Optical Signal Processing Techniques and Applications of Optical Phase Modulation in High-Speed Communication Systems

DENG, Ning

A Thesis Submitted in Partial Fulfilment
of the Requirements for the Degree of
Doctor of Philosophy
in
Information Engineering

© The Chinese University of Hong Kong
August 2007

The Chinese University of Hong Kong holds the copyright of this thesis. Any person(s) intending to use a part or whole of the materials in the thesis in a proposed publication must seek copyright release from the Dean of Graduate School

UMI Number: 3302446

INFORMATION TO USERS

The quality of this reproduction is dependent upon the quality of the copy submitted. Broken or indistinct print, colored or poor quality illustrations and photographs, print bleed-through, substandard margins, and improper alignment can adversely affect reproduction.

In the unlikely event that the author did not send a complete manuscript and there are missing pages, these will be noted. Also, if unauthorized copyright material had to be removed, a note will indicate the deletion.

UMI Microform 3302446

Copyright 2008 by ProQuest LLC.

All rights reserved. This microform edition is protected against unauthorized copying under Title 17, United States Code.

ProQuest LLC
789 E. Eisenhower Parkway
PO Box 1346
Ann Arbor, MI 48106-1346

Acknowledgement

First and foremost, I would like to express my heartfelt gratitude to my thesis supervisor Prof. Calvin Chun-Kit Chan, for his persistent guidance and support throughout my postgraduate study. Prof. Chan not only taught me research methodology and professional knowledge, but also gave me invaluable suggestions on paper writing and presentation skills. I believe Prof. Chan's ingenuity and preciseness will continue inspiring me in my future research and work.

I have also benefited a lot from Prof. Lian-Kuan Chen and Prof. Chinlon Lin in the Lightwave Communications Laboratory. They kindly provided plenty of illuminative suggestions, and brought me into wider and deeper research perspectives in photonics and optical communications. Thanks also go to Prof. Frank Tong and Prof. K.W. Cheung in the Laboratory. Besides, I also benefited from the suggestion and discussion from Prof. Chester Shu (CUHK), Prof. H.K. Tsang (CUHK), Prof. Kenneth Wong (HKU) and Prof. Chao Lu (PolyU). Many thanks to all of them.

It is my great pleasure to have worked or be working together with so many smart and diligent labmates. I have learned a lot from them and have shared a lot of happiness of research with them. I would like to express my sincere thanks to the graduated and the current labmates during recent five years. I would like to particularly mention Dr. Li Huo and Dr. Zhaoxin Wang for their help and the discussions with them.

I would like to thank IEEE LEOS for their generous Graduate Student Fellowship, as well as the best paper award and the travel grant offered by their sponsored conferences. Thanks must also go to the Graduate School and the Department of Information Enginnering of CUHK for the conference grants, which enabled me to have many opportunities to attend international conferences.

Last but not the least, I am extremely indebted to my family for their continuous care and encouragement. I would like to say, I love them.

Abstract

In recent years, optical phase modulation has attracted much research attention in the field of fiber optic communications. Compared with the traditional optical intensity-modulated signal, one of the main merits of the optical phase-modulated signal is the better transmission performance. For optical phase modulation, in spite of the comprehensive study of its transmission performance, only a little research has been carried out in terms of its functions, applications and signal processing for future optical networks.

These issues are systematically investigated in this thesis. The research findings suggest that optical phase modulation and its signal processing can greatly facilitate flexible network functions and high bandwidth which can be enjoyed by end users. In the thesis, the most important physical-layer technology, signal processing and multiplexing, are investigated with optical phase-modulated signals. Novel and advantageous signal processing and multiplexing approaches are proposed and studied. Experimental investigations are also reported and discussed in the thesis.

Optical time-division multiplexing and demultiplexing: With the ever-increasing demand on communication bandwidth, optical time division multiplexing (OTDM) is an effective approach to upgrade the capacity of each wavelength channel in current optical systems. OTDM multiplexing can be simply realized, however, the demultiplexing requires relatively complicated signal processing and stringent timing control, and thus hinders its practicability. To tackle this problem, in this thesis a new OTDM scheme with hybrid DPSK and OOK signals is proposed. Experimental investigation shows this scheme can greatly enhance the demultiplexing timing misalignment and improve the demultiplexing performance, and thus make OTDM more practical and cost effective.

All-optical signal processing: In current and future optical communication systems and networks, the data rate per wavelength has been approaching the speed limitation of electronics. Thus, all-optical signal processing techniques are highly desirable to

support the necessary optical switching functionalities in future ultrahigh-speed optical packet-switching networks. To cope with the wide use of optical phase-modulated signals, in the thesis, an all-optical logic for DPSK or PSK input signals is developed, for the first time. Based on four-wave mixing in semiconductor optical amplifier, the structure of the logic gate is simple, compact, and capable of supporting ultrafast operation. In addition to the general logic processing, a simple label recognition scheme, as a specific signal processing function, is proposed for phase-modulated label signals. The proposed scheme can recognize any incoming label pattern according to the local pattern, and is potentially capable of handling variable-length label patterns.

Optical access network with multicast overlay and centralized light sources: In the arena of optical access networks, wavelength division multiplexing passive optical network (WDM-PON) is a promising technology to deliver high-speed data traffic. However, most of proposed WDM-PONs only support conventional point-to-point service, and cannot meet the requirement of increasing demand on broadcast and multicast service. In this thesis, a simple network upgrade is proposed based on the traditional PON architecture to support both point-to-point and multicast service. In addition, the two service signals are modulated on the same lightwave carrier. The upstream signal is also remodulated on the same carrier at the optical network unit, which can significantly relax the requirement on wavelength management at the network unit.

摘 要

近年來，高速光通訊技術的發展一日千里。光相位調製(optical phase modulation)作為一種重要的調製方法，引起了學術界的高度重視。已有的研究成果表明，與傳統的光幅度調製相比，光相位調製的訊號擁有更好的傳輸性能。但是，除了其傳輸性能，幾乎沒有研究涉足到光相位調製在下一代光網路中的功能、應用及其訊號處理。

本論文將系統地研究這些問題。研究發現光相位調製可以更好地支援寬頻通訊以及更加靈活的網路功能。光相位調製的訊號複用(signal multiplexing)以及訊號處理(signal processing)，作為網路物理層的核心技術在本文中作了詳細研究。一些新的提案首次在本文中提出，並通過實驗做了進一步的探索。

光時分複用及解複用： 光時分複用(OTDM)是一種有效提高每個波長容量的技術。OTDM 系統的難點在於其解複用(demultiplexing)，因其需要高速的光開關和嚴格的時鐘控制。為了解決這一難題，本文首次提出了一種新型的開關鍵控(OOK)和差分相移鍵控(DPSK)兩種混合調製的 OTDM 系統框架。實驗發現這種方法可以極大地提高解複用對時鐘偏移的容忍度從而顯著地提高解複用性能。因此，這一方法使得 OTDM 更加高效實用。

全光訊號處理： 未來的高速光通訊網路系統將會超出電子系統的處理容限。所以，下一代光網路交換處理系統將會需要超高速的全光訊號處理技術。然而此前的研究並未涉及到光相位調製訊號的全光處理。本文首次提出了針對 DPSK 調製格式的全光邏輯門(all-optical logic)。基於半導體光放大器中的四波混頻(FWM)原理，此邏輯門結構簡單、體積小、支援超高速處理。本文還提出了一種新型的光標籤識別(optical label recognition)技術，它可以識別任意的相位調製的標籤。

支援點對點和多播功能的光接入技術： 波分複用無源光網路(WDM-PON)是一種前景廣闊的光接入解決方案。然而，此前的 WDM-PON 方案只支援點對點的資料業務，這顯然不能滿足日益增長的廣播及多播視頻業務的需求。本文提出了一種非常簡單實用的方案，將原來的點對點接入網升級成為同時支持點對點和多播雙重業務的新型接入網路。兩種業務只需要一套光源，同時光網路單元(ONU)亦不需要光源。這大大簡化了波長管理和維護開銷。

Table of Contents

List of Figures

1 Introduction

1.1 Recent research developments in optical communication networks

Along with human beings stepping into the Information Age, communication network is becoming a basic demand of people and an important sign of civilization. Optical fiber is the best candidate to transmit high capacity of data (supported bandwidth as high as 25 THz) to ultra long distance (thousands of kilometers). With the development of modern technology, trans-ocean fiber deployment has been replacing satellite voice communication since 1980s and 1990s. In late 1990s, the exponential growth of the emerging Internet traffic greatly stimulated the research, development, and investment of optical communications.

Although people have acquired huge achievements in developing communication networks, people are still at the beginning stage of the "informationization" process. The following forthcoming problems are challenging the research and development of optical communication networks. First, the data flow on the Internet doubles around every eight months, which suggests continuously increasing bandwidth of backbone transmission networks; Second, the increasing bandwidth is exceeding the capability of electronic processing in network nodes (such as routing, switching, etc.), and thus much faster processing mechanism such as all-optical processing is expected; Third, video traffic experiences significant augmentation in recent years. Internet-protocol based television (IPTV) has been developing very quickly, and high-definition (HD) video is the future trend of video casting, which requires high-bandwidth enabled access solutions. Fig. 1.1 shows the bandwidth demand for various applications versus the capacity of different access technologies [1]. It is obvious that optical access technology, or namely fiber to the premise (FTTP), is the unique solution in the future.

Therefore, the main research efforts lie in the following: increasing the network capacity by improving transmission performance and data modulation; pondering better network architecture that is more low-latency, bandwidth-efficient and flexible; speeding the information processing by all-optical means; and so on. Nowadays, researchers have achieved 25 Tb/s in backbone transmission [2], 10 Gb/s in access networks [3], and 640 Gb/s in signal processing [4] in research laboratories.

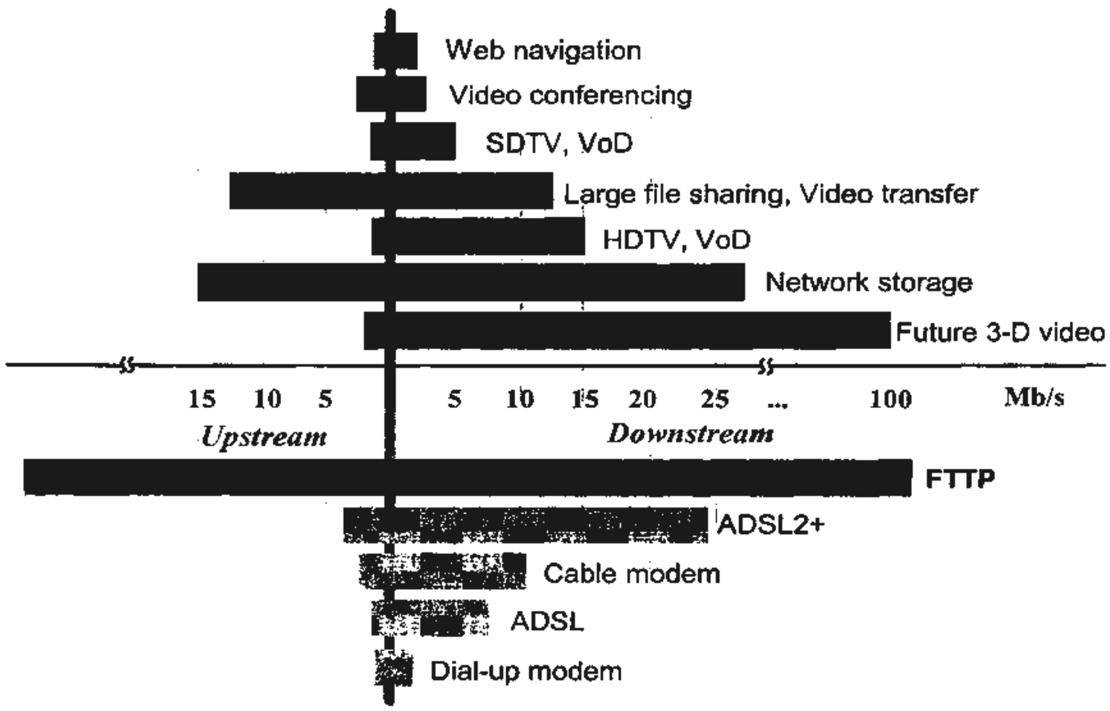

Fig. 1.1 The bandwidth demand of various end-user applications (upper) and the available bandwidth provided by various access technologies (lower) [1].

1.2 Utilization of optical phase modulation in optical communication networks

Optical phase modulation for data communications first attracted much attention in late 1980s and early 1990s. Most of the research work was focused on coherent system and the main emphasis led in the receiver sensitivity. With optical amplifiers having become mature in 1990s, research and development efforts returned to on-off keying (OOK) modulation format, in either nonreturn-to-zero (NRZ) or return-to-zero

(RZ) form. With the data encoded on the intensity of the optical carrier, an OOK signal can be directly detected at the receiver.

Recently, with the continuous increase of the data rate per wavelength channel, people started to revisit optical phase modulation, especially the optical differential-phase-shift keying (DPSK) modulation format. Intensive research efforts have been paid in studying the DPSK format, and its superior transmission performance has been proven. Using balanced detection, DPSK signals require about 3-dB lower optical signal-to-noise ratio (OSNR) to achieve the same performance compared with OOK signals [5, 6]. Moreover, DPSK has also been shown to be very robust against the degradation due to fiber nonlinearities [2, 5]. It is not surprising that many of recent transmission records at per-channel rates of 10 or 40 Gb/s are held by optical systems based on DPSK.

In next chapter, we shall review the fundamental concept of optical phase modulation and the signal performance of optical phase modulation. Coherent PSK or DPSK system will be introduced first, and then noncoherent DPSK system with direct detection will be discussed in detail. After that, we shall summarize the current research status of DPSK applications in optical communication networks of different scales, including backbone, metro and access networks.

1.3 Major contribution of the thesis

Optical phase modulation, especially the DPSK modulation format, is very promising modulation technology for next-generation optical communications. Previously, the main research efforts have been paid to the transmission and receiver performance of optical phase modulation. In this thesis, I concentrate on the investigation of the signaling and processing of optical phase modulation in network applications.

My research in optical phase modulation, especially in the DPSK modulation format, is focused on their functions, applications and signal processing in future optical networks. Up to now, only a little research has been carried out in this aspect, in spite of the comprehensive study of optical phase modulation in terms of the transmission and receiver performance. In my research, I find out that employing optical phase modulation can greatly facilitate signal processing or network functions, which can make the subsystem and the whole network simpler, more flexible and of higher performance.

In the thesis, I propose a novel OTDM scheme with hybrid modulation formats of DPSK and OOK. With this kind of hybrid OTDM scheme, the performance degradation in demultiplexing due to adjacent-channel crosstalk can be effectively suppressed. Therefore, the demultiplexing performance can be greatly enhanced. Meanwhile, the requirement on the timing control circuit can be greatly relaxed. These lead the OTDM to become more practical and cost effective.

All-optical signal processing is regarded as an important approach to improve the network efficiency for future optical networking. My research in optical phase-modulated signal processing is focused on the all-optical logic function and all-optical label recognition. The thesis reports the world's first demonstration of an all-optical XOR logic for DPSK signals. In addition, the proposed XOR gate can support three input signals, for the first time, which can increase the feasibility and flexibility for cascaded operation.

Optical access is becoming a hot topic in optical communications, as the high bandwidth offered by the backbone networks has not yet been efficiently enjoyed by end users. My research findings suggest that employing optical phase modualtion can effectively enhance the value-added services and reduce the cost of optical access networks. I propose a novel WDM-PON architecture to support a multicast overlay on a traditional PON for point-to-point service only. As the multicast data is modulated on the same lightwave carrier with the point-to-point signal, the scheme is cost effective. Moreover, the scheme can achieve colorless optical network unit and wavelength-management-free operation.

1.4 Outline of the thesis

Chapter 2 introduces the basic concept and recent research thrust on optical phase modulation. First, optical phase modulation, PSK, DPSK, and multi-level PSK are introduced. Second, the transmitters and receivers for optical DPSK are discussed. Last but not the least, a detailed analysis on the performance of optical DPSK signal is given. The performance between DPSK and OOK is compared.

Chapter 3 proposes a novel OTDM scheme with hybrid modulation formats of DPSK and OOK. After the principle of operation, the enhanced tolerance to timing misalignment and improved performance using the hybrid OTDM is demonstrated in 40-Gb/s and 80-Gb/s OTDM demultiplexing. A special case of the hybrid OTDM is discussed: a two-channel OTDM signal can be directly detected without demultiplexing.

Chapter 4 focuses on the all-optical logic gate for DPSK signals. The XOR logic is implemented based on FWM in SOA. Two-input case and three-input case are experimentally demonstrated, respectively.

Chapter 5 proposes a new label recognition scheme for phase-modulated label signals. The principle is explained in detail and an experiment is demonstrated.

Chapter 6 proposes a WDM-PON architecture with multicast overlay and centralized light sources. The network is demonstrated in a proof-of-principle experiment. The practical issue such as power budget and signal performance is analyzed.

Chapter 7 gives a summary of the thesis and suggests the possible future work.

References

[1] M.A. Wegleitner, "Maximizing the impact of optical technology," in *Optical Fiber Communication Conference and Exposition and The National Fiber Optic Engineers Conference (OFC/NFOEC)* 2007, Anaheim, USA, Plenary talk.

[2] A.H. Gnauck, G. Charlet, P. Tran, P. Winzer, C. Doerr, J. Centanni1, E. Burrows, T. Kawanishi, T. Sakamoto, K. Higuma, "25.6-Tb/s C+L-Band transmission of polarization-multiplexed RZ-DQPSK signals," in *Optical Fiber Communication Conference and Exposition and The National Fiber Optic Engineers Conference (OFC/NFOEC)* 2007, Anaheim, USA, paper PDP19.

[3] W. Hung, C.K. Chan, L.K. Chen, F. Tong, "An optical network unit for WDM access networks with downstream DPSK and upstream re-modulated OOK data using injection-locked FP laser," P*hotonics Technology Letters*, vol. 15, no. 10, pp. 1476-1478, 2003.

[4] E. Tangdiongga, Y. Liu, X. Shu, I. Bennion, H. De Waardt, G.D. Khoe, A.M.J. Koonen, H.J.S. Dorren, "640-to-40 Gb/s all-optical demultiplexing using a single SOA assisted by an optical filter," *IEEE Lasers and Electro-Optics Society Annual Meeting (LEOS)* 2006, Montreal, Canada, paper PD1.6.

[5] C. Xu, X. Liu, and X. Wei, "Differential phase-shift keying for high spectral efficiency optical transmitters," *Journal of Selected Topics in Quantum Electronics*, vol. 10, no. 2, pp. 281-293, 2004.

[6] P.A. Humblet and M. Azizoglu, "On the bit rate of lightwave systems with optical amplifiers," *Journal of Lightwave Technology*, vol. 9, pp. 1576-1582, 1991.

2 Optical Phase Modulation in Communication Networks

2.1 Phase modulation and phase-shift keying

2.1.1 Introduction

Modern optical communications systems are largely based on a simple digital transmission scheme in which the intensity of the optical carrier is modulated with binary data and the optical signal is detected directly with a photodiode to convert it to the original digital signal in electrical domain. Such scheme is usually referred to as intensity modulation with direct detection (IM/DD). An alternative modulation scheme is to transmit information by modulating the phase (or frequency) of the optical carrier, usually using an electro-optic phase modulator. This approach was well studied in the 1980s in the context of coherent detection due to its superior receiver sensitivity comparing with IM/DD systems. However, coherent transmission systems based on phase modulation was never deployed for field application owing to the introduction of optical amplifiers in the early 1990s. During the last few years, however, there have been renewed interests in optical phase shift keying and its potential application in amplified ultra long-haul DWDM transmission system at 10 Gb/s and higher bit rates. The research interest in this area is in line with the continuing effort of telecommunications industry to improve the transmission distance and capacity of long-haul transport network.

Instead of coherent detection, recent research efforts mainly concentrate on optical phase modulation which can facilitate direct detection. Optical differential phase shift keying (DPSK) is one such modulation format. A Mach-Zehnder delay interferometer (DI) can be employed to allow adjacent phase-modulated bits to interfere, thus recovering the on-off keyed (OOK) signal for direct detection at the DI output. One of the attractive features of DPSK compared to OOK is that it requires an almost 3-dB lower optical signal-to-noise ratio (OSNR) to reach a given Q factor (or equivalently, BER) provided a balanced receiver is implemented at the receiver side [1, 2, 5]. Another interesting feature of DPSK is that its intensity is almost constant despite the presence of phase data. When all channels in a DWDM system are modulated in DPSK format, the cross-phase modulation (XPM) penalty can be effectively reduced allowing wavelength channels to be placed even closer to each other. With the use of DPSK (either NRZ-DPSK or RZ-DPSK), some impressive ultra long-haul DWDM transmission experiments were reported recently [10-14].

In addition to the extensive research of optical phase modulation formats in next-generation long-haul transmission network has been studied intensively, there are also some research activities on the system applications of optical phase modulation in future next-generation optical access and metropolitan area networks. The combined signal of intensity modulation and phase modulation has been demonstrated in a WDM metro network to facilitate the network functions [35]. However, their scheme was based on coherent detection. More recently, directly-detected optical DPSK was proposed to be used in OLS networks for packet labeling in European STOLAS project [44]. In this scheme, the extinction ratio (ER) of the intensity modulated packet was purposely reduced and the label is phase-modulated onto the entire packet body.

In this chapter, the fundamental concept of optical phase modulation and the signal performance of optical phase modulation will be reviewed. Coherent PSK or DPSK system will be first introduced, and then noncoherent DPSK system with direct detection will be discussed in detail. After that, we shall summarize the current research status of DPSK applications in optical communication networks of different scales, including backbone, metro and access networks.

2.1.2 Basic concept of phase-shift keying

In optical digital communication systems, the representation of information is generally realized by modulating the amplitude, or the frequency, or the phase of a lightwave carrier. In the case of optical phase modulation (PM), information is coded on the optical carrier by altering the phase of different bits, which is known as optical phase-shift keying (PSK). In a binary system, space ("0") or mark ("1") information is represented by different phase values of the optical carrier, which are usually chosen to be "0" and "π".

Mathematically, an optical PSK signal can be represented as

$$E_{PSK}(t) = \sum_n u(t - nT)\exp[-j\omega_c t - j\pi b_n] \tag{1.1}$$

where b_n is the bit information (either 1 or 0), ω_c is the optical carrier angular frequency, $u(t)$ is the signal baseband waveform which is ideally a rectangular window function.

Optical differential-phase-shift keying (DPSK) is a derivative format of optical PSK. A DPSK signal carries information in its phase transit between its every two adjacent bits, instead of the absolute phase value in each bit as in a PSK signal. A main advantage of DPSK compared with PSK is that it does not need a reference phase for detection at a receiver. Note that in this thesis, we use DPSK to only refer to the binary DPSK (also known as DBPSK), which is widely accepted in literature.

Fig. 2.1 depicts the constellation diagram of the electrical field of an optical PSK or DPSK signal. The constellation for an optical OOK signal is also shown for comparison. From the diagram, we can find the difference between the two formats lies in both the amplitude and the phase. For the same received power, the symbol distance of a DPSK signal is $\sqrt{2}$ times of that of an OOK signal. Therefore, only a half of the received power is needed for a DPSK signal to achieve the same symbol distance as compared with an OOK signal. This gives a simple explanation why a DPSK signal has better receiver performance than an OOK signal. However, it should be noted that such a benefit can only be realized by balanced detection, and a more precise explanation will be given in later sections.

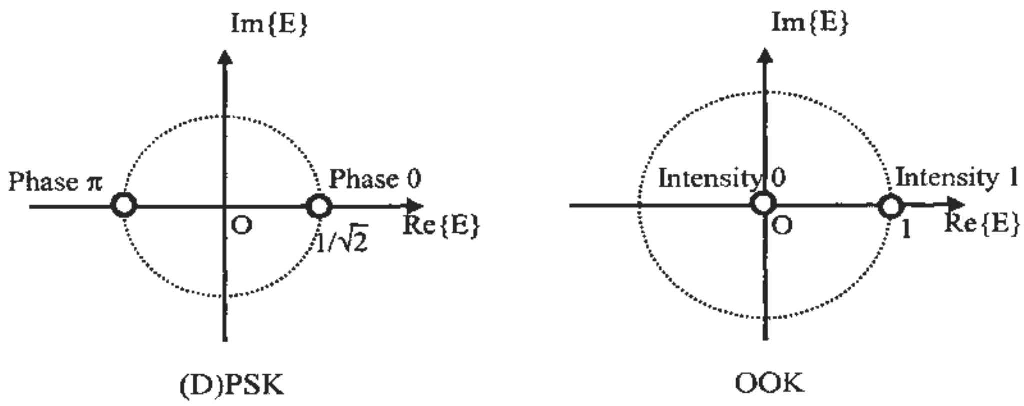

Fig. 2.1 The respective constellation diagrams of an optical (D)PSK and an optical OOK signal.

To generate an optical DPSK signal, the data signal should first be differentially pre-coded. A direct implementation of the differential pre-coder is shown in Fig. 2.2, which consists of an XOR logic gate and a feedback tap of one-bit delay. The output of the pre-coder is

$$c_k = c_{k-1} \oplus d_k \tag{1.2}$$

where d_k is the k^{th} input original data bit and c_k is the k^{th} output data bit.

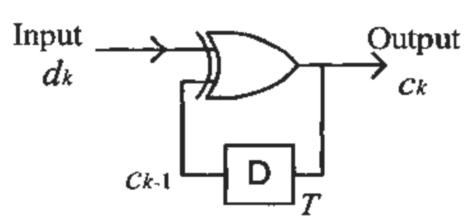

Fig. 2.2 A direct implementation of the differential pre-coder. D: one-bit delay.

For experimental investigation using commercial bit error rate test set (BERT), the differential pre-coder can usually be ignored. This is due to a special property of the commonly used pseudorandom binary sequences (PRBS) generator in a BERT. For a 2^n-1 PRBS sequence, the generating polynomial implemented in a BERT is of the form: $1+x^{n-1}+x^n$. The output from the differential pre-coder would be the exact same sequence as the input except that the whole sequence is shifted by (n-1) bits.

To convert an electrical pre-coded data signal to an optical DPSK signal, a phase modulator is required. Phase modulation can either be achieved by a straight-line $LiNbO_3$ phase modulator (SL-PM) or a Mach-Zehnder modulator (MZM), as shown in Fig. 2.3. A SL-PM only modulates the phase of the optical field, resulting in a constant-envelop signal. Since phase modulation does not occur instantaneously, it introduces chirp across bit transitions, as shown in Fig. 2.3(a).

On the other hand, to conduct phase modulation with a MZM, it is biased at the null point of its transmission response, and is driven at twice of the switching voltage required for OOK modulation. Alternatively, a dual-drive MZM can be employed with push-pull operation. The pre-coded data signal and its complementary signal at normal switching voltage are used to drive the MZM. It can achieve much faster phase transition compared with a SL-PM, and thus it realizes almost chirp-free operation.

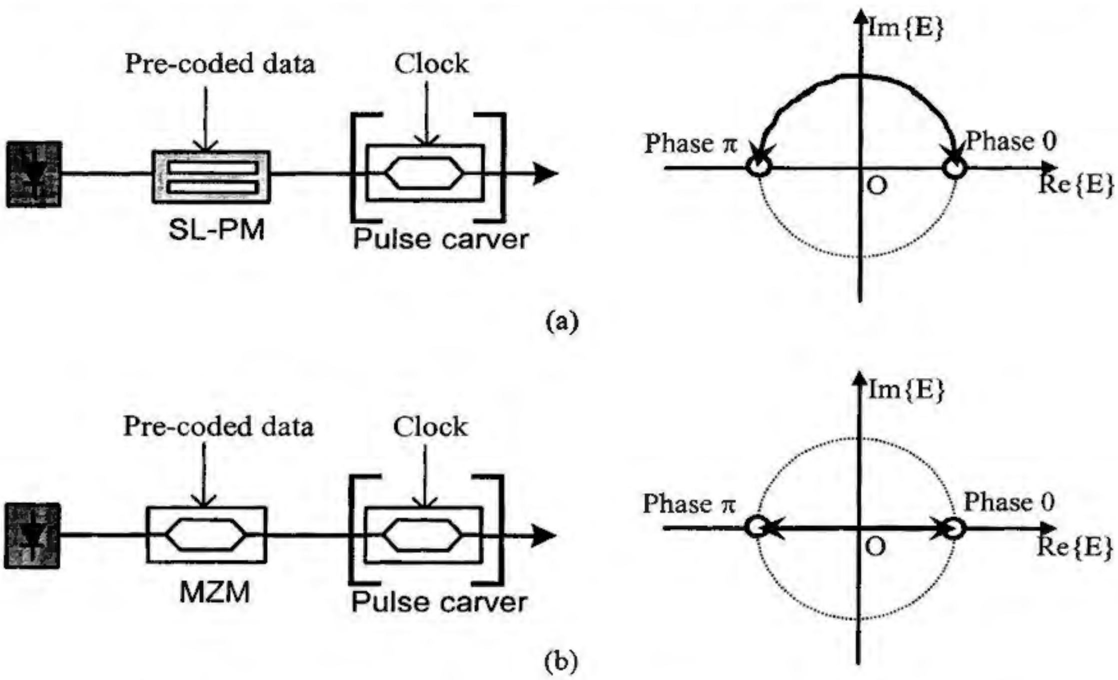

Fig. 2.3 Two types of optical DPSK transmitters and their modulation principle represented in constellation diagrams. (a) SL-PM, (b) MZM.

Sometimes, another MZM or electro-absorption modulator (EAM) is inserted after the phase modulator as a pulse carver. A constant-intensity DPSK signal becomes a series of phase-modulated pulses, which is called RZ-DPSK. As discussed before, the phase modulator may cause chirps to the signal at phase transition positions. With proper pulse carving, the chirps can be eliminated, which results in one advantage of RZ-DPSK signals. Another merit of RZ-DPSK format is its better transmission performance compared with DSPK, which will be discussed in later sections.

2.1.3 Receiver for PSK or DPSK signals

Basically there are two classes of methods to receive an optical DPSK signal – coherent detection and noncoherent detection. Coherent detection is a method to achieve superior performance, which can approach theoretical receiver sensitivity and excellent spectral efficiency. Coherent system attracted considerable attention in late 1980s and early 1990s. Fig. 2.4 shows a typical coherent receiver for DPSK system. A local oscillating laser (LO), coupled with the incoming optical signal, is fed into a photodiode. The mixed optical field of the received optical signal and the local CW is converted into electrical radio-frequency (RF) signal through photo-detection. Since such opto-electrical (OE) conversion is achieved by means of square-law envelope detection, there appears an output term containing the multiplication between the two optical fields, in addition to the two other output terms proportional to the squares of the two optical fields. The multiplication term consists of not only the amplitude parameter of the received optical signal but also the optical frequency and phase parameters. Thus the data information carried by the optical PSK or DPSK signal can be extracted from the multiplication term of the output electrical RF signal. Relying on whether the carrier frequencies of received optical signal and LO are the same or not, two approaches namely homodyne and heterodyne coherent detection have been proposed [3-4].

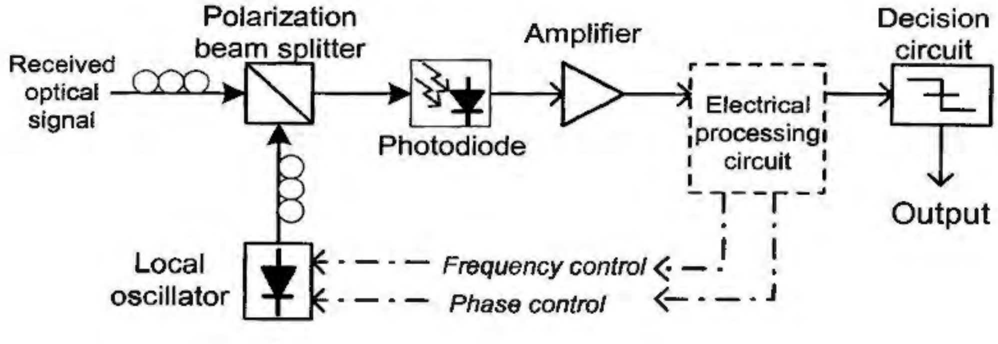

Fig. 2.4 The coherent receiver for optical PSK or DPSK signals.

Compared with the commonly-used direct detection, though coherent detection can offer advantages as better receiver sensitivity and narrower permissible frequency spacing of the optical PSK signals, it requires accurate local oscillator's frequency/phase control and sophisticated electronic circuits after the photodiodes. In late years, non-coherent detection has become prevailing for optical DPSK reception for its simplicity. A general optical DPSK receiver comprises a demodulator and a photo-detector. An optical delay-line interferometer (DI) [1, 6, 7], or an optical bandpass filter (OBPF) [8, 9], can serve as an optical DPSK demodulator. It converts the phase modulation into intensity modulation so that the output signal can be directly detected by a photodiode.

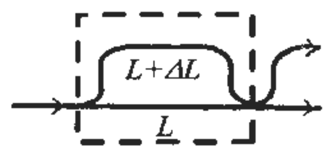

(a)

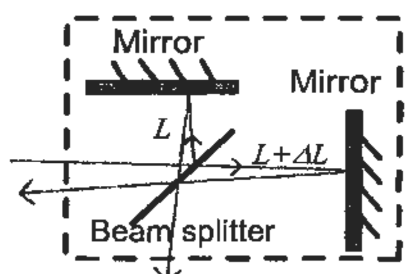

(b)

Fig. 2.5 Optical delay interferometer for DPSK demodulation. (a) based on fiber or PLC structure, (b) based on free-space optics [7].

The delay tap in a DI is usually made of a piece of fiber or a planar lightwave circuit (PLC). Since the refractive index of the delay tap is sensitive to temperature variation, the transmission response of a DI and the demodulated DPSK performance are also very sensitive to temperature variation. Therefore, accurate temperature control must be incorporated to stabilize a DI. In 2005, a new DI based on free space optics was proposed, which was almost independent on temperature changes [7]. Based on free-space Michelson interferometer, the DI consists of an optical beam splitter and two reflection mirrors, as shown in Fig. 2.5. As the length difference between the two paths varies less than 10 nm over a temperature range between 0°C and 70°C, the demodulation performance change is negligible.

After demodulation, both of the DI output ports carry full logically-complementary information, and either of them can be used for detection, which is so-called single-ended detection. To achieve better detection performance, balanced detection can be employed by connecting the two output ports with two balanced photodiodes, as shown in Fig. 2.6. A balanced receiver requires identical path lengths between the output point and the point of subtraction of the two branches. In a linear communication channel dominated by amplifier noise, DPSK with balanced detection requires approximately 3-dB lower OSNR than OOK for the same bit error rate (BER). In the following we analytically explain the reason based on the analysis in [1].

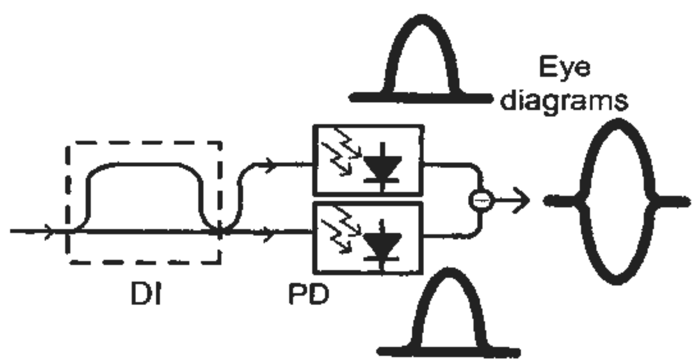

Fig. 2.6 Balanced detector of optical DPSK signals. DI: delay interferometer, PD: photo-detector.

In an optical transmission channel where amplifier spontaneous emission (ASE) noise dominates [1,2], the electrical field of a DPSK signal can be expressed

$$s(t) = \left[\sum_{n=0}^{N-1} a_n u(t-nT) + z(t)\right] \exp(-j\omega_c t) + \text{c.c.} \tag{2.2}$$

where a_n and $u(t-nT)$ are the complex amplitude and the waveform function of the n^{th} bit, respectively; $z(t)$ is the accompanied noise that is assumed to be additive white Gaussian noise (AWGN); ω_c is the angular frequency of the optical carrier and T is the bit period. In front of the receiver, a matched filter is employed with an impulse response function

$$h(t) = \frac{1}{\sqrt{E_b}} u(-t)\exp(j\omega_c t) + \text{c.c.} \tag{2.3}$$

where $E_b = \int u^*(t)u(t)\mathrm{d}t$ is the energy per bit.

The output of the matched filter is the convolution of $s(t)$ and $h(t)$. At the center of the n^{th} bit, the sampled signal is

$$F_n(t) = f_n e^{-j\omega_c t} + \text{c.c.} \tag{2.4}$$

$$f_n = a_n\sqrt{E_b} + z_n \tag{2.5}$$

$$z_n = \int_{(n-1/2)\mathrm{T}}^{(n+1/2)T} z(t)u^*(t-nT)\mathrm{d}T \tag{2.6}$$

The filtered noise amplitude $z(t)$ consists of a real part and an imaginary part, i.e. $z_n = x_n + jy_n$, and they are independent zero-mean Gaussian random variables with the variance

$$\langle x_n^2 \rangle = \langle y_n^2 \rangle = \sigma^2 \tag{2.7}$$

Then the filtered DPSK signal is demodulated using a DI, as shown in Fig. 2.6. The optical output of the DI is constructive interference or destructive interference between the adjacent bits, depending on the phase difference between f_n and f_{n-1}. The signals measured by the two photodiodes are

$$I_+ = \left|\frac{f_n + f_{n-1}}{2}\right|^2 \text{ and } I_- = \left|\frac{f_n - f_{n-1}}{2}\right|^2 \tag{2.8}$$

The balanced output is the subtraction between them

$$\begin{aligned} I_b = I_+ - I_- &= \frac{f_n f_{n-1}^* + f_n^* f_{n-1}}{2} \\ &= (a_n\sqrt{E_b} + x_n)(a_{n-1}\sqrt{E_b} + x_{n-1}) + y_n y_{n-1} \end{aligned} \tag{2.9}$$

Let $V = (a_n\sqrt{E_b} + x_n)$, $W = (a_{n-1}\sqrt{E_b} + x_{n-1})$, $X = y_n$, $Y = y_n$, I_b can be written as

$$I_b = VW + XY \tag{2.10}$$

It is obvious to see that V and W are independent identical-distribution (i.i.d.) random variables, with the mean being either $+E_b$ or $-E_b$ (depending on $a_n \cdot a_{n-1}$) while the variance being σ^2. X and Y are also i.i.d., with zero-mean and the variance of σ^2. In the following, we calculate the distribution of I_b, through which we can calculate the BER of the balanced detected DPSK signal.

The characteristic function of I_b is

$$\phi_{I_b}(u) = E\left[e^{jI_b}\right] = E\left[e^{j(VW+XY)}\right] = E\left[e^{jVW}\right] + E\left[e^{jXY}\right] \tag{2.11}$$

Based on the distribution

$$V,W \sim N(0,\sigma^2) \tag{2.12a}$$

$$X,Y \sim N(\mu,\sigma^2) \tag{2.12b}$$

where $\mu = +E_b$ for the current bit 1 (written as I_{b1}) while $\mu = -E_b$ for the current bit 0 (written as I_{b0}), the characteristic function is derived as

$$\phi_{I_b}(u) = \frac{1}{1+u^2\sigma^4} e^{\frac{ju\mu^2}{1-ju\mu^2}} \tag{2.13}$$

To obtain the BER, we first calculate the error probability that a bit 1 is erroneously detected as a bit 0. That is,

$$\begin{aligned}
&Prob[I_{b1} < 0] \\
&= \int_{-\infty}^{0} p(x)\mathrm{d}x = \int_{-\infty}^{0}\left(\frac{1}{2\pi}\int_{-\infty}^{\infty}\phi_{I_{b1}}(u)e^{-jux}\mathrm{d}u\right)\mathrm{d}x \\
&= \frac{1}{2\pi}\int_{-\infty}^{\infty}\phi_{I_{b1}}(u)\int_{-\infty}^{0}e^{-jux}\mathrm{d}x\mathrm{d}u \\
&= -\frac{1}{2\pi j}\int_{-\infty+j\varepsilon}^{\infty+j\varepsilon}\frac{\phi_{I_{b1}}(u)}{u}\mathrm{d}u \\
&= \frac{1}{2}e^{-E_b/(2\sigma^2)}
\end{aligned} \tag{2.14}$$

The last integral is calculated employing the residue theorem. Similarly, we can calculate the error probability of a bit 0, and the result is the same with the error probability of a bit 1. Therefore, if assuming equal distribution of bits 0s and 1s, the BER of the balanced detected DPSK signal can be expressed as

$$\mathrm{BER} = \frac{1}{2}\exp\left(-\frac{E_b}{2\sigma^2}\right) \tag{2.15}$$

On the other hand, the BER for an optical OOK signal has been extensively studied, and is given by [3]

$$\mathrm{BER}_{\mathrm{OOK}} = \frac{1}{2}\mathrm{erfc}\left(\frac{1}{\sqrt{2}}\cdot\sqrt{\frac{E_b}{2\sigma^2}}\right) \approx \sqrt{\frac{\sigma^2}{\pi E_b}}\exp\left(-\frac{E_b}{4\sigma^2}\right) \tag{2.16}$$

Neglecting the prefactors in front of the exponential functions, Eqs. (2.15) and (2.16) show an approximately 3-dB advantage in receiver sensitivity by using DPSK format compared with OOK format. As a more precise reference, Fig. 2.7 plots the relation between the BER and the signal-to-noise ratio (SNR) $E_b/(2\sigma^2)$. Again, we find that the receiver sensitivity of DPSK is 2.8 dB (around 3 dB) lower than that of OOK at a BER of 10^{-9}.

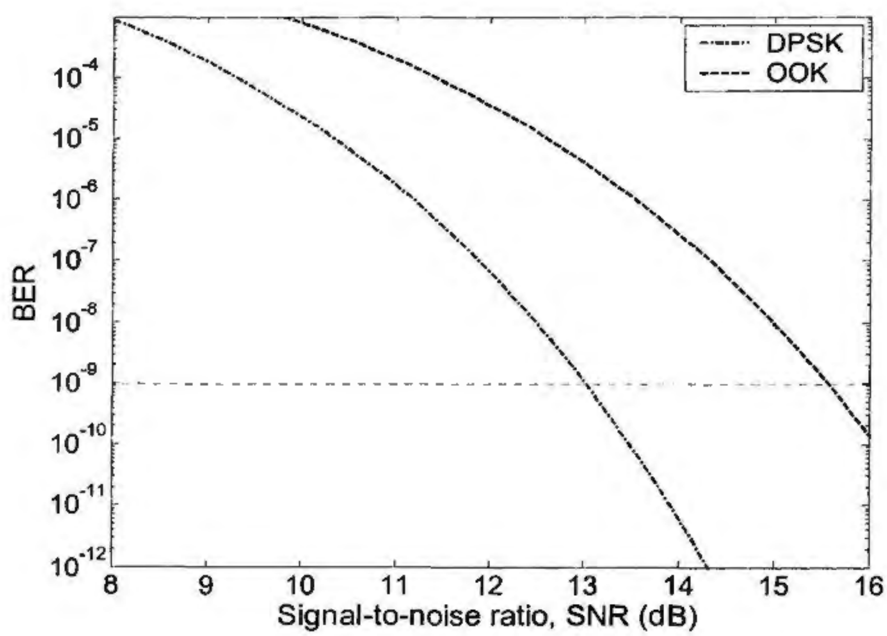

Fig. 2.7 Respective BER of OOK and DPSK signals versus SNR, plotted based on Eqs. (2.15) and (2.16).

2.2 DPSK in Backbone Transmission Networks

Data communications have experienced drastic revolution over the past ten years. In terms of the scale, communication networks can be classified as backbone networks, metro networks and access networks. Backbone networks connect the main network nodes located in the main cities in the world across long distance of land and ocean. Today's backbone long-haul networks utilize wavelength-division multiplexing (WDM) or time-division multiplexing (TDM) technology to realize high-capacity transmission. They also utilize erbium-doped fiber amplifiers (EDFAs) to compensate the attenuation in the optical fiber links. In recent years, optical DPSK, as a high-performance modulation format, has been extensively investigated for backbone transmission [1, 4, 5, 7, 10-14].

2.2.1 Wavelength-division multiplexing (WDM)

In an optical WDM system, multiple optical carriers at different wavelengths are modulated by using independent electrical data streams and are then transmitted over the same fiber. Therefore, the capacity per fiber is greatly increased. For example, some deployed systems have 160 channels with each channel carrying 10-Gb/s data, thus the capacity per fiber is easily increased to 1.6 Tb/s. The optical signal at the receiver is demultiplexed into separate channels by using an optical technique. Fig. 2.8 shows the system architecture of an optical WDM system.

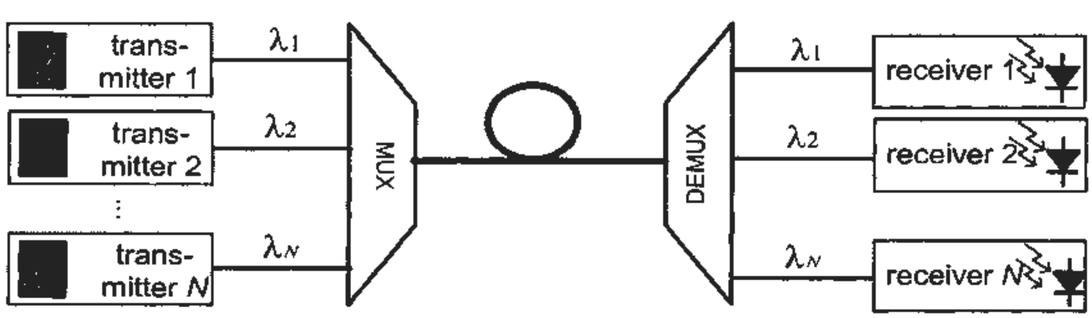

Fig. 2.8 System architecture of an optical WDM backbone transmission network.

As mentioned in previous sections, almost all the transmission records, in terms of the capacity, spectral efficiency, distance, are held by WDM systems based on phase modulation. Table 2.1 summarizes the most recent transmission results reported in the Optical Fiber Communication Conference and the National Fiber Optic Engineers Conference (OFC/NFOEC) 2007. All the investigations support high-capacity long-distance transmission, but they also have their respective specific features. For example, the first experiment achieved extremely high spectral efficiency of 3.2 b/s/Hz, which was realized by differential quadrature phase-shift keying (DQPSK) and polarization multiplexing, within a 50-GHz spacing WDM system. On the other hand, the last two experiments were focused on the physical-layer transmission of next-generation 100-Gbit/s Ethernet, which is a promising network architecture compatible with the wide use of Ethernet.

Table 2.1

Bitrate (Bitrate per ch.)	No. of λ	Transmission distance	Modulation technique	Spectral efficiency	Reference	Highlight
25.6 Tb/s (85.4Gb/s)	160 (50GHz spacing)	3×80 km	RZ-DQPSK & Pol. Multiplexing	**3.2 b/s/Hz**	Bell Labs [10]	Highest capacity& efficiency
20.4 Tb/s (111Gb/s)	**102 (100 GHz spacing)**	3×80 km	CSRZ-DQPSK & Pol. Multipl.	2 b/s/Hz	NTT [11]	Widest optical spectrum
2 Tb/s (10Gb/s)	100	49×**150** km	RZ-DPSK	60%	Tyco [14]	Long repeater spacing
1 Tb/s (55.5Gb/s)	10 **(50GHz spacing)**	25×95 km	RZ-DQPSK & Pol. Multiplexing	2 b/s/Hz	Coreoptics Siemens [12]	For 100G Ethernet
1 Tb/s (107Gb/s)	10 (200 GHz spacing	6×80 km	**NRZ-OOK**	50%	Alcatel-Lucent [13]	For 100G Ethernet 100G ETDM

DQPSK is a multi-level format of DPSK, and its constellation diagram and example waveform are presented in Fig. 2.9. Each symbol of a DQPSK signal carries two bits of information. For instance, the phase difference of "0" may stand for bits 00, "$\pi/2$" for bits 01, "π" for bits 10, while "$3\pi/2$" for bits 11. The main advantage if DQPSK is its improved spectral efficiency of as twice as that of DPSK. However, the main difficulty of implementing DQPSK is that a set of complicated transmitter and receiver is required, and the frequency offset of the transmitter and receiver needs to be much smaller than binary DPSK [1,5,10,11]. Therefore, in terms of commercialization, DPSK is more promising in coming years.

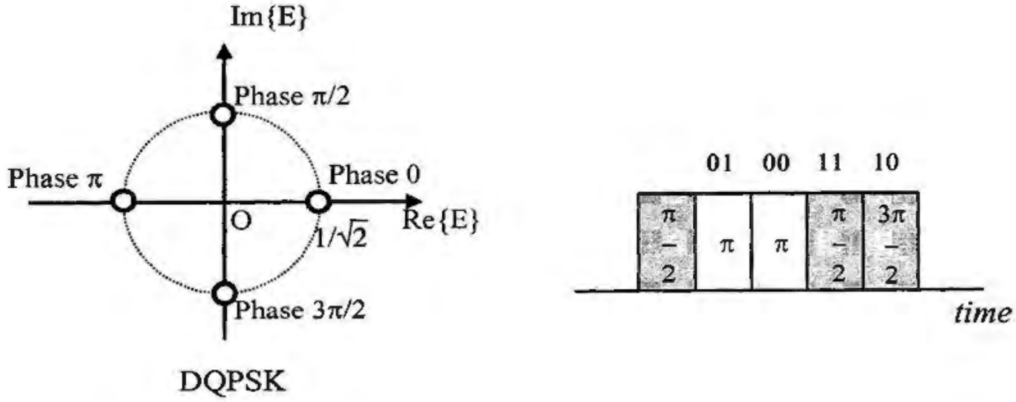

Fig. 2.9 Constellation diagram of an optical DQPSK signal and its example waveform.

2.2.2 Optical time division multiplexing (OTDM)

As another method to aggregate low-speed data signals into a high-speed signal, time division multiplexing (TDM) can be realized by electrical means (ETDM) or by optical means (OTDM). Only one wavelength carrier is required to carry the high-speed signal. At present, the first 40-Gb/s system based on ETDM has been installed, and the first 100-Gb/s ETDM has been experimentally demonstrated in laboratory [14]. However, the ultrahigh-speed electronics is still costly and beyond-100-GHz electronic technology is under development. Therefore, to achieve ultrahigh-speed multiplexing, OTDM is a good choice.

In an optical OTDM system, several optical signals at a bit rate B shares the same carrier frequency and are multiplexed optically to form a composite bit stream at the bit rate NB, where N is the number of channels. An OTDM transmitter can be designed based on the delay line technique, as shown in Fig. 2.10. The bit stream in the nth branch is delayed by $1/N$ of the pulse repetition rate. The output of all braches is then combined to form a composite OTDM signal. Therefore, the transmitter requires a light source generating optical pulse train at the repetition rate equal to the single-channel bit rate B. Generally the generated pulse width should be narrower than the OTDM bit period. Fig. 2.10 shows the whole system architecture of an OTDM system.

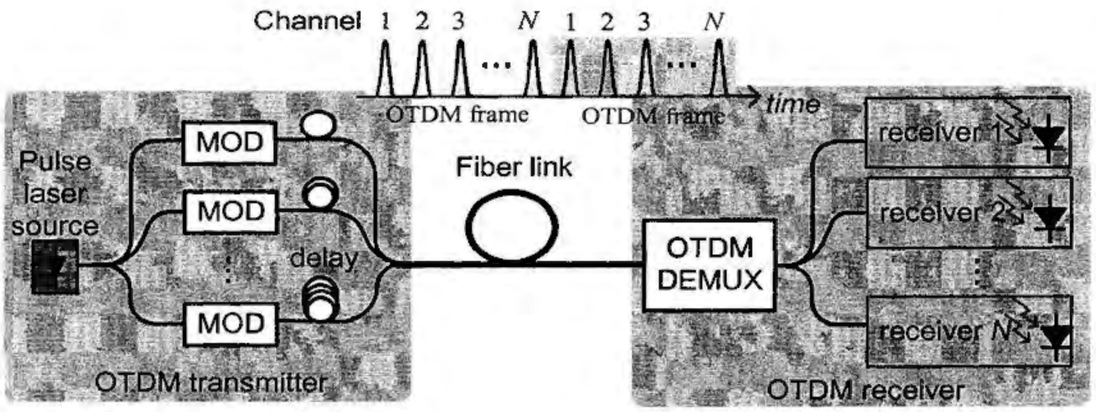

Fig. 2.10 OTDM system architecture. Inset shows an OTDM signal waveform.

Demultiplexing of an OTDM signal requires electro-optical or all-optical techniques. However, all of the demultiplexing techniques require a clock signal at the base repetition rate. Therefore, a clock recovery circuit is essential at the OTDM receiver. After the base-repetition-rate clock is recovered, it is used to control a fast switch gate to select the target demultiplexing channel. The process is shown in Fig. 2.11. As the electro-optical approach for the fast switch, the electro-absorption modulator (EAM) is an excellent candidate [15-18]. Compared with other electro-optical switches, it can realize very narrow switching window. Compared with all-optical approaches, using EAM is more economical, and the device is compact and of good controllability.

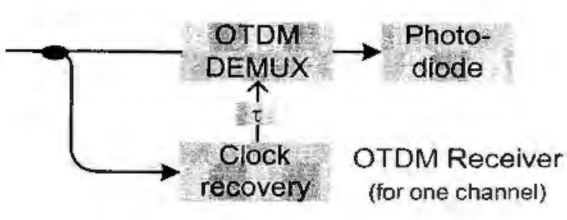

Fig. 2.11 An OTDM receiver consists of a clock recovery unit and an OTDM demultiplexer.

In spite of high cost and difficult control, all-optical OTDM demultiplexer has its advantages. It is capable achieving extremely narrow switching window. One all-optical technique makes use of a nonlinear optical loop mirror (NOLM) constructed by a fiber loop whose ends are connected to the two output ports of a 3-dB fiber coupler [19]. Alternatively, OTDM demultiplexing can also be achieved by using four-wave mixing (FWM) in a nonlinear medium [20], which actually serves as a logic AND operation between the recovered clock signal and the OTDM signal. The three kinds of OTDM demultiplexers mentioned above are depicted in Fig. 2.12.

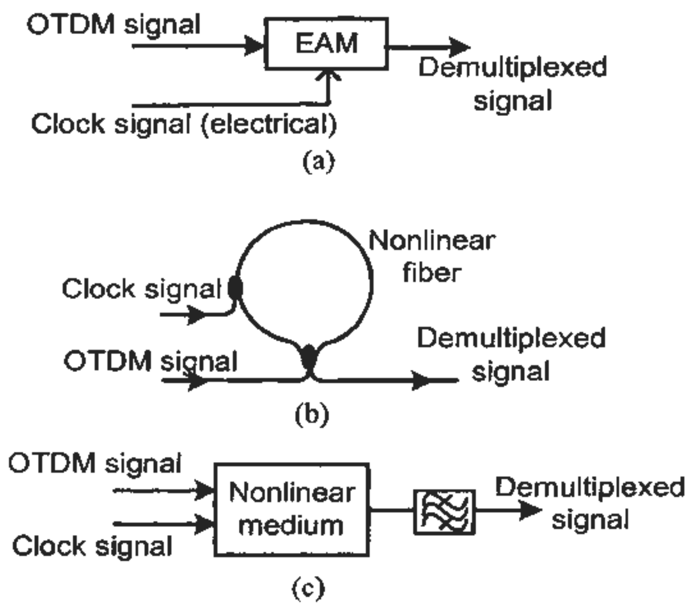

Fig. 2.12 OTDM demultiplexers based on (a) EAM, (b) NOLM, (c) FWM.

OTDM multiplexing, demultiplexing and transmission has been extensively studied for more than ten years. Major efforts were put into the OTDM systems at 80 or 160 Gb/s, since such systems can achieve stable and good performance of transmission and demultiplexing. Higher-bit-rate OTDM systems involve much more consideration and difficulty in demultiplexing and transmission. For demultiplexing, extremely narrow switching window and highly precise timing control should be guaranteed; for transmission, higher-order dispersion compensation should be adopted. There are also a lot of reports about 320-Gb/s or 640-Gb/s OTDM systems [19, 21, 22]. The highest bit rate realized by OTDM on a single wavelength is 1.28 Tb/s [23].

In early years, OTDM systems mainly adopted RZ-OOK as the modulation format. In recent years, OTDM systems based on RZ-DPSK, RZ-DQPSK have been reported [15-16]. It was observed that the system based on DPSK format had better performance than that on OOK format. Moreover, the waveform of a DPSK OTDM signal has a constant envelope, which can alleviate the possible patterning effect induced signal degradation. Patterning effect is the waveform distortion caused by pattern dependent system nonlinearity, for example, the pattern dependent gain of a semiconductor optical amplifier (SOA). It was reported that DPSK OTDM system could greatly reduce the penalty compared with OOK OTDM system, in a SOA based all-optical demultiplexer [24,25].

2.3 DPSK in Metropolitan and Access Networks

The above discussed optical backbone networks span interregional distances (1000 km or more) and provide large tributary connectivity between regional and metro domains, and therefore they are optimized for transmission. From the backbone network nodes, data traffic are delivered to relative regions around 10-100 km through metropolitan networks, or simply named metro networks. Metro networks today are based on synchronous optical network (SONET) or synchronous digital hierarchy (SDH) ring architectures. However, to achieve more bandwidth efficiency and low latency, packet based architecture will be the trend of next-generation networks. Recently, IP routing based framework has been proposed to support TDM-style guarantees in bandwidth, delay and loss, namely the multi-protocol label switching (MPLS) framework.

With the advent of high-speed communication networks, the ever-increasing number of subscribers and the emerging bandwidth-hungry applications lead to remarkably accruing traffic loads. Packet switching technology, potentially providing faster and more efficient routing and forwarding functionalities in networks, has attracted much research attention in recent years. MPLS has been emerging as one of the best candidates for packet switching framework. MPLS uses the technique of packet forwarding based on labels to enable the implementation of a simple high-performance packet-oriented engine. An extended version of MPLS is the generalized multiprotocol label switching (GMPLS) [26], which is suitable for optical connection-oriented networks.

Based on the concepts above, we can illustrate the procedure of optical label switching in the following. In such a network, the routing/forwarding information is transmitted together with the payload data, entitled as an optical "label" (a.k.a. "header"). When an optical packet is transmitted along an established label switched path (LSP), the routing information is distilled from the label at each intermediate core node where the payload is piloted to proceed with forwarding. On the other hand, the label should then be updated so as to successfully induct the next node's forwarding function. The whole procedure in an OLS network is described in Fig. 2.13.

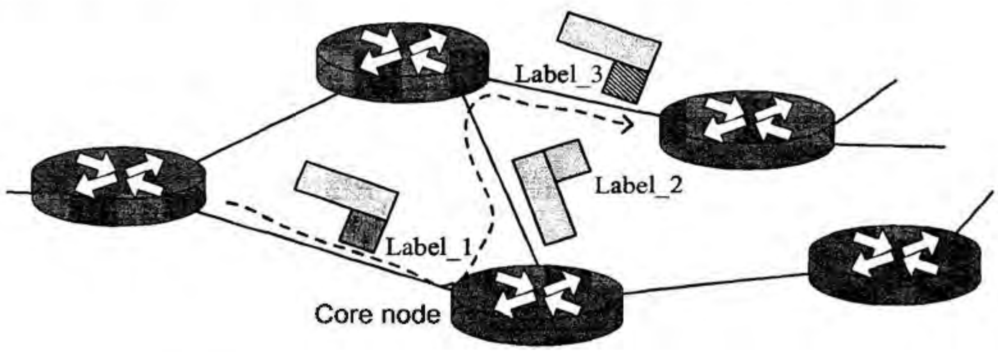

Fig. 2.13 The procedure of optical label switching in a MPLS network

Optical phase modulation, especially DPSK, as a promising modulation method in next-generation networks, has been widely employed in various OLS network proposals [27-32], which can be classified as follows. (1) In an optical packet, an optical phase modulated label is located before the payload in time, which is so-called bit-serial labeling scheme [28, 29]. (2) The optical label and payload are overlapped with each other in time, for example, the DPSK label superimposed on the OOK payload [30]. (3) Conversely, the label can be in OOK format superimposed on DPSK payload. The above two schemes are named orthogonal labeling [31, 32].

After the network traffic is transmitted from one central office (CO) to another via metro networks and backbone networks, it should be delivered to end users. The last one to several kilometers' reach is achieved by access networks. Current access solutions include: Modem, xDSL, Cable Modem, etc. For future scenarios, optical access and wireless access are quite attractive for their high capacity and flexibility. Optical local area networks are promising and play an important role as a wide-bandwidth access architecture [32].

As a matter of fact, the research of optical local area networks has been started in late 1980's. Several typical examples include LAMBDANET [33], RAINBOW [34], etc. All of them are broadcast-and-select networks supporting wavelength division multiplexing access (WDMA). Compared with the conventional connections via copper, optical access technology is capable of providing several tens and even hundred times bandwidth, solving the problems of the last mile bottleneck. Furthermore, optical local network infrastructure has some inherent properties suitable for multicast function, which meets the requirements of many access services.

In a typical passive optical access network (PON), downstream traffic is disseminated from an optical line terminal (OLT) to all optical network units (ONU) through a passive splitter at the remote node (RN). ONUs further deliver the downstream data to the subscribers via optical or electrical means. Furthermore, upstream traffic from the subscribers is carried back to the OLT to support interactive application and data networking. Among various PON architectures, the one using WDM technology is promising as the data traffic is delivered to each ONU via a designated distinct wavelength channel. If only one wavelength is allocated for one data channel, there must be two fiber lines between the OLT and the RN, each for the downstream data and the upstream data, respectively, to avert from Rayleigh back scattering induced signal degradation. Alternatively, $2n$ wavelengths in one fiber line can be employed, with n wavelength assigned for downstream channels and the rest assigned for the upstream channels. WDM-PON has the advantages of high capacity and easy handling.

DPSK format has been proposed to employ in optical access networks for over ten years. Optical signaling and network control is an important function in access architecture, and sometimes a control signal is designed to accompany with the main body of a data signal. The control signal and the data signal can be transmitted in a TDM manner, however, the effective bandwidth is reduced and the separation between them should be considered. Therefore, some researchers proposed to superimpose a DPSK control signal onto the OOK data signal, and thus the control signal can be easily processed [35].

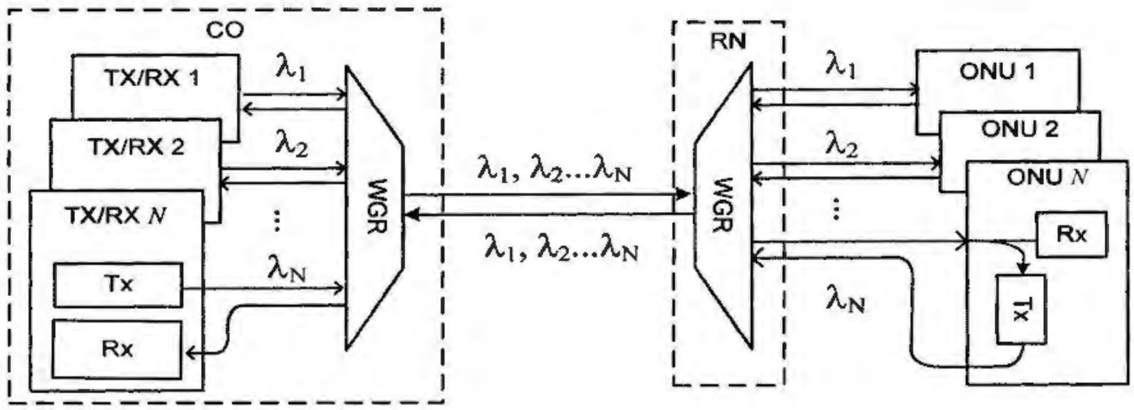

Fig. 2.14 The CLS WDM-PON architecture. CO: central office, RN: remote node, ONU: optical network unit, WGR: arrayed wavelength grating router.

In the future, a very attractive WDM-PON architecture may be the centralized-light-source (CLS) architecture [36-38]. In such a network as shown in Fig. 2.14, part of the downstream optical power is reused at the ONUs as the upstream data carrier and it is re-modulated with the upstream data. Light sources at the ONUs are thereby retrenched and not necessarily wavelength registered. A more important property of this architecture is that the upstream optical carrier in each channel has exactly the same wavelength with the downstream one, because of light reuse. Therefore, the upstream optical signals are expectedly routed through the same wavelength routers with the downstream ones, without any wavelength management troubles in traditional WDM-PON. Thus this architecture is a potentially robust and economical solution. DPSK has been proposed and demonstrated to serve as the downstream modulation format of the CLS WDM-PON [38]. Since an optical DPSK signal has constant intensity, the upstream data can be directly remodulated onto the same lightwave carrier, without any crosstalk. With the downstream DPSK signal, both the downstream and the upstream signals can achieve very good signal performance and there is no need of any processing at the ONU side.

References

[1] C. Xu, X. Liu, and X. Wei, "Differential phase-shift keying for high spectral efficiency optical transmitters," *Journal of Selected Topics in Quantum Electronics*, vol. 10, no. 2, pp. 281-293, 2004.

[2] P.A. Humblet and M. Azizoglu, "On the bit rate of lightwave systems with optical amplifiers," *Journal of Lightwave Technology*, vol. 9, pp. 1576-1582, 1991.

[3] G.P. Agrawal, *Fiber-Optic Communication Systems*, 3rd Ed, Wiley-Interscience, New York, pp. 250-253, 2002.

[4] L.G. Kazovsky, G. Kalogerakis and Wei-Tao Shaw, "Homodyne phase-shift-keying systems: past challenges and future opportunities," *Journal of Lightwave Technology*, vol. 24, no. 12, pp. 4876-4884, 2006.

[5] A.H. Gnauck and P.J. Winzer, "Optical phase-shifted keying transmission," *Journal of Lightwave Technology*, vol. 23, no. 1, pp.115-130, 2005.

[6] D.O. Caplan, M.L. Stevens and J.J. Carney, "High-sensitivity demodulation of multiple-data-rate WDM-DPSK signals using a single interferometer," in *Optical Fiber Communication Conference and Exposition and The National Fiber Optic Engineers Conference (OFC/NFOEC)* 2007, Anaheim, USA, paper OThD3.

[7] A.H. Gnauck, X. Liu, S. Chandrasekhar, X. Wei, "Optical duobinary format from demodulation of DPSK using athermal delay interferometer," *Photonics Technology Letters*, vol. 18, no. 4, pp. 637-639, 2006.

[8] I. Lyubomirsky, S. Shetty, J. Roman, and M. Y. Frankel, "Optimum 10-Gb/s NRZ receiver bandwidths for ultradense WDM transmission systems," *Photonics Technology Letters*, vol. 14, no. 6, pp. 870-872, 2002.

[9] L. Christen, Y.K. Lize, S. Nuccio, J.Y. Yang, P. Saghari, A.E. Willner and L. Paraschis, "Fiber Bragg grating balanced DPSK demodulation," *IEEE Lasers and Electro-Optics Society Annual Meeting (LEOS)* 2006, Montreal, Canada, paper WP2.

[10] A.H. Gnauck, G. Charlet, P. Tran, P. Winzer, C. Doerr, J. Centanni1, E. Burrows, T. Kawanishi, T. Sakamoto, K. Higuma, "25.6-Tb/s C+L-Band transmission of polarization-multiplexed RZ-DQPSK signals," in *Optical Fiber Communication Conference and Exposition and The National Fiber Optic Engineers Conference (OFC/NFOEC)* 2007, Anaheim, USA, paper PDP19.

[11] H. Masuda1, A. Sano, T. Kobayashi, E. Yoshida1, Y. Miyamoto, Y. Hibino, K. Hagimoto, T. Yamada, T. Furuta, H. Fukuyama, "20.4-Tb/s (204×111 Gb/s) transmission over 240 km using bandwidth-maximized hybrid Raman/EDFAs," in *Optical Fiber Communication Conference and Exposition and The National Fiber Optic Engineers Conference (OFC/NFOEC)* 2007, Anaheim, USA, paper PDP20.

[12] C. R. S. Fludger, T. Duthel, D. van den Borne, C. Schulien1, E-D. Schmidt, T. Wuth, E. de Man, G. D. Khoe, H. de Waardt, "10×111 Gbit/s, 50 GHz spaced, POLMUX-RZ-DQPSK transmission over 2375 km employing coherent equalisation," in *Optical Fiber Communication Conference and Exposition and The National Fiber Optic Engineers Conference (OFC/NFOEC)* 2007, Anaheim, USA, paper PDP22.

[13] K. Schuh, B. Junginger, E. Lach, G. Veith, "1 Tbit/s (10×107 Gbit/s ETDM) NRZ Transmission over 480km SSMF," in *Optical Fiber Communication Conference and Exposition and The National Fiber Optic Engineers Conference (OFC/NFOEC)* 2007, Anaheim, USA, paper PDP23.

[14] D. G. Foursa, A. Lucero, C.R. Davidson, J.-X. Cai, W. Anderson, Y. Cai, P.C. Corbett, W.W. Patterson, H. Li, M. Mazurczyk, M. Nissov, A. N. Pilipetskii, N. Bergano, " 2Tb/s (200x10Gb/s) data transmission over 7,300km using 150km spaced repeaters enabled by ROPA technology," in *Optical Fiber Communication Conference and Exposition and The National Fiber Optic Engineers Conference (OFC/NFOEC)* 2007, Anaheim, USA, paper PDP25.

[15] H.G. Weber, R. Ludwig, S. Ferber, C. Schimidt-Langhorst, M. Kroh, V. Marembert, C. Boerner, and C. Schubert, "Ultrahigh-speed OTDM transmission technology," *Journal of Lightwave Technology*, vol. 24, no. 12, pp. 4616-4627, 2006.

[16] J. P. Turkiewicz, E. Tangdiongga, G. Lehmann, H. Rohde, W. Schairer, Y.R. Zhou, E.S.R. Sikora, A. Lord, D.B. Payne, G.D. Khoe, H. de Waardt, "160 Gb/s OTDM networking using deployed fiber," *Journal of Lightwave Technology*, vol. 23, no. 1, pp. 225-235, 2005.

[17] F. Futami, S. Ono, S. Watanabe, "160-Gb/s optical demultiplexing with enhanced timing tolerance by unequally aligning pulse position," in *European Conference on Optical Communication (ECOC)*, paper We2.2.6, Glasgow, UK, 2005.

[18] E.S. Awad, P.S Cho, N. Moulton, J. Goldhar, "All-optical timing extraction with simultaneous optical demultiplexing from 40 Gb/s using a single electroabsorption modulator," *Photonics Technology Letters*, vol. 15, no. 1, pp. 126-128, 2003.

[19] A.I. Siahlo, A.T. Clausen, L.K. Oxenlowe, J. Seoane, P. Jeppesen, "640 Gb/s OTDM transmission and demultiplexing using a NOLM with commercially available highly non-linear fiber," *Conference on Lasers and Electro-Optics (CLEO)* 2005, paper CTuO1, Baltimore, USA.

[20] S.L. Jansen, M. Heid, S. Spalter, E. Meissner, C.-J. Weiske, A. Schopflin, D. Khoe, H. de Waardt, "Demultiplexing 160 Gbit/s OTDM signal to 40 Gbit/s by FWM in SOA," *Electronics Letters*, vol. 38, no. 17, pp. 978-980, 2002.

[21] N. Yamada, S. Nogiwa, H. Ohta, "640-Gb/s OTDM signal measurement with high-resolution optical sampling system using wavelength-tunable soliton pulses," *Photonics Technology Letters*, vol. 16, no. 4, pp. 1125-1127, 2004.

[22] A.I. Siahlo, J. Seoane, A.T Clausen, L.K. Oxenlowe, L.K.; P. Jeppesen, "320 Gb/s single-polarization OTDM transmission over 80 km standard transmission fiber," in *Optical Fiber Communication Conference and Exposition and The National Fiber Optic Engineers Conference (OFC/NFOEC)* 2005, Anaheim, USA, paper OFF3.

[23] M. Nakazawa, T. Yamamoto, K.R. Tamura, "1.28 Tbit/s-70 km OTDM transmission using third- and fourth-order simultaneous dispersion compensation with a phase modulator," *Electronics Letters*, vol. 36, no. 24, pp. 2027-2029, 2000.

[24] K. Chan, C.K. Chan, L.K. Chen, F. Tong, "Mitigation of pattern-induced degradation in SOA-based all-optical OTDM demultiplexers by using RZ-DPSK modulation format," *Photonics Technology Letters*, vol. 15, no. 9, pp. 1264-1266, 2003.

[25] Y.C. Ku, K.Chan, C.K. Chan, L.K. Chen, "Patterning effect avoidance of SOA-based demultiplexer in 80-Gb/s OTDM system using RZ-DPSK modulation format," *Opto-Electronics and Communications Conference (OECC)* 2006, paper 7C1-4, Kaohsiung, Taiwan,

[26] "draft-ietf-ccamp-gmpls-architecture-07.txt", work in progress, Internet draft in www.ietf.org, 2003.

[27] D. J. Blumenthal, B. E. Olsson, G. Rossi, T. E. Dimmick, L. Rau, M. Masanovic, O. Lavrova, R. Doshi, O. Jerphagnon, J. E. Bowers, V. Kaman, L. A. Coldren and J. Barton, "All-optical label swapping networks and technologies," *Journal of Lightwave Technology*, vol. 18, no. 12, pp. 2058-2075, 2000.

[28] W. Hung, C.K. Chan, L.K. Chen, F. Tong, "A bit-serial optical packet label swapping scheme using DPSK encoded labels," *Photonics Technology Letters*, vol. 15, no. 11, pp. 1630-1632, 2003.

[29] N. Calabretta, G. Contestabile, A. D'Errico, E. Ciaramella, "All-optical label processor/erasure for label swapping of 12.5 Gbit/s spectrally separated bit-serial DPSK label and payload," *Electronics Letters*, vol. 41, no. 9, pp. 541-543, 2005.

[30] X. Liu, Y. Su, X. Wei, J. Leuthold, and R. Giles, "Optical-label switching based on DPSK/ASK modulation format with balanced detection for DPSK payload," paper Tu4.4.3, in *European Conference on Optical Communication (ECOC)*, Rimini, 2003.

[31] N. Deng, Y. Yang, C.K. Chan, W. Hung, and L.K. Chen, "Intensity-modulated labeling and all-optical label swapping on angle-modulated optical packets," *Photonics Technology Letters*, vol. 16, no. 4, pp. 1218-1220, 2004.

[32] C. Lin, K.L. Deng, and C.K Chan, "Broadband optical access networks", in *Conference on Lasers and Electro-Optics in Pacific Rim (CLEO/PR)*, Vol. 2, pp. II-256, 2001.

[33] M. S. Goodman, H. Kobrinski, M. P. Vecchi, R. M. Bulley, and J. L. Gimlett, "The LAMBDANET multiwavelength network: architecture, applications, and demonstrations," *Journal on Selected Areas in Communications*, vol. 8, no. 6, pp. 995-1004, 1990.

[34] E. Hall, J. Kravitz, R. Ramaswami, M. Halvorson, S. Tenbrink, and R. Thomsen, "The Rainbow-II gigabit optical network," *Journal on Selected Areas in Communications*, vol. 14, no. 5, pp. 814-823, 1996.

[35] M. Hickey and L. Kazovsky, "The STARNET coherent WDM computer communication network: experimental transceiver employing a novel modulation format," *Journal of Lightwave Technology*, vol. 12, no. 5, pp. 876-884, 1994.

[36] N. J. Frigo, P.P. Iannone, P. D. Magill, T. E. Darcie, M. M. Downs, B. N. Desai, U. Koren, T. L. Koch, C. Dragone, H. M. Presby, and G. E. Bodeep, "A wavelength-division multiplexed passive optical network with cost-shared components," *Photonics Technology Letters*, vol. 6, no. 11, pp. 1365-1367, 1994.

[37] N. Deng, C.K. Chan, L.K. Chen, "A centralized-light-source WDM access network utilizing inverse-RZ downstream signal with upstream data remodulation," *Optical Fiber Technology*, vol. 13, no. 1, pp.18-21, 2007.

[38] W. Hung, C.K. Chan, L.K. Chen, F. Tong, "An optical network unit for WDM access networks with downstream DPSK and upstream re-modulated OOK data using injection-locked FP laser," *Photonics Technology Letters*, vol. 15, no. 10, pp. 1476-1478, 2003.

[39] I.T. Monroy, E. van Breusegem, T. Koonen, J.J.V. Olmos,; J. van Berkel, J. Jennen, C. Peucheret, E. Zouganeli, "Optical label switched networks: laboratory trial and network

emulator in the IST-STOLAS project," *IEEE Communications Magazine*, vol. 44, no. 8, pp. 43-51, 2006.

3 A Novel OTDM Scheme with Hybrid Modulation Format

3.1 Demultiplexing issues of OTDM signals

With the ever-increasing demand on communication bandwidth, optical time division multiplexing (OTDM) is an effective approach to upgrade the capacity of each wavelength channel in current optical systems [1-8]. At the receiver side, an aggregated high-speed OTDM signal has to be time demultiplexed to the base channel rate before detection. All of the demultiplexing techniques require a clock signal at the base repetition rate. Therefore, a clock recovery circuit is essential at the OTDM receiver. Chapter 2 has introduced several OTDM demultiplexing approaches. Generally they can be classified into electro-optical approaches [1-4] and all-optical approaches [5-8]. For the former, the recovered electrical clock is used to control an electro-optical switch to extract the target demultiplexing channel; for the latter, the recovered clock is in optical domain and is used to control an all-optical switch, which is usually realized based on nonlinear effects in fiber or semiconductor devices.

Fig. 2.12 depicts an electro-optical demultiplexing scheme based on EAM and two all-optical schemes based on NOLM and FWM, respectively. Generally, although the latter ones could realize narrow switching window, the EAM based demultiplexer is more preferred in practice, because of its simpler configuration and better controllability. Moreover, EAM based demultiplexers may be the best choice for medium-bit-rate OTDM demultiplexing due to its proper width of switching window.

The switching window of an OTDM demultiplexer should have a reasonable width to avoid crosstalk from the adjacent channels and to have some tolerance against timing misalignment in demultiplexing. That is, the switching window cannot be either too wide or too narrow, as described in Fig. 3.1. Usually, EAM based demultiplexers can meet such requirements, as they offer switching window a little smaller than or comparable to the bit period of a medium-bit-rate OTDM signal [3,8,10]. Thus, even with a small amount of timing misalignment $\Delta\tau$ in demultiplexing, the signal pulse of the target demultiplexed channel can still be contained in the switching window. However, part of an adjacent bit may still be included in the misaligned switching window, and the target channel would be degraded due to the crosstalk from the adjacent channels.

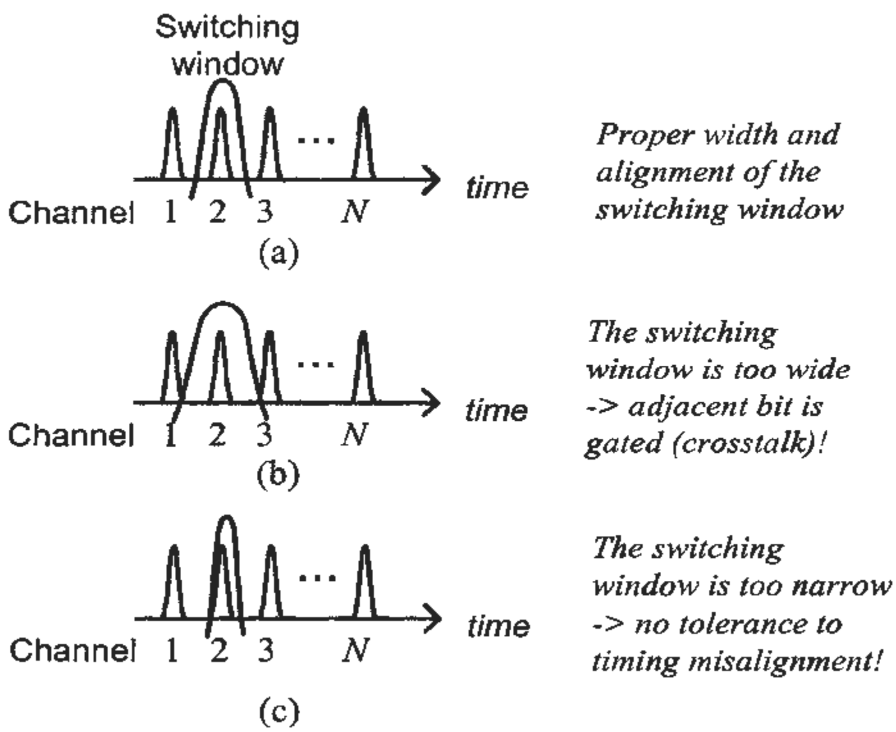

Fig. 3.1 Considerations on the switching window of OTDM demultiplexing. (a) a proper switching window. (b) If the switching window is too wide, part of the bit in the adjacent channel(s) may be gated and crosstalk occurs. (c) If the switching window is too narrow, there is no tolerance to any timing misalignment in demultiplexing. Most all-optical techniques can produce a relatively narrow switching window as (c) while EAM based demultiplexers have a switching window like (a) or (b).

To reduce the channel crosstalk due to timing misalignment in demultiplexing, a scheme was proposed by altering the pulse position of different OTDM channels [3]. The authors added an optical phase modulator (PM) and a dispersion medium in the OTDM demultiplexer, as shown in Fig. 3.2. The recovered clock was used to drive the

PM and it was well aligned with the incoming OTDM signal, such that it induced proper chirp to the OTDM pulses. With such properly induced chirp, after passing through the dispersion medium, the adjacent pulses of the target demultiplexing channel were de-centralized and the target switching window could be wider or have more timing misalignment. Although the experimental demonstration showed that the tolerance to timing misalignment could be enhanced, this scheme drastically increased the complexity and cost of the demultiplexer. Moreover, the recovered clock needed to well align with the incoming OTDM signal at the added PM, in which misalignment might also occur and thus make this scheme fail to work.

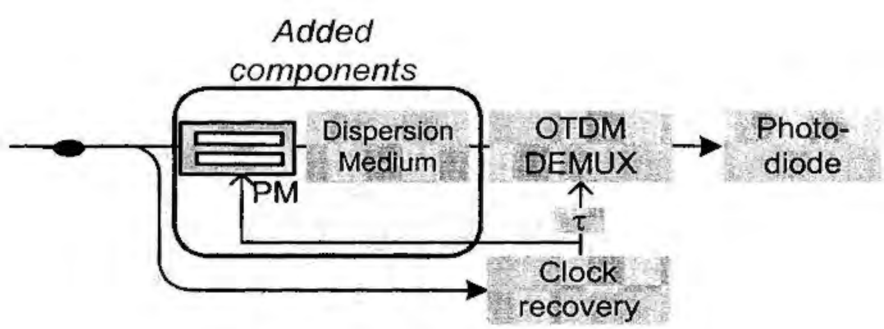

Fig. 3.2 A scheme to enhance the tolerance to demultiplexing timing misalignment, by adding an optical phase modulator (PM) and a dispersion medium at the demultiplexer [3].

Therefore, besides the significant increase of the cost and complexity, this scheme introduced one more timing alignment problem at the demultiplexer by adding some components. Other than altering the simplest EAM based demultiplexer, may we find another method to enhance the misalignment tolerance and improve the demultiplexing performance? The answer is yes. In our research, we propose a novel OTDM scheme to achieve this goal. Compared with the conventional OTDM scheme, the new scheme does not increase any complexity but greatly improves the demultiplexing performance.

3.2 Proposed OTDM scheme with hybrid modulation formats

Fig. 3.3(a) depicts the conventional OTDM scheme, in which all the channels are in the same modulation formats. A lot of work employed binary amplitude-shift keying (ASK), also known as on-off keying (OOK), as the signal modulation format [3-7]; while some recent reports employed DPSK as the modulation format [1, 2, 8].

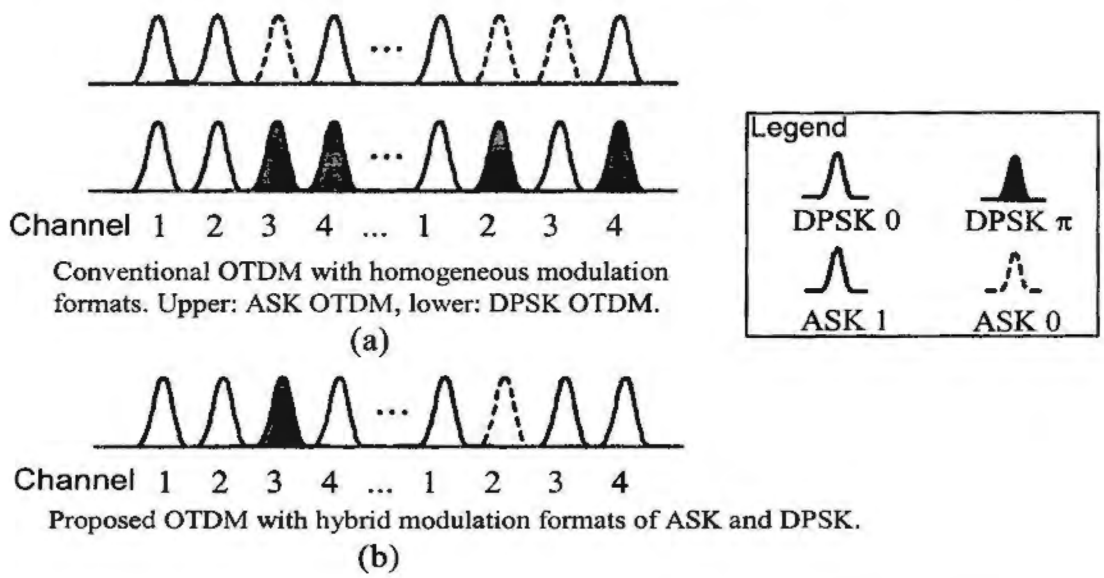

Fig. 3.3 Example waveforms of (a) conventional OTDM with homogeneous modulation format (either RZ-ASK or RZ-DPSK), (b) our proposed OTDM scheme with hybrid RZ-ASK and RZ-DPSK formats.

We propose a novel OTDM scheme with hybrid ASK channel and DPSK channel signals. An example of the waveform based on the hybrid OTDM is shown in Fig. 3.3(b). With these two different modulation formats, the performance degradation induced by crosstalk from adjacent channels in a hybrid OTDM is much less than that in a conventional OTDM signal with homogeneous modulation formats. Therefore, the demultiplexing performance can be greatly enhanced and the requirement on the control circuit can be relaxed. In the following we explain the principle of operation.

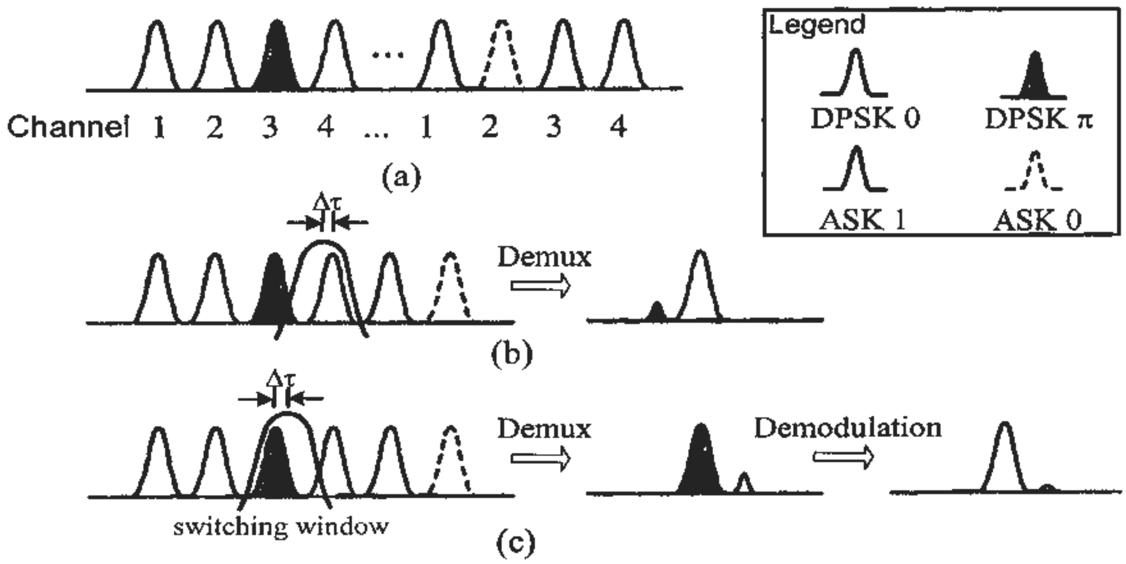

Fig. 3.4 Proposed OTDM with hybrid modulation formats and its demultiplexing in case of timing misalignment. (a) an example waveform, (b) demultiplexing of an ASK channel, (c) demultiplexing of a DPSK channel, in case of timing misalignment.

In our proposed hybrid OTDM scheme, every even channel is in RZ-ASK format while every odd channel is in RZ-DPSK format, as illustrated in Fig. 3.4(a). In other words, the RZ-ASK channels are interleaved with the RZ-DPSK channels. One of the main advantages of this hybrid OTDM system is that every channel suffers much less crosstalk induced error from its two adjacent channels, in case of improper demultiplexing. Fig. 3.4(b) shows the demultiplexing of an RZ-ASK channel in which the time gating (switching window) has some timing misalignment. The width of the switching window is comparable with a bit period. With some timing misalignment, part of the signal in the adjacent channel is also gated in the window. In a conventional ASK OTDM case (all channels in ASK format), the gated adjacent bit may have no power (ASK "0") or may have some power (ASK "1"). This crosstalk causes the target channel to become having multiple levels, which would induce significant errors in detection. However, for an ASK channel in the proposed hybrid OTDM case, the gated adjacent DPSK bit always have the same power, which would not lead to crosstalk induced erroneous decision. Similarly, for a DPSK channel, demultiplexing with timing misalignment will gate part of the adjacent ASK bits.

However, in the process of DPSK demodulation, the gated part of the ASK bit will destructively interfere with that of its previous bit. After the demodulation, the gated power of the ASK bit will disappear or become as little as a quarter of its original power, depending whether its two consecutive bits are the same or not. Therefore, the DPSK channel demodulation process can greatly alleviate the crosstalk from the adjacent ASK channel.

3.3 Enhanced tolerance to timing misalignment in 40-Gb/s OTDM demultiplexing

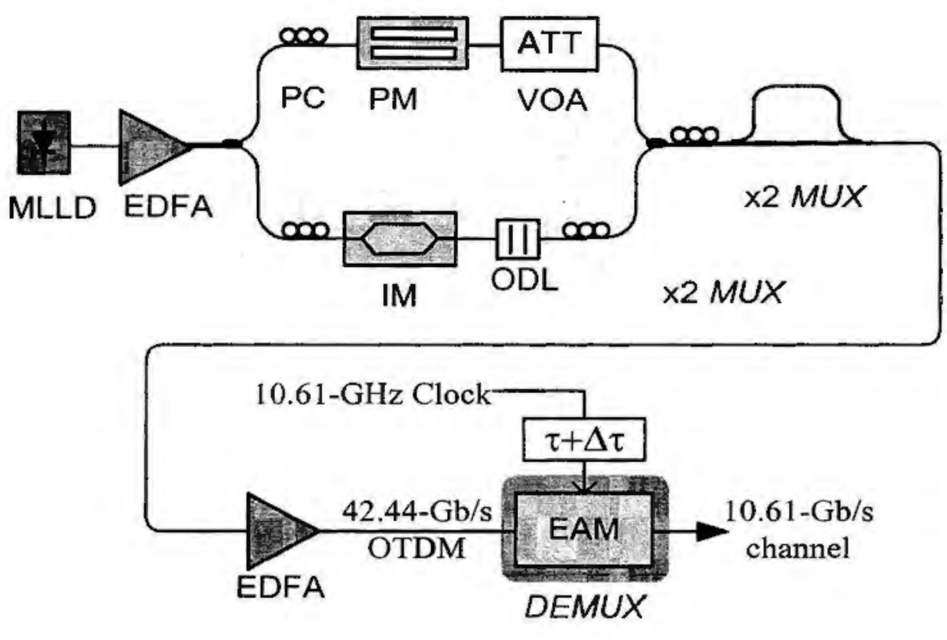

Fig. 3.5 Experimental setup of 42.44-Gb/s hybrid OTDM demultiplexing. MLLD: mode-locked laser diode; PM: phase modulator; EDFA: Erbium doped fiber amplifier; VOA: variable optical attenuator; ODL: optical delay line; PC: polarization controller; EAM: electro-absorption modulator.

We first carry out a 42.44-Gb/s to 10.61-GTb/s demultiplexing experiment to show the effectiveness of the proposed hybrid OTDM in enhancing the demultiplexing misalignment tolerance. Fig. 3.5 depicts the experimental setup. A semiconductor mode-locked laser diode (MLLD) generated an optical pulse train with a pulse width of about 1.5 ps (FWHM) at a repetition rate of 10.61 GHz. After power boosting, it was separated and modulated by decorrelated patterns via an optical phase modulator and an intensity modulator, respectively to generate an RZ-DPSK and an RZ-ASK tributaries. The two channels were properly time multiplexed to 21.22 Gb/s via the tunable optical delay line (ODL). A polarization controller and a variable optical attenuator (VOA) were used, to assure the two tributaries having the same peak power and polarization. The hybrid OTDM signal was upgraded to 42.44 Gb/s via a second stage of multiplexer. After proper amplification, the 42.44-Gb/s was fed into an EAM, driven by a 10.61-GHz clock signal for demultiplexing. The switching window of the EAM demultiplexer was around 15 ps. The RZ-ASK channels were directly detected while the RZ-DPSK channels were first demodulated via a delay interferometer (DI) with a relative delay of 94.3 ps before single-ended detection.

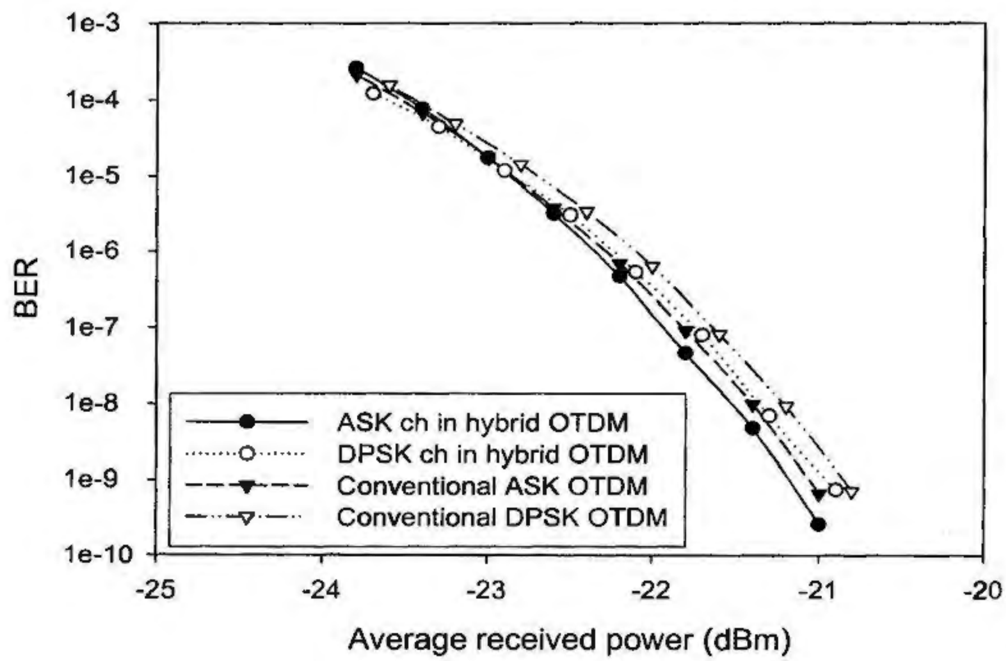

Fig. 3.6 BER of a demultiplexed ASK channel (●) and a DPSK channel (○) from the hybrid OTDM signal; and BER of a demultiplexed channel from the conventional ASK (▼) OTDM and DPSK (▽) OTDM, respectively.

We have measured the BER performance of the demultiplexed signals both in the 42.44-Gb/s hybrid OTDM and the conventional 42.44-Gb/s OTDM cases. The results are depicted in Fig. 3.6. For conventional OTDM using either ASK or DPSK, the four demultiplexed channels had similar performance, thus the respective BER of only one channel is plotted ("▼" for RZ-ASK OTDM case and "▽" for RZ-DPSK OTDM case), for clarity. In the hybrid OTDM case, the results for one demultiplexed RZ-ASK channel ("●") and one RZ-DPSK channel ("O") are plotted. It is found that all of them had very similar performance, which means the switching window extracted the target channel only and the demutiplexing timing is properly aligned. Under this condition, the demultiplexed channel suffered nearly no crosstalk from adjacent channels.

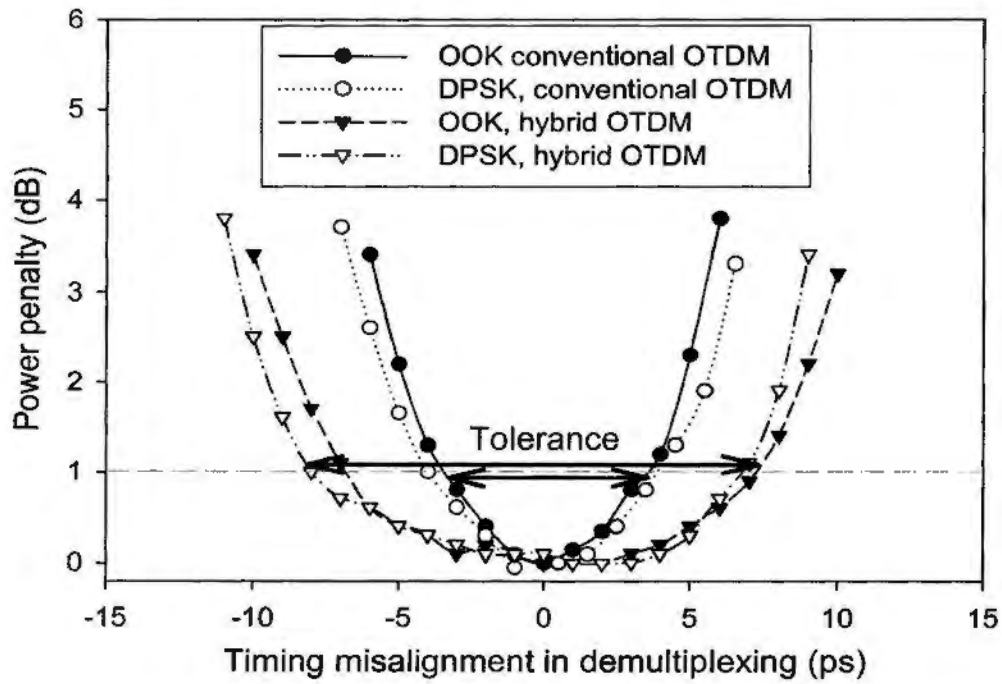

Fig. 3.7 The power penalty under the condition of timing misalignment, of a demultiplexed channel from a conventional RZ-OOK OTDM signal (●), a demultiplexed channel from a conventional RZ-DPSK OTDM signal (○), a demultiplexed OOK channel (▼) and a demultiplexed DPSK channel (▽) from a hybrid 42.44-Gb/s OTDM signal, respectively.

Fig. 3.7 depicts the measurements of the 42.44-Gb/s demultiplexing performance under the condition of timing misalignment. The 1-dB tolerance of timing misalignment was around 7 ps (from −3.5 ps to +3.5 ps), for either conventional pure RZ-OOK OTDM or RZ-DPSK OTDM, respectively. With our proposed hybrid OTDM scheme, the 1-dB tolerance for RZ-OOK channels was greatly enhanced to around 14.5 ps. The tolerance for RZ-DPSK channels also had an obvious enhancement to 15 ps.

To conclude this section, we have experimentally demonstrated 42.44-Gb/s demultiplexing, for both conventional OTDM and our proposed hybrid OTDM. In normal operation with proper switching window and timing alignment, the demultiplexing performance of the hybrid OTDM is similar with that of the conventional OTDM with homogeneous modulation format. In case of timing misalignment in demultiplexing, our proposed hybrid OTDM performed much better than the conventional one. The tolerance to timing misalignment was increased from around 7 ps (conventional OTDM case) to around 15 ps (hybrid OTDM case), that is, by more than one hundred percent.

3.4 Performance improvement in 80-Gb/s OTDM demultiplexing

Based on the operating principle described in Chapter 3.2, the enhancement of the demultiplexing performance using our proposed hybrid OTDM will be more significant in systems at bit rate higher than 40 Gb/s, since the requirement on the demultiplexing switching window is more stringent. In this section, we shall study the 80-Gb/s OTDM demultiplexing based on EAM.

Usually, an EAM-based demultiplexer has a relatively wide switching window, which may limit its demultipelxing performance. Generally, a 160-Gb/s (or 40-Gb/s) OTDM signal could be easily demultiplexed to its base rate 40 Gb/s (or 10 Gb/s) [2-4]. To realize higher-ratio 8:1 or 16:1 demultiplexing, some sophisticated measure should be taken into account [11-12], which requires either two sets of clock signals plus radio-frequency (RF) amplifiers or an expensive high-power RF amplifier with applied voltage exceeding the normal operation range of general commercial EAMs. In addition, the demultiplexer requires a complex and costly timing control circuit to guarantee the performance.

Without employing such sophisticated scheme, in this section, we experimentally demonstrate that our proposed hybrid OTDM can support 8:1 demultiplexing with an EAM based demultiplexer operated at normal condition. The success benefits from the demultiplexing performance improvement because of the enhanced tolerance to adjacent-channel crosstalk by using the hybrid OTDM approach. Fig. 3.8 shows the principle of the performance improvement by using hybrid OTDM. In a conventional OTDM signal, all channels employ either RZ-ASK or RZ-DPSK formats. However, in our proposed hybrid OTDM scheme, every even channel is in RZ-ASK format while every odd channel is in RZ-DPSK format, as illustrated in Fig. 3.8(a). In other words, the RZ-ASK channels are time-interleaved with the RZ-DPSK channels. Fig. 3.8(b) shows the 8:1 demultiplexing of an RZ-ASK channel in which the switching window covers not only the target demultiplexed channel but also part of its two adjacent channels (The switching window of an EAM at normal operation is between 1/4 and 1/8 of the base bit period). In a conventional ASK OTDM signal in which all channels are in RZ-ASK formats, such demultiplexing would induce severe crosstalk from adjacent channels and may severely deteriorate the target demultiplexed channel. However, for an ASK channel in our proposed hybrid OTDM signal, the crosstalk from adjacent channels are part of the adjacent DPSK bits, having the same amount of power for either DPSK "0" or "1". This is equivalent to add a small amount of constant power into the target ASK channel, which may alter the detection threshold but will not induce erroneous detection due to crosstalk from adjacent channels.

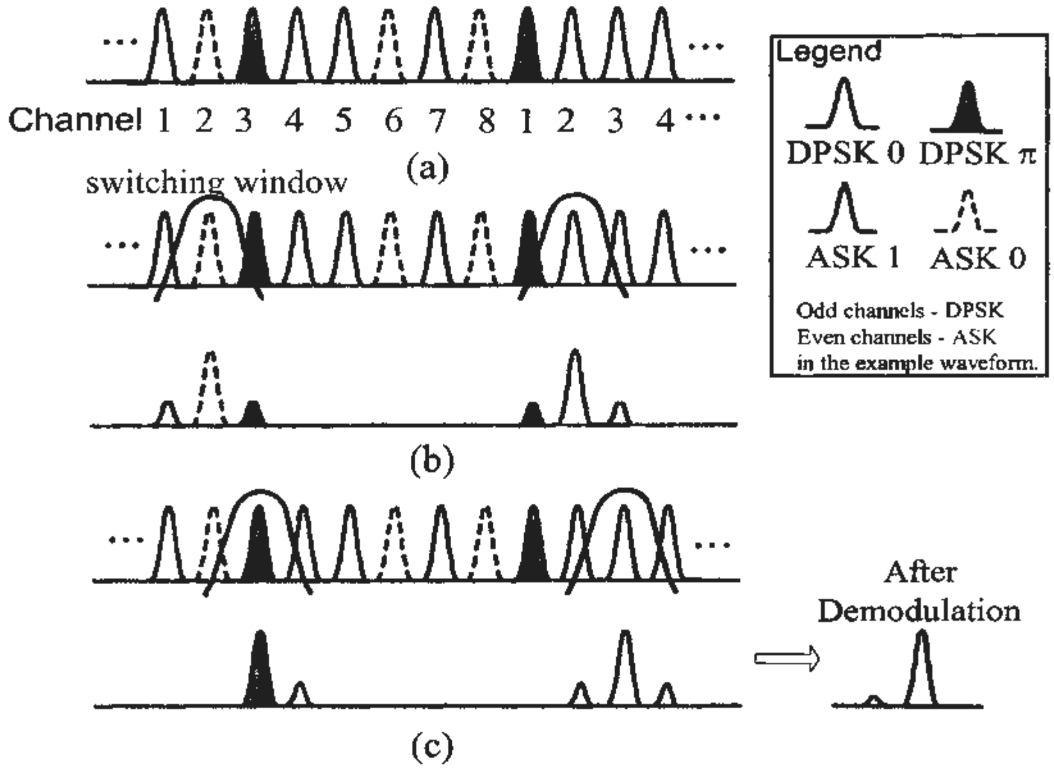

Fig. 3.8 (a) The signal format of the hybrid OTDM approach (8 channels), (b) demultiplexing of an ASK channel, (c) demultiplexing of a DPSK channel.

Similarly, for a DPSK channel in a hybrid OTDM signal, the demultiplexing will gate part of the adjacent ASK bits. However, after DPSK demodulation, the gated part of the ASK bit will destructively interfere with that of its previous bit. That is, the gated power of the ASK bit will disappear or become as little as a quarter of its original power, depending whether its two consecutive bits are the same or not, respectively. Therefore, the DPSK channel demodulation process can greatly alleviate the crosstalk from the adjacent ASK channels, as compared with the demultiplexing of a conventional RZ-DPSK OTDM signal.

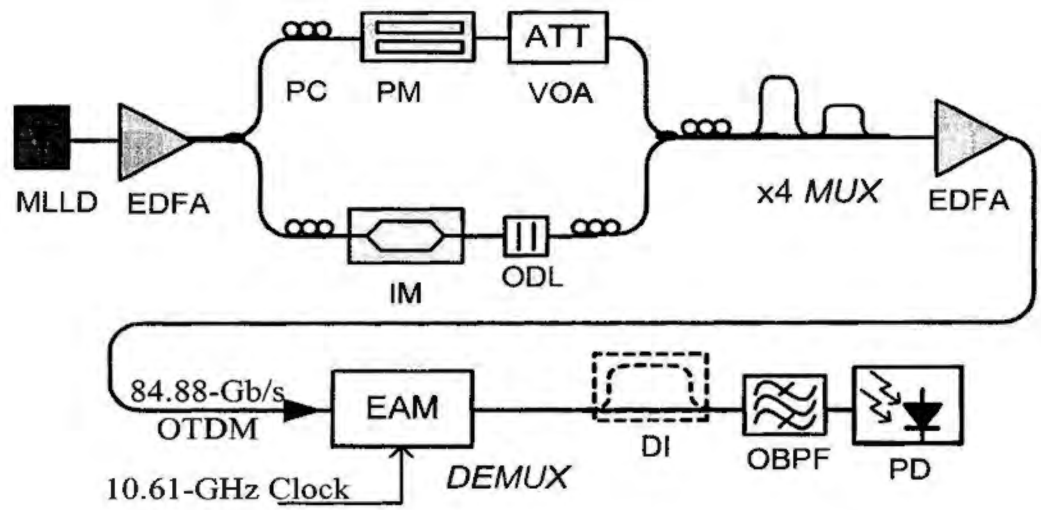

Fig. 3.9 Experimental setup. MLLD: mode-locked laser diode; EDFA: Erbium doped fiber amplifier; PC: polarization controller; PM: phase modulator; VOA: variable optical attenuator; IM: intensity modulator; ODL: optical delay line; EAM: electro-absorption modulator; DI: delayed interferometer; OBPF: optical bandpass filter; PD: photo-detector.

We have conducted an 84.88-Gb/s to 10.61-Gb/s demultiplexing experiment using the hybrid OTDM scheme. The experimental setup is similar with the previous one and is shown in Fig. 3.9. A semiconductor mode-locked laser diode (MLLD) generated 10.61-GHz pulse train (1.5-ps FWHM, pulse extinction ratio > 20 dB) was first separated into two braches. Then the two pulse trains were respectively phase modulated and intensity modulated by 10.61-Gb/s decorrelated 2^{31}-1 data patterns. The RZ-ASK signal was adjusted by a tunable optical delay line (ODL) to have a delay of 11.8 (or 94.3/8) ps, relative to the RZ-DPSK signal. A polarization controller and a variable optical attenuator (VOA) were used, to assure the two branches having the same peak power and polarization. Then the interleaved RZ-ASK/DPSK signal was 1:4 time-multiplexed to form an 84.88-Gb/s hybrid OTDM signal as shown in Fig. 3.10(a). After proper amplification, it was fed into a commercial EAM, driven by a 10.61-GHz clock signal for demultiplexing. The bias voltage for the EAM was –3.2 V and the RF peak-to-peak voltage was 6 V. The switching window of the EAM was measured to be around 15 ps (FWHM), which was wider than the bit period of the OTDM signal (11.8 ps). The demultiplexed RZ-ASK channels were directly detected while the RZ-DPSK channels were first demodulated via a delay interferometer (DI) with a relative delay of 94.3 ps before single-ended detection.

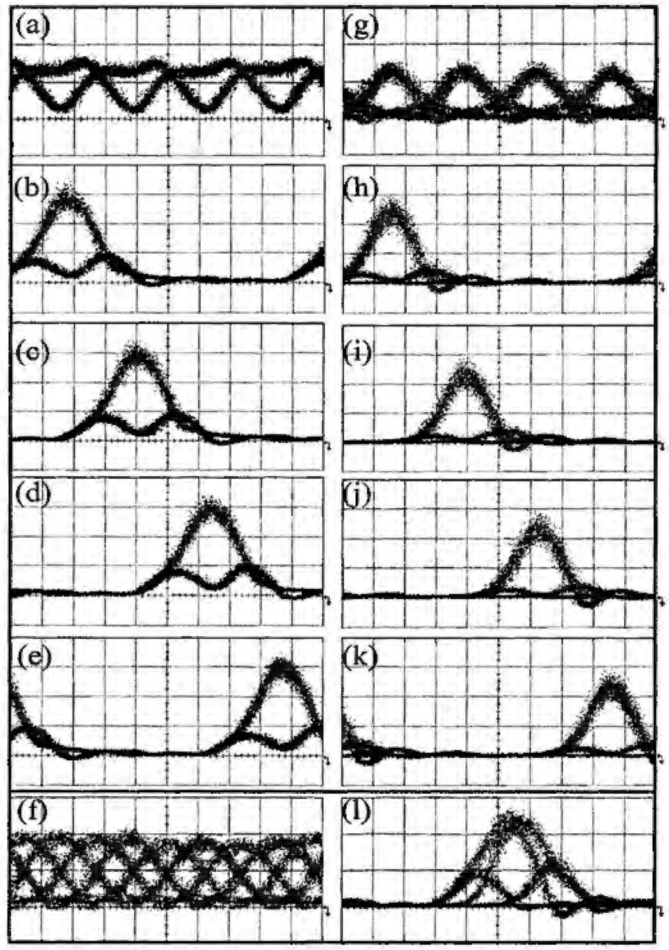

Fig. 3.10 Eye diagrams of (a) the 84.88-Gb/s hybrid OTDM signal, (g) after DI, (b)-(e) four demultiplexed ASK channels, (h)-(k) four demultiplexed and demodulated DPSK channels, (f) an 84.88-Gb/s conventional ASK OTDM signal, (l) and one of its demultiplexed channels, all detected with a 50-GHz photodiode. Time scale: 10 ps/div.

Fig. 3.10(b)-(e) show the four demultiplexed ASK channels from the 84.88-Gb/s hybrid OTDM signal. We could observe the crosstalk from the adjacent DPSK channels but the eye is clearly open. As a comparison, Fig. 3.10(l) shows a demultiplexed ASK channel from an 84.88-Gb/s conventional OTDM signal (Fig. 3.10(f)), in which the crosstalk from adjacent channels severely distorted the eye and consequently degraded data detection. Similar distorted eye diagram was observed in the case of demultiplexing in a conventional DPSK OTDM signal, after DI demodulation. On the contrary, using our proposed hybrid OTDM, the eye diagrams of the demultiplexed and demodulated DPSK channels from our proposed hybrid OTDM were clearly open, as shown in Fig. 3.10(h)-(k). Again we could see the greatly enhanced tolerance to the adjacent crosstalk by employing hybrid OTDM signals.

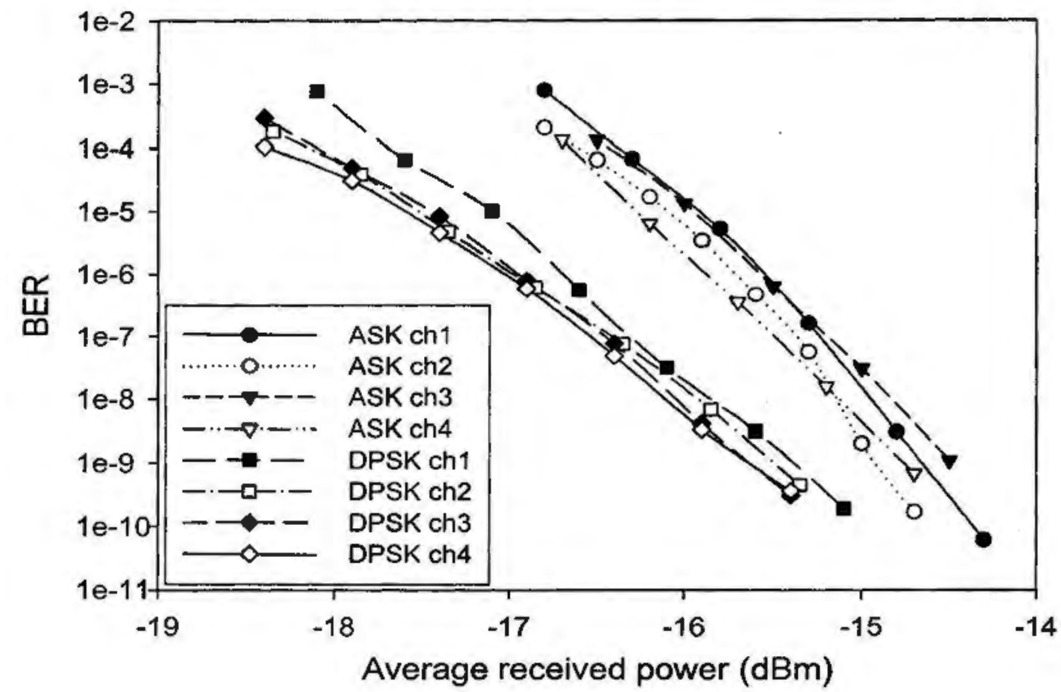

Fig. 3.11 BER measurements of four ASK and four DPSK channels demultiplexed from the 84.88-Gb/s hybrid OTDM signal.

We have measured the bit error rates (BER) of the eight 10.61-Gb/s demultiplexed channels from the hybrid OTDM signal, as shown in Fig. 3.11. Although they had around 4-dB penalty due to the wide demultiplexing switching window, compared with a 10.61-Gb/s back-to-back signal, all channels could achieve error free detection (BER<10^{-9}). Comparatively, we also attempted to measure the demultiplexing performance of conventional ASK or DPSK OTDM signals, using the EAM with the same operation condition. However, synchronization loss occurred and BER could not be measured. This showed that hybrid OTDM can greatly enhance the demultiplexing performance against the adjacent-channel crosstalk. In Fig. 3.11, DPSK channels showed a little better receiver sensitivity than ASK channels, which agreed with the eye diagram performance, as shown in Fig. 3.10.

In summary for this section, by employing our proposed novel OTDM scheme with hybrid RZ-ASK and RZ-DPSK modulation formats, we have demonstrated that it could offer enhanced demultiplexing performance through a successful experiment of 80-Gb/s to 10-Gb/s demultiplexing, based on a commercial EAM operated at normal condition. On the contrary, 80-Gb/s to 10-Gb/s could not be demultiplexed by using conventional OTDM with the same EAM.

3.5 A two-channel hybrid OTDM system without demultiplexing

In this section, we investigate a special case of the hybrid OTDM system. We have demonstrated that using hybrid OTDM could greatly enhance the demultiplexing performance. In the following, we shall show that there is no need of demultiplexing at all for a two-channel hybrid OTDM system. Therefore, the hybrid OTDM approach provides a simple and cost-effective way to double the capacity of a wavelength channel without optical demultiplexing.

The two-channel ASK/DPSK hybrid OTDM signal format and its transmitter and receiver are depicted in Fig. 3.12. Two optical tributaries, one in ASK format while the other in DPSK format, are first individually generated at the same bit rate, say m b/s. Both of them are then time-interleaved, via an optical delay line circuit, to form an ASK/DPSK hybrid OTDM signal, at a doubled aggregate data rate of $2m$ b/s. At the receiver, no optical time demultiplexing technique is required to separate the two tributaries before simple direct detection at each tributary's bit rate of m b/s. In each detection time period ($1/m$ seconds), there are two bits present, one is RZ-ASK bit and the other is RZ-DPSK bit. As every RZ-DPSK bit has an optical pulse, and thus constant power in each detection period, simple direct detection at m b/s is equivalent to RZ-ASK signal detection with a degraded extinction ratio. On the other hand, if a delay interferometer (DI) is placed before the photodiode, the RZ-DPSK pulses would be demodulated and detected at *m* b/s. However, in addition to the demodulated RZ-DPSK pulses, the RZ-ASK pulse in the detection period would also lead to a residual pulse with power being 1/4 of the input pulse power if the ASK consecutive bits are not the same (that is, either "10" or "01") while no residual pulse would be present if the ASK consecutive bits are the same (that is, "11" or "00"). In this way, both tributaries could be detected without any optical time demultiplexing.

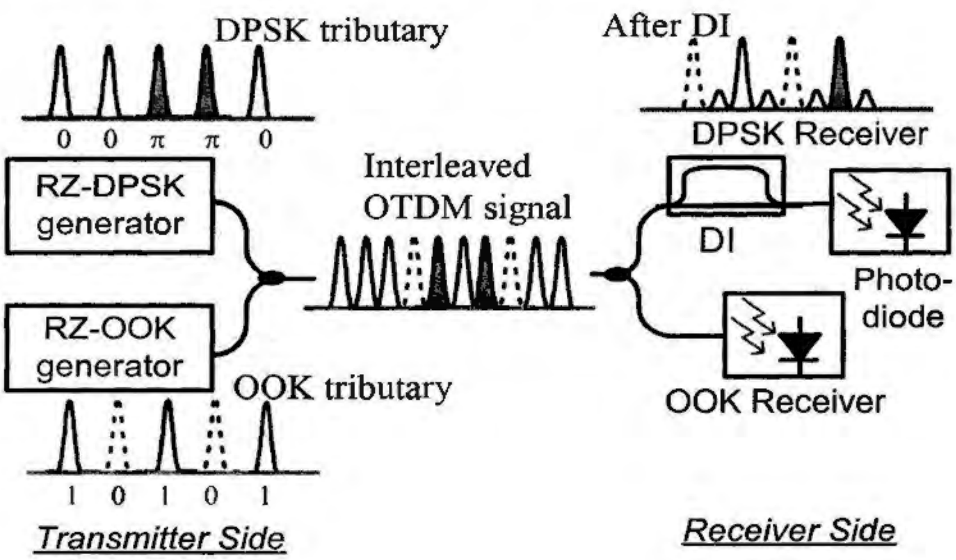

Fig. 3.12 Two-channel ASK/DPSK hybrid OTDM signal format and its transmitter and receiver.

We have experimentally investigated the generation and reception of such an ASK/DPSK hybrid OTDM signal. Transmission over a medium-range distance has also been demonstrated. A semiconductor mode-locked laser diode (MLLD) generated optical pulse train (wavelength 1554 nm, FWHM ~1.5 ps, repetition rate 10.61 GHz) were separated and modulated by decorrelated patterns via an optical phase modulator and an intensity modulator, respectively to generate the two individual RZ-DPSK and RZ-ASK tributaries. The choice of pulsewidth can be much broader as far as the pulses have no overlap after interleaving. A tunable optical delay line (ODL) was inserted to let the optical 10.61-Gb/s RZ-DPSK pulses properly time-interleave with the 10.61-Gb/s RZ-ASK signal pulses to form a 21.22-Gb/s hybrid OTDM signal. A polarization controller and a tunable optical attenuator were used, to assure the two tributaries having the same peak power and polarization. The hybrid OTDM signal was then amplified to around 0 dBm and was coupled into a piece of 40-km single mode fiber (SMF) with corresponding dispersion compensation. The ASK/DPSK interleaved signal is detected by the receiver unit as shown in Fig. 3.12. The delay interferometer (DI) used has a relative arm delay of 94.3 ps for DPSK demodulation.

Fig. 3.13(a) shows the back-to-back eye diagrams of the ASK/DPSK hybrid OTDM signal when a 50-GHz wideband p-i-n photodiode was employed. By direct detection using a 10-GHz p-i-n receiver, the RZ-ASK signal can be simply detected, as shown in Fig. 3.13(b). When the hybrid OTDM is passed through the DI, the RZ-DPSK signal is demodulated, as shown in Fig. 3.13(c). However, the RZ-ASK tributary signal may or may not contribute a residual pulse in each detection period, depending on its bit pattern, as discussed. As the RZ-DPSK signal dominates, it can be detected by using a 10-GHz p-i-n receiver, as shown in Fig. 3.13(d).

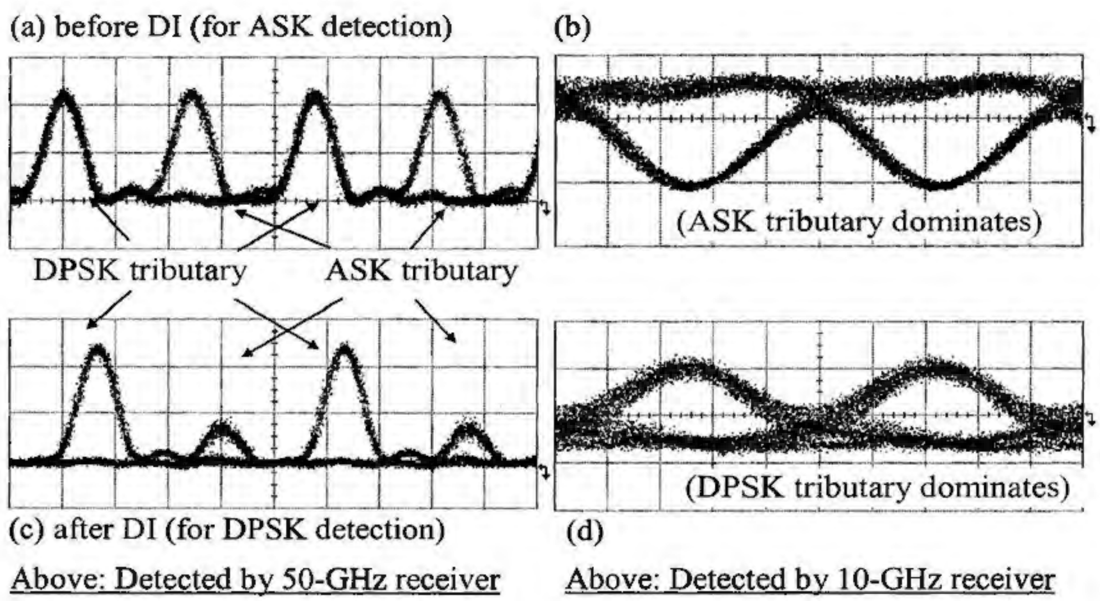

Fig. 3.13 Back-to-back eye diagrams of the ASK/DPSK hybrid OTDM signal detected by receivers with different electrical bandwidths. Time scale: 20 ps/div.

We have measured the bit error rate (BER) of the ASK/DPSK hybrid OTDM signal, as shown in Fig. 3.14. Both tributaries were modulated by $2^{23}-1$ pseudo random binary sequence, yet the two optical signals were decorrelated via ODL. The receiver unit shown in Fig. 3.12 was employed, and the received optical powers were measured before the p-i-n photodiodes. The back-to-back receiver sensitivities for the ASK and DPSK tributaries were measured to be around −16 and −19 dBm, respectively and error-free operation was achieved in both cases. There were about 4.5-dB or 1.5-dB power penalties compared with the measured conventional RZ-ASK or RZ-DPSK sensitivities, respectively. For the ASK tributary reception, the average power of the DPSK pulses, which was twice that of the ASK tributary, was counted into the received power of the ASK tributary signal. Therefore, two thirds of the received power was useless for ASK detection and led to degraded extinction ratio, which corresponded to ~4.5 dB of power penalty. Similarly, for DPSK reception, the power penalty could be attributed to the degraded eye due to the presence of the residual ASK pulse.

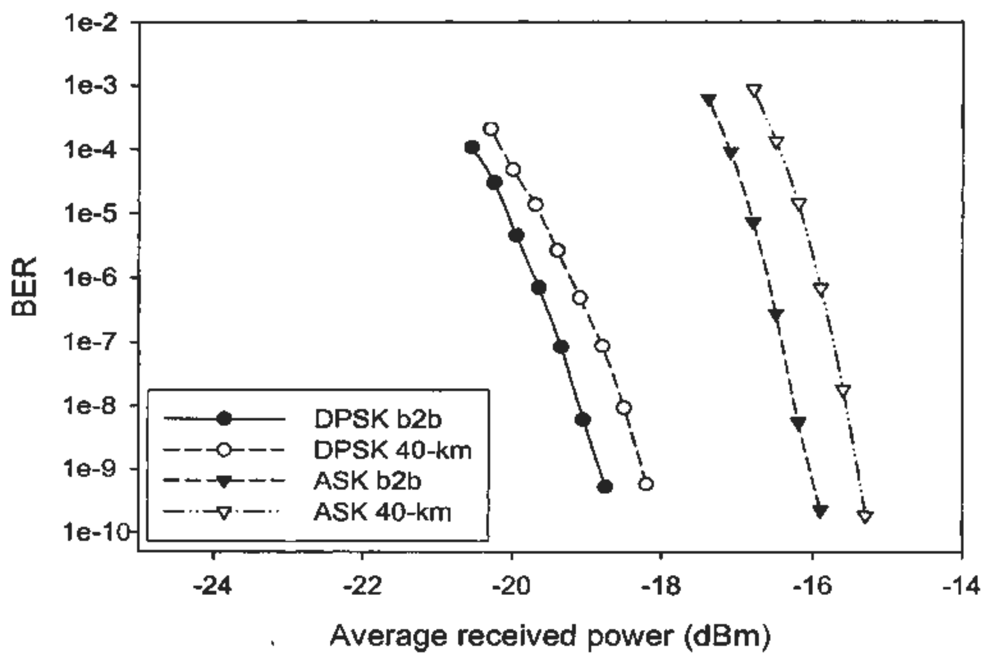

Fig. 3.14 BER measurements of the DPSK and ASK tributaries of a 21.22-Gb/s hybrid OTDM signal.

After 40-km transmission with corresponding dispersion compensation, both the received RZ-DPSK and RZ-ASK tributaries had a power penalty of about 0.5 dB, which might be caused by the wide spectrum of optical pulses and the residual fiber dispersion. In the above measurements, the two tributaries were evenly time-interleaved. It is expected that the detection performance depends on proper interleaving alignment of the two tributaries. Fig. 3.15 shows the measured power penalty of both tributaries under different interleaving misalignment. It is shown that the interleaving misalignment tolerances were around ±10 ps and ±20 ps for the RZ-ASK and the RZ-DPSK tributaries, respectively, at a 1.5-dB power penalty.

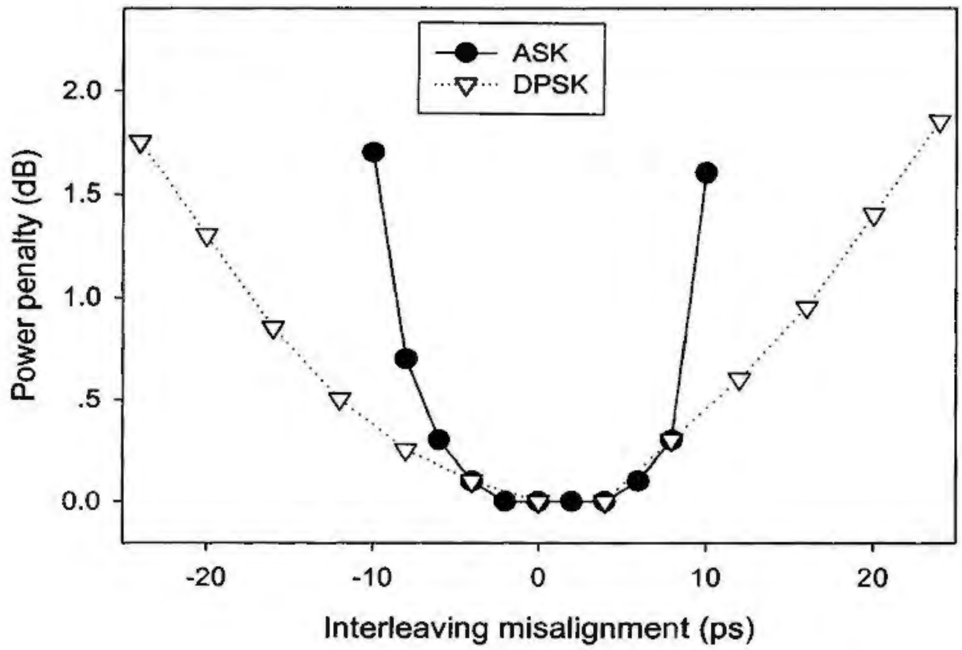

Fig. 3.15 Power penalty of the ASK and DPSK tributaries due to interleaving misalignment.

3.6 An application in label-switching networks

As introduced in Chapter 2, optical label switching (OLS) is an attractive approach to support low-latency and efficient packet routing and forwarding for future high-speed optical packet networks. In OLS networks, an optical label is encapsulated into every incoming optical packet at the ingress router to provide routing information for the next hop. Label swapping is performed at each core router to update the content of the label. Among various optical labeling schemes, optical differential phase-shift keying (DPSK) has been widely adopted as the labeling format [13-17]. In [13-14], the optical DPSK label was superimposed onto the optical on-off keying (OOK) payloads by means of orthogonal modulation. However, the extinction ratio of the OOK payload had to be reduced to optimize the performance of both the label and the payload. In [15-17], bit-serial return-to-zero (RZ)-DPSK labeling was proposed to guarantee the performance of both the label and the payload signals. However, this approach required careful adjustment of the guard band between the label and the payload. Moreover, dedicated optical processing might be required to separate the label and the payload at the core router [17].

In this work, we propose to employ the idea of hybrid OTDM in the application of optical labeling. We time interleave the optical RZ-DPSK label signal into the optical payload, instead of placing it in front of the payload. As the label is interleaved in the payload, the packet structure is more compact and thus the effective network bandwidth is improved. No guard band between the label and the payload is required. Both of the label and the payload signals can be detected without any time-division demultiplexing technique to separate the two signals. We have experimentally demonstrated optical packet generation at 21.22-Gb/s line-rate, with 10.61-Gb/s DPSK labels and 10.61-Gb/s OOK payloads. 40-km transmission and optical label swapping have also been demonstrated with small induced power penalty.

The proposed labeling scheme and the packet format are depicted in Fig. 3.16. Both the label and the payload signals are in RZ formats and are of the same tributary bit rates. Therefore, an optical RZ-DPSK label can be attached with an optical RZ-OOK payload by simply time-interleaving the label bits with the payload bits, via an optical delay line circuit. Such packet format can also be regarded as an optical time-division-multiplexed composite signal, with hybrid modulation formats of DPSK and OOK and at a doubled aggregate bit rate. The reception of such packet signal is simple and it requires no dedicated optical processing for separation of the label and the payload. The RZ-OOK payload tributary can be retrieved by directly detecting the composite packet signal at its tributary bit rate. The presence of an additional constant-intensity RZ-DPSK pulse in every tributary period only produces an offset to both the "zero" and the "one" bit levels of the RZ-OOK signal during power integration at the detector. Thus, by optimizing the detection threshold, good detection performance of the RZ-OOK payload can be achieved. On the other hand, a traditional optical DPSK receiver, comprising an optical delay interferometer (DI) and a photodiode, can be used to demodulate and detect the RZ-DPSK label tributary signal. In addition to the demodulated RZ-DPSK pulses, the RZ-OOK pulse at the destructive output port of the DI, in every detection time period, would lead to no pulse or a residual pulse with power being a quarter of the input pulse power [15], depending on its bit pattern.

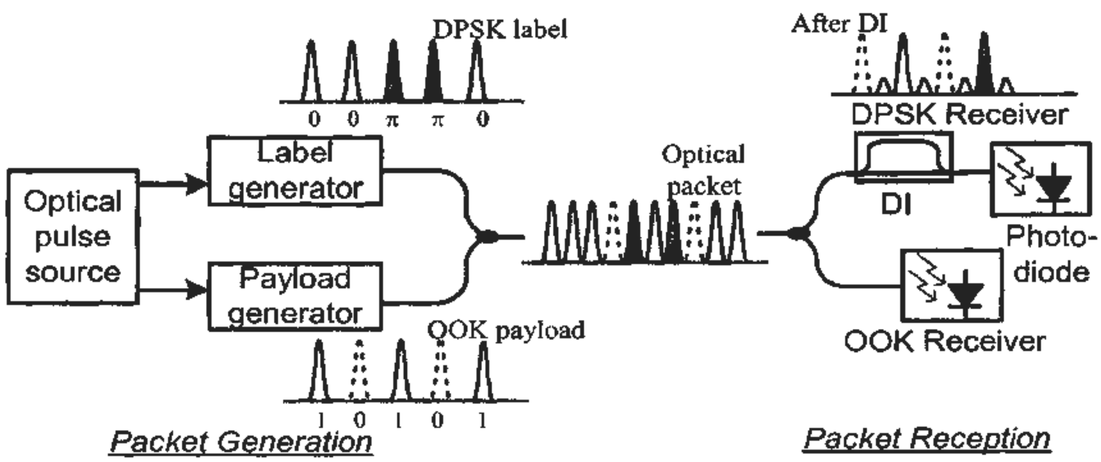

Fig. 3.16 The proposed DPSK-interleaved labeling scheme and the corresponding optical packet generator and receiver.

In the above description, every RZ-OOK bit is assumed to be accompanied by an RZ-DPSK bit, which means the payload might have the same length with the label. However, in a practical optical packet, the length of the label may be smaller than that of the payload. In this case we may attach a few unmodulated pulses to the original RZ-DPSK label to make the label have the same length as the payload, in order to assure packet reception with a stable performance. Another important issue in an optical packet-switching network is label swapping. According to the old label and the expected new label patterns, a control pattern can be computed, which is the binary exclusive-OR logical result between the old label and the new label. The control pattern is used to modulate the intensity of a locally generated optical pulse train at the label's pulse rate. This optical control signal will be used to modify the incoming optical RZ-DPSK label pulses via cross-phase modulation (XPM), thus this realizes all-optical label swapping, without any label/payload separation processing. Under proper operation conditions, only the phase of the DPSK label signal is changed; while both the intensity and the phase of the OOK payload can be preserved.

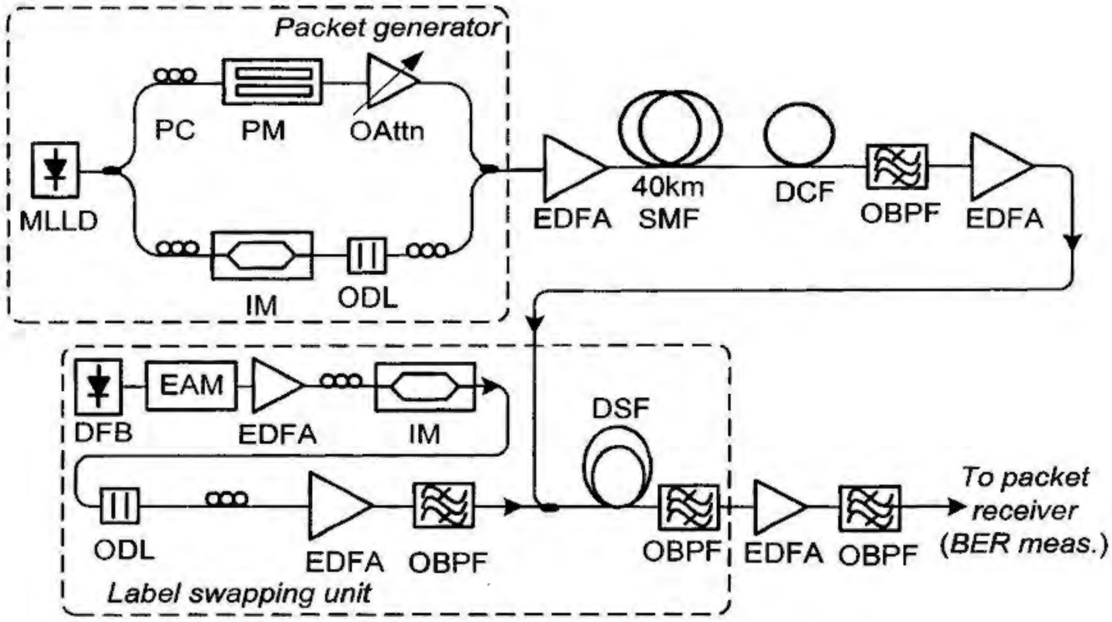

Fig. 3.17 Experimental setup. MLLD:mode-locked laser diode; PC: polarization controller; PM: phase modulator; OAttn: optical attenuator; IM: intensity modulator; ODL: optical delay line; EDFA: Erbium doped fiber amplifier; SMF: single-mode fiber; DCF: dispersion compensating fiber; OBPF: optical bandpass filter; DFB: distributed feedback laser; EAM: electro-absorption modulator; DSF: dispersion-shifted fiber.

Fig. 3.17 shows the experimental setup. A 10.61-GHz optical pulse train at 1554 nm and with a pulse-width of 1.5-ps FWHM was generated from a semiconductor mode-locked laser diode (MLLD). It was then split into two streams which were modulated via an optical phase modulator and an optical intensity modulator, respectively, for DPSK label and OOK payload generation. The choice of such narrow pulse-width was due to our equipment availability. Broader pulses would also work as far as the pulses have no temporal overlapping after interleaving in our proposed scheme. A tunable optical delay line (ODL) was inserted to let the 10.61-Gb/s RZ-DPSK label pulses interleave into the 10.61-GHz RZ-OOK payload pulses to form an optical packet signal. A polarization controller (PC) and a tunable optical attenuator (OAttn) were used, to guarantee the two signals to have the same polarization and peak power, respectively. The composite packet signal was amplified to around 0 dBm and was coupled into a piece of 40-km standard single mode fiber (SMF) with corresponding dispersion compensation.

All-optical label swapping for such an OOK/DPSK interleaved packet has also been experimentally demonstrated. A 10.61-GHz optical pulse train at 1545-nm and with 20-ps FWHM was encoded by the control pattern via an intensity modulator to form the local control signal. The optical intensity-modulated control signal was properly delayed to align with the incoming DPSK label pulses. It was amplified to about 20 dBm before being fed into a 4-km dispersion-shifted fiber (DSF) together with the 21.22-Gb/s OOK/DPSK interleaved packet signal for the recoding of the DPSK label signal via XPM. The label-recoded OOK/DPSK signal was then extracted by an optical bandpass filter (OBPF). At the receiver, the received OOK/DPSK packet signal was detected by the receiver unit, as shown in Fig. 1. The DI used had a relative arm delay of 94.3 ps.

We have measured the bit error rate (BER) of the OOK/DPSK interleaved signal, and the results are depicted in Fig. 4. Both the label and the payload signals were modulated by $2^{23}-1$ pseudo random binary sequence (PRBS). We employed the receiver unit shown in Fig. 1, and the received optical powers were measured before the 10-GHz p-i-n diode. The back-to-back receiver sensitivities for the OOK and the DPSK tributaries in the OOK/DPSK interleaved packet signal were measured to be around −16 and −19 dBm, respectively. The difference in the sensitivities is reasonable as the label information is usually regarded to be more critical and important in label-switching networks. There were about 4.5-dB or 1.5-dB of power penalty compared with the measured sensitivities of single RZ-OOK or RZ-DPSK signals, respectively. For the OOK tributary reception, the power of the DPSK pulses, which was twice of the OOK tributary average power, was counted towards the received power of the OOK tributary signal. Therefore, two thirds of the received power was useless for OOK detection, which was equivalent to about 4.5-dB power penalty. Similar explanation could be applied to the case of the DPSK tributary signal; however, the over-counted power was much less, thus led to smaller power penalty (1.5 dB).

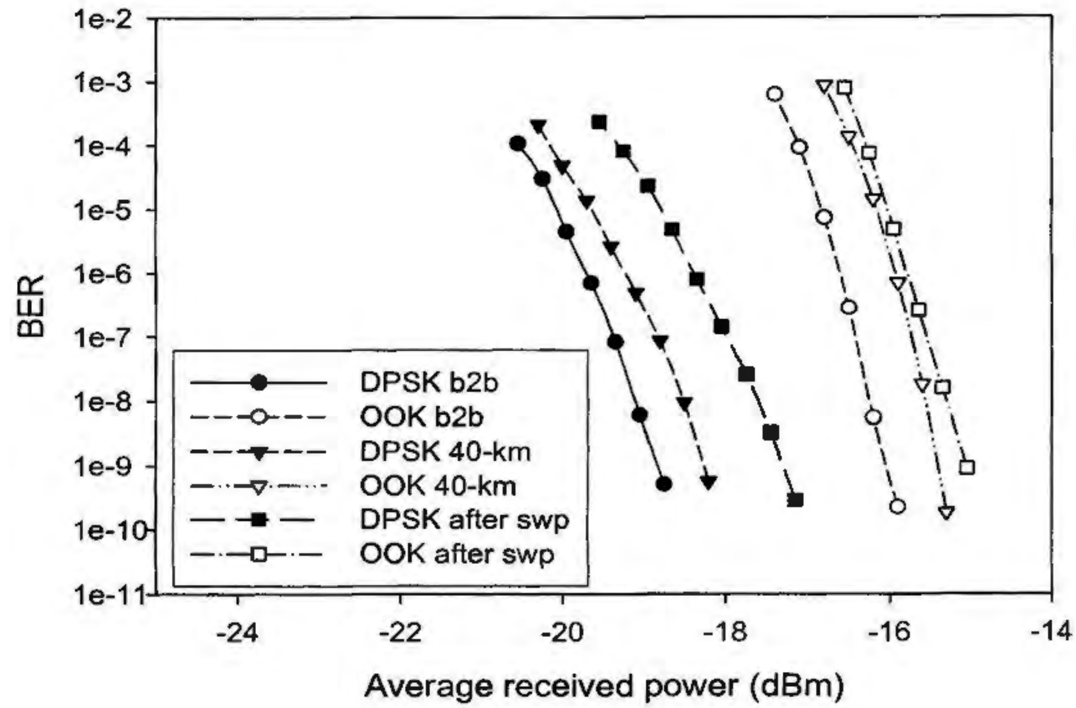

Fig. 3.18 BER measurements of the DPSK label and the OOK payload tributaries of a 21.22-Gb/s line-rate packet signal.

We then transmitted the 21.22-Gb/s OOK/DPSK interleaved packet signal over a piece of 40-km SMF with corresponding dispersion compensation. Both the DPSK label signal and the OOK payload signal suffered from a power penalty of about 0.5 dB, which might be caused by the wide spectra of optical pulses and the residual fiber dispersion. Next, we performed all-optical label swapping based on XPM. After the DPSK label signal was modified by the locally-generated control signal via XPM, the optical DPSK label was recoded, however, suffered from a power penalty of about 1 dB. The performance of the swapped label signal depended on both of the original DPSK label signal and the control signal. The incomplete (non-π) phase modulation or modification from either of the two signals would degrade the swapped label signal. The measurements also showed that the XPM-based label swapping resulted in negligible penalty on the OOK payload tributary. From the BER measurements, the OOK and DPSK interleaved signal was suitable for packet labeling and transmission in label-switching networks. In addition, such an interleaved signal has an optical pulse in each DPSK tributary period no matter the OOK bit is one or zero. This could avoid obvious power dynamics and thus would alleviate patterning effect of the packet signal in SOA-amplified networks, compared with the other labeling formats.

As the summary of the section, we have proposed and demonstrated to interleave an RZ-DPSK label signal into an RZ-OOK payload signal, to simplify the separation and detection of the label and the payload. No optical time division demultiplexing is needed to separate the label and the payload. The label and the payload data can be detected with their traditional receivers at tributary bit rate. The 20-Gb/s aggregate rate can be fully realized by 10-Gb/s components, without requirement to upgrade the speeds of the electrical and optical components at the transmitter or receiver. Experimental results showed good performance of such interleaved packet signal in transmission and all-optical label swapping via XPM. Furthermore, the nearly constant envelope of the OOK/DPSK interleaved signal can potentially alleviate patterning effect induced signal degradation.

3.7 Summary

We have proposed and experimentally demonstrated a novel OTDM scheme with hybrid modulation formats of ASK and DPSK, and studied its demultiplexing performance in detail. The multiplexer implementation of the hybrid OTDM is the same with that of the conventional OTDM, while the demultiplexing performance can be greatly improved. Therefore, this can significantly improve the simplicity and feasibility of OTDM systems. We have described the principle in the first part of this chapter.

Then, we experimentally demonstrated a 42.44-Gb/s OTDM demultiplexing. It showed that our proposed hybrid OTDM could enhance the tolerance to timing misalignment in demultiplexing by a factor of 2, compared with conventional OTDM with homogenous modulation formats. In addition, we successfully demonstrated hybrid OTDM demultiplexing using a commercial EAM demultiplexer operated at normal condition. On the contrary, 84.88-Gb/s demultiplexing based on conventional OTDM could not be realized using the same EAM with the same operating condition.

Again, this revealed that our proposed hybrid OTDM could enhance the tolerance to adjacent-channel crosstalk and thus improve the demultiplexing performance. Third, we demonstrated that a two-channel hybrid OTDM signal could be directly detected without demultiplexing. This can be used as a simple way to double the channel data rate without additional complexity. Finally, we reported an application of the hybrid OTDM in packet switching networks. With the RZ-DPSK label time interleaved in the RZ-OOK payload, compact packet signal and simple label/payload separation can be achieved. Optical labeling and label swapping were successfully demonstrated.

References

[1] H.G. Weber, R. Ludwig, S. Ferber, C. Schimidt-Langhorst, M. Kroh, V. Marembert, C. Boerner, and C. Schubert, "Ultrahigh-speed OTDM transmission technology," *Journal of Lightwave Technology*, vol. 24, no. 12, pp. 4616-4627, 2006.

[2] J. P. Turkiewicz, E. Tangdiongga, G. Lehmann, H. Rohde, W. Schairer, Y.R. Zhou, E.S.R. Sikora, A. Lord, D.B. Payne, G.D. Khoe, H. de Waardt, "160 Gb/s OTDM networking using deployed fiber," *Journal of Lightwave Technology*, vol. 23, no. 1, pp. 225-235, 2005.

[3] F. Futami, S. Ono, S. Watanabe, "160-Gb/s optical demultiplexing with enhanced timing tolerance by unequally aligning pulse position," in *European Conference on Optical Communication (ECOC)*, paper We2.2.6, Glasgow, UK, 2005.

[4] E.S. Awad, P.S Cho, N. Moulton, J. Goldhar, "All-optical timing extraction with simultaneous optical demultiplexing from 40 Gb/s using a single electroabsorption modulator," *Photonics Technology Letters*, vol. 15, no. 1, pp. 126-128, 2003.

[5] A.I. Siahlo, A.T. Clausen, L.K. Oxenlowe, J. Seoane, P. Jeppesen, "640 Gb/s OTDM transmission and demultiplexing using a NOLM with commercially available highly non-linear fiber," *Conference on Lasers and Electro-Optics (CLEO)* 2005, paper CTuO1, Baltimore, USA.

[6] S.L. Jansen, M. Heid, S. Spalter, E. Meissner, C.-J. Weiske, A. Schopflin, D. Khoe, H. de Waardt, "Demultiplexing 160 Gbit/s OTDM signal to 40 Gbit/s by FWM in SOA," *Electronics Letters*, vol. 38, no. 17, pp. 978-980, 2002.

[7] M. Nakazawa, T. Yamamoto, K.R. Tamura, "1.28 Tbit/s-70 km OTDM transmission using third- and fourth-order simultaneous dispersion compensation with a phase modulator," *Electronics Letters*, vol. 36, no. 24, pp. 2027-2029, 2000.

[8] K. Chan, C.K. Chan, L.K. Chen, F. Tong, "Mitigation of pattern-induced degradation in SOA-based all-optical OTDM demultiplexers by using RZ-DPSK modulation format," *Photonics Technology Letters*, vol. 15, no. 9, pp. 1264-1266, 2003.

[9] C. Schubert, J. Berger, S. Diez, H.J. Ehrke, R. Ludwig, U. Feiste, C. Schmidt, H.G. Weber, G. Toptchiyski, S. Randel, K. Petermann, "Compasison of interferometric all-optical switches for demultiplexing applications in high-speed OTDM systems," *Journal of Lightwave Technology*, vol. 20, no. 4, pp. 618-624, 2002.

[10] S. Kieckbusch, S. Ferber, H. Rosenfeldt, R. Ludwig, C. Boerner, A. Ehrhardt, E. Brinkmeyer, H.-G. Weber, "Automatic PMD compensator in a 160-Gb/s OTDM transmission over deployed fiber using RZ-DPSK modulation format," *Journal of Lightwave Technology*, vol. 23, no. 1, pp. 165-171, 2005.

[11] M.J. Guy, S.V. Chernikov, J.R. Taylor and D.G. Moodie, "Demonstration of the feasibility of dual frequency operation of an electroabsorption modulator for demultiplexing in a 16 channel 40Gbit/s OTDM system," *Electronics Letters*, vol. 32, no. 12, pp. 1138-1139, 1996.

[12] D.G. Moodie, A.D. Ellis, and C.W. Ford, "Generation of 6.3 ps optical pulses at a 10GHz repetition rate using a packaged electroabsorption modulator and dispersion compensating fiber," *Electronics Letters*, vol. 30, no. 20, pp. 1700-1701, 1994.

[13] T. Koonen, Sulur, I. T. Monroy, J. Jennen, H. Waardt, "Optical labelling of packets in IP-over-WDM networks," in *European Conference on Optical Communication (ECOC)*, Paper 5.5.2, 2002.

[14] N. Chi, L. Xu, L. Chritiansen, K. Yvind, J. Zhang, P. Holm-Nielsen, C. Peucheret, C. Zhang, and P. Jeppesen, "Optical label swapping and packet transmission based on ASK/DPSK orthogonal modulation format in IP-over-WDM networks," in *Optical Fiber Communication Conference (OFC)*, Paper FS2, 2003.

[15] W. Hung, C.K. Chan, L.K. Chen, F. Tong, "A Bit-Serial Optical Packet Label Swapping Scheme using DPSK Encoded Labels," *Photonics Technology Letters*, vol. 15, no. 11, pp. 1630-1632, 2003.

[16] D. Klonidis, R. Nejabati, C. Politi, M. O'Mahony, "All-Optical Packet Switching of 40Gb/s Variable Length Packets Using Dual-Pump FWM Controlled by Fast Tunable Laser," in *European Conference on Optical Communication (ECOC)*, paper Th1.6.2, Stockholm, Sweden, 2004.

[17] J .J. V. Olmos, I. T. Monroy, J. P. Turkiewicz, Y. Liu and A. M. J. Koonen, "Self-controlled all-optical label and payload separator for variable length bursts in a time-serial IM/DPSK scheme," *Photonics Technology Letters*, 17, pp. 1692-1694, 2005.

4 Optical Logic Gate for DPSK Signals based on FWM in SOA

4.1 All-optical XOR logic gate

In current and future optical digital communication systems and networks, the data rate per wavelength has been approaching the speed limitation of electronics. Thus, all-optical signal processing techniques are highly desirable to support the necessary optical switching functionalities in future ultrahigh-speed optical packet-switching networks. Moreover, all-optical signal processing can avoid cumbersome electrical-optical-electrical conversions, and thus can lead to transparent optical network nodes in spite of different electrical signal formats and protocols.

Since optical logic gate is the basic construction element for all-optical digital signal processing, it has been extensively studied in recent years. Among various logic functions including AND, OR, exclusive-OR (XOR), etc, optical XOR has been investigated most thoroughly, as it can realize many functions in packet data processing. Fig. 4.1 shows the truth table of a two-input XOR gate. The useful optical processing functions include data encoding and parity checking [1], label recognition and label swapping [2], advanced all-optical processing such as half-adder, full-adder, etc. [3]. Fig. 4.2 shows the function of label swapping and half-adder implemented with all-optical XOR logic gate. In the network node of an optical label switching network, the old optical label should be removed and a new optical label should be attached with the optical packet payload. With all-optical swapping based on XOR operation, the label removal and label rewrite can be accomplished in one step. A local pattern can be calculated by the network management unit, which is the XOR result of the incoming label and the new label. Then the incoming label and the local pattern are synchronized and fed into the all-optical XOR gate, and the output is exactly the new label. For all-optical half-adder, it is comprised of an all-optical XOR gate and an all-optical AND gate. This is an example of combination of different optical logic gate that is capable of advanced optical digital signal processing.

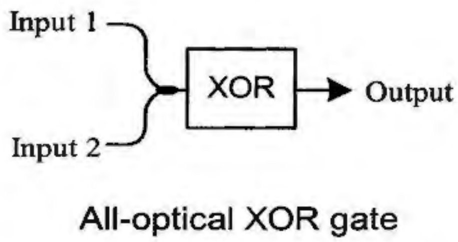

In1	*In2*	*Output*
0	0	0
0	1	1
1	0	1
1	1	0

Truth table

Fig. 4.1 Truth table of a two-input XOR gate.

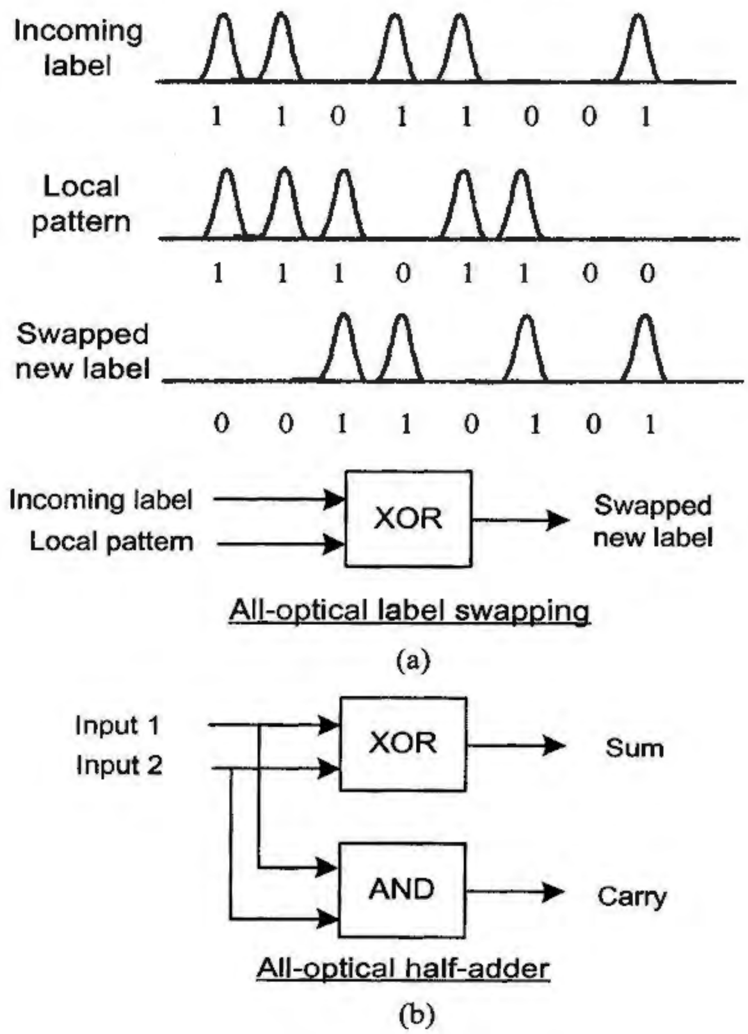

Fig. 4.2 All-optical digital signal processing circuits and applications based on XOR gate.

Previously, all-optical XOR gate was all designed for optical OOK modulation format. All the demonstrations were limited to two-input XOR gate. They were realized based on the nonlinearity in optical fiber or semiconductor optical amplifier (SOA). For example, all-optical XOR gate based on a nonlinear optical loop mirror (NOLM) has been demonstrated. However, its bulky size and poor power efficiency hindered its practicality. On the other hand, it could be realized by utilizing cross-gain modulation [2] and cross-polarization modulation [4] in a semiconductor optical amplifier (SOA), at 10- and 5-Gb/s signal speeds, respectively. Higher speed (at 20-Gb/s ~ 40-Gb/s) operation was reported by utilizing cross-phase modulation (XPM) in an SOA with differential inputs and in different configurations, including terahertz optical asymmetric demultiplexer (TOAD) [5], ultrafast nonlinear interferometer (UNI) [6], and SOA Mach–Zehnder interferometer (SOA-MZI) [7]. However, the data patterning effect in SOA always induced severe system degradations when the input signals were in on-off keying (OOK) format.

As discussed in previous chapters, DPSK or RZ-DPSK modulation format has been recently studied extensively for its higher tolerance against transmission impairments, improved receiver sensitivity with the help of balanced detection, reduced patterning effect induced degradation in high-speed optical systems, as well as its labeling function in optical packet switching networks. To cope with the wide use of optical phase modulated signals, all-optical XOR gates for RZ-DPSK signals are essential. In this project, we propose an all-optical XOR gate based on four-wave mixing (FWM) in an SOA with RZ-DPSK modulated input signals. In addition to its simplicity and alleviated patterning effect, it can potentially support much higher speed operation than the XPM-based schemes, since the intraband processes, such as carrier heating and spectral hole burning, leading to FWM have much shorter scattering time than the interband process [8-9]. Furthermore, compared with the previous schemes [1-7], our proposed XOR gate can accommodate three-input XOR operation in one unit. This feature is particularly suitable for multiple-input XOR operations such as full-adder and parity checking, to avoid too many cascaded XOR gates.

Before we report our proposed XOR logic gate for RZ-DPSK signals, we first give a brief introduction to FWM in SOA.

4.2 Four-wave mixing in semiconductor optical amplifier

Optical wave mixing refers to the nonlinear interaction among several optical waves in a medium. It is a kind of parametric process because it involves modulation of a medium parameter such as the refractive index. The origin lies in the nonlinear response of bound electrons of a material to an applied optical field. The polarization induced in the medium is not linear in the applied field but contains nonlinear terms whose magnitude is governed by the nonlinear susceptibilities [10-11]. Four-wave mixing (FWM) belongs to the third-order parametric process since the third-order susceptibility $\chi^{(3)}$ is responsible.

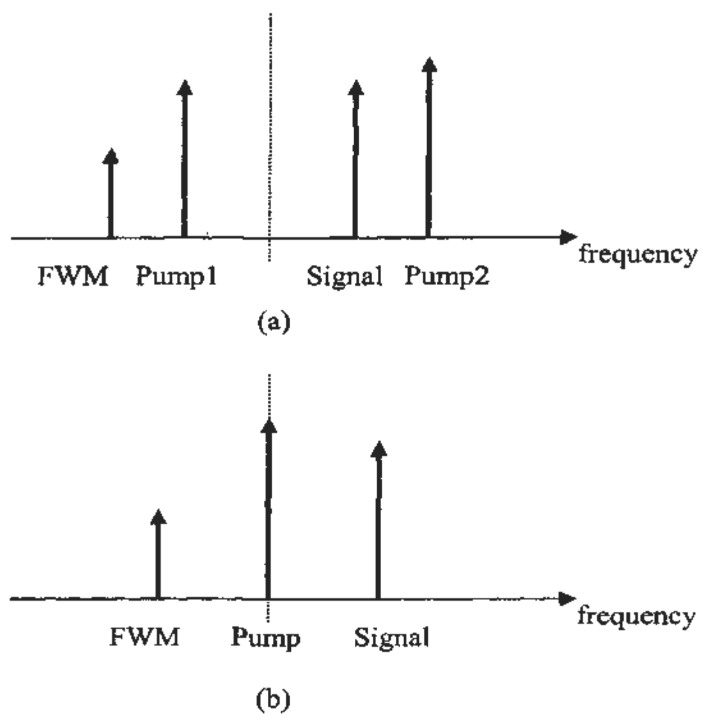

Fig. 4.3 Optical frequency of four-wave mixing process: (a) non-degenerate case, (b) partially degenerate case..

The physical process of four-wave mixing (FWM) can be understood as follows. When a light field containing multiple frequency components is applied to a nonlinear medium, it induces in the atoms or molecules of that medium electronic dipoles oscillating at the beat frequencies of the input field components. Any two input components can be considered to beat and drive the material excitations. The material excitation wave thus produced can mix with a third input component, yielding a nonlinear polarization at the resultant beat frequency. This nonlinear polarization field radiates electromagnetic energy, generating a coherent output at a fourth frequency, which is known as the FWM-produced light wave. This procedure is shown in Fig. 4.3.

In terms of optical frequency configurations, FWM can be classified into three major types: non-degenerate FWM, partially-degenerate FWM and degenerate FWM. Non-degenerate FWM (NDFWM) is the most general case, with three different input optical frequencies, as shown in Fig. 4.3(a). If two out of the three input frequencies are the same, the FWM is named partially-degenerate FWM, as in Fig. 4.3(b). If all the three frequencies are the same, degenerate FWM occurs. The material excitation at zero frequency leads to a static refractive index variation, which can cause a phenomenon known as self-phase modulation (SPM).

A number of physical mechanisms have been proposed to account for the process of four-wave mixing in semiconductor media. All are forms of electronic excitation. Beating between two input waves can result in carrier population pulsations, that is, the modulation of the carrier density at the beat frequency [12]. This is referred to as an interband process, because it is the total carrier population in the conduction band which is modulated. Four-wave mixing via carrier population pulsations is characterized by high conversion efficiency, but its 3-dB bandwidth is limited by the carrier lifetime to the order of a few gigahertz [12]. There are also two intraband modulation processes which are commonly associated with four-wave mixing in semiconductors. Intraband processes do not result in changes in the total carrier numbers, but in changes in the distribution of carriers in the conduction band.

Dynamic carrier heating [9] results from intraband processes which tend to increase the temperature of the carrier distribution above the lattice temperature. The most significant processes contributing to carrier heating are stimulated emission, which removes carriers from close to the band-edge, and free-carrier absorption which transfers carriers to higher energies in the bands. Spectral hole burning [9] is an intraband process which arises as a result of the finite time taken for carriers in the conduction band to establish a quasi-equilibrium Fermi distribution in the presence of strong fields which deplete carriers at particular energies. Many investigations have indicated that both carrier heating and spectral hole burning contribute to the optical nonlinearity of semiconductor materials. The intraband processes are characterized by extremely fast response times, and have a bandwidth into the terahertz range. However, they are less efficient sources of four-wave mixing than carrier population pulsations, which dominate the mixing process for input waves separated by up to a hundred gigahertz.

The modelling of FWM in travelling-waveguide SOA has been well established [8-13]. We shall summarize the basic results here to facilitate explaining our proposed XOR gate based on FWM in SOA. The configuration to be considered in the theoretical model is shown schematically in Fig. 4.4. The SOA is a travelling-wave device, with near-ideal AR coatings on the end facets such that the residual reflectivity can be neglected. The optical field propagates unidirectionally through the device parallel to the z-axis, and is strongly constrained by the waveguiding properties of the active region. Constant direct-current is injected from an external current source, and the current density is assumed to be uniform along the length of the device.

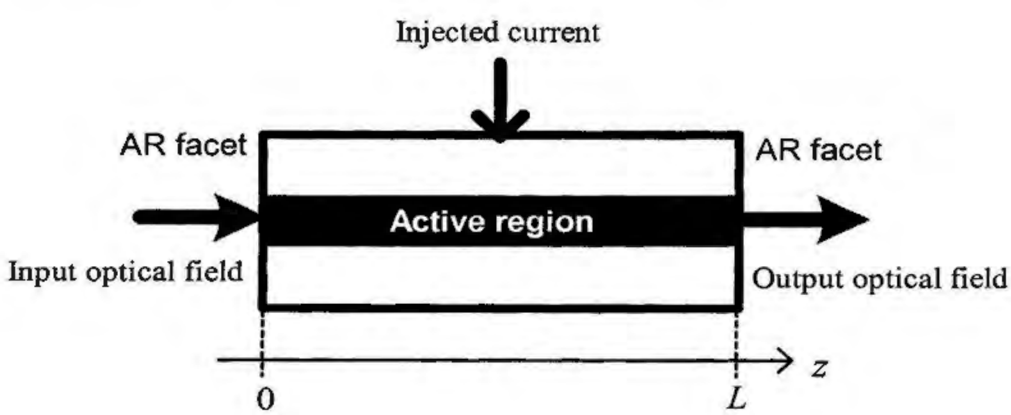

Fig. 4.4 Modelling a travelling-waveguide semiconductor optical amplifier.

Taking into account carrier population pulsation only, the generated nonlinear polarization field (the l^{th} mode) by FWM is

$$\frac{1}{\varepsilon_0} P_{l,CPP}^{NL} = \frac{nc}{\omega_l} g(\overline{N}) \frac{(\alpha + j)/P_e}{1+j\Delta\omega_{ij}\tau_e} A_i^* A_j A_k \tag{4.1}$$

where ε_0 is the vacuum permittivity, c is the velocity of light in a vacuum, n is the refractive index of the active region, ω_l is the angular frequency of the FWM generated field (the l^{th} mode), $g(\cdot)$ is the gain of the mode, α is the linewidth enhancement factor, P_e is the saturation intensity, τ_s is the spontaneous carrier lifetime. A_i, A_j, A_k are the three input optical fields. The imaginary part of the above expression represents gain modulation, and the real part represents refractive index modulation.

Calculation of the contribution to the nonlinear susceptibility by spectral hole burning and carrier heating requires a detailed quantum-mechanical analysis. The most common approach taken in the literature uses the density matrix formalism to describe transitions within the conduction band [8]. To avoid this complexity, a simple phenomenological model is adopted here to account for the effects of spectral hole burning and carrier heating. Using this model, the nonlinear polarization resulting from intraband effects is given at ω_l by

$$\frac{1}{\varepsilon_0}P^{NL}_{l,SHB+CH}=\frac{nc}{\omega_l}g(\overline{N})\sum_{m=shb,ch}\frac{(\beta_m+j)\varepsilon_m}{1+j\Delta\omega_{ij}\tau_m}A_i^*A_jA_k \tag{4.2}$$

where the $\{\varepsilon_m\}$ are inverse saturation powers, representing the strength of the nonlinearity, the $\{\beta_m\}$ are equivalents to the linewidth enhancement factor, representing the relative contributions of the gain and index modulation at all frequencies, and the $\{\tau_m\}$ are characteristic relaxation times associated with the nonlinear processes. The summation is performed over all contributing processes, namely spectral hole burning ($m = shb$) and carrier heating ($m = ch$). This model has been used by a number of researchers to obtain good agreement with experimental results by using curve-fitting techniques to determine the parameters [13-14].

Therefore, The total nonlinear polarization can be written as

$$\frac{1}{\varepsilon_0}P^{NL}_l=\frac{nc}{\omega_l}g(\overline{N})\sum_{\substack{m=cpp,shb,\\ ch}}\frac{(\beta_m+j)\varepsilon_m}{1+j\Delta\omega_{ij}\tau_m}A_i^*A_jA_k \tag{4.3}$$

where an additional term has been added to the summation representing carrier population pulsations ($m = cpp$). The corresponding parameters are, from Equation (17), $\varepsilon_{cpp} = 1/P_e$, $\beta_{cpp} = \alpha$ and $\tau_{cpp} = \tau_e$.

Usually, if we only consider FWM process qualitatively and emphasize on the optical frequency relations, the above equation can also be simplified as

$$E_4(\text{or } E_{132}) = (A_1 \square A_3)\, r(\omega_1 - \omega_3)\, A_2 \exp[j(\omega_1 + \omega_2 - \omega_3)t + (\phi_1 + \phi_2 - \phi_3)] \quad (4.4)$$

where A_i $(i \in 1,2,3)$, ω_i and ϕ_i are the respective input field amplitudes, angular frequencies and phases, $r(\omega_1 - \omega_3)$ determines the conversion efficiency and E_4 (or E_{132}) is the FWM-generated field. We shall employ this simplified equation to explain our proposed XOR gate for DPSK signals based on FWM in SOA as follows.

4.3 Proposed three-input XOR gate for RZ-DPSK signals

In Eq. (4.4), with the phases of the input fields ϕ_1, ϕ_2, ϕ_3 taking values either "0" or "π", the possible phase of the generated new field will be "0", "π", "2π" or "−π". Due to the periodicity of the phases, a phase of "π" is equivalent to "−π", and similar property applies to the phases of "2π" and "0". By assuming Boolean values "0" and "1" as the signal phases of "0" and "π", respectively, the FWM process can be regarded as a three-input XOR Boolean operation in the phase domain, i.e. $\phi_{132} = \phi_1 \oplus \phi_2 \oplus \phi_3$. This can be seen clearly from the truth table in Fig. 4.5.

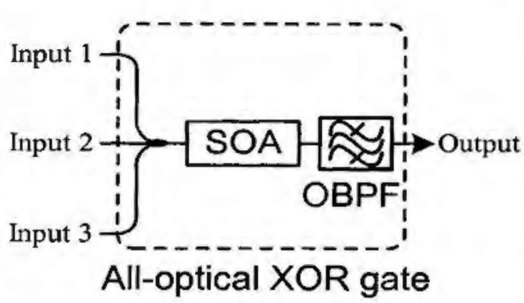

ϕ_1	ϕ_2	ϕ_3	$\phi_1+\phi_2-\phi_3$	Boolean
0	0	0	0	0
0	0	π	−π	1
0	π	0	π	1
0	π	π	0	0
π	0	0	π	1
π	0	π	0	0
π	π	0	2π	0
π	π	π	π	1

Fig. 4.5 The proposed all-optical XOR logic gate and the truth table discovering the phase evolution based on FWM in a SOA. OBPF: optical bandpass filter.

To achieve such FWM-based Boolean operation, RZ-DPSK is employed as the modulation format of the input signals, in which the "0" and the "1" bits are represented in form of phase change between adjacent optical pulses. A three-input XOR gate can be realized with the input fields $E_1(A_1, \omega_1, \phi_1)$, $E_2(A_2, \omega_2, \phi_2)$ and $E_3(A_3, \omega_3, \phi_3)$, which are all RZ-DPSK modulated, that is,

$$k_{1\_i} = \phi_{1\_i} \oplus \phi_{1\_(i-1)};\ k_{2\_i} = \phi_{2\_i} \oplus \phi_{2\_(i-1)} \text{ and } k_{3\_i} = \phi_{3\_i} \oplus \phi_{3\_(i-1)} \quad (4.5)$$

where k_{j_i} (either "0" or "1") is the i^{th} binary value and ϕ_{j_i} (either "0" or "π") is the phase value for the i^{th} RZ-DPSK coded optical pulse, j is the input wavelength index. When FWM occurs in the SOA with these three input fields, one of the generated fields has an angular frequency of $(\omega_1 + \omega_2 - \omega_3)$, and a resultant phase of $(\phi_1 \oplus \phi_2 \oplus \phi_3)\pi$. After demodulation using a delayed-interferometer (DI), the i^{th} output binary value, k_{132_i}, is:

$$k_{132\_i} = (\phi_{1\_i} \oplus \phi_{2\_i} \oplus \phi_{3\_i}) \oplus (\phi_{1\_(i-1)} \oplus \phi_{2\_(i-1)} \oplus \phi_{3\_(i-1)}) = k_{1\_i} \oplus k_{2\_i} \oplus k_{3\_i} \quad (4.6)$$

Thus, the output of the DI represents the XOR Boolean operation among the respective binary values for the input fields $E_1(A_1, \omega_1, \phi_1)$, $E_2(A_2, \omega_2, \phi_2)$ and $E_3(A_3, \omega_3, \phi_3)$. Hence, all-optical XOR Boolean operation for RZ-DPSK modulated input signals can be realized by FWM in a SOA.

4.4 Demonstration of two-input XOR gate

Two-input XOR operation is the common basic XOR operation, which can be realized by our proposed XOR gate. Partially degenerate FWM occurs in the SOA when there are only two input light waves, and Eq. (4.4) can be modified as

$$E_{121} = (A_1 \Box A_2)\, r(\omega_1 - \omega_2)\, A_1 \exp[j(2\omega_1 - \omega_2)t + (2\phi_1 - \phi_2)] \quad (4.7)$$

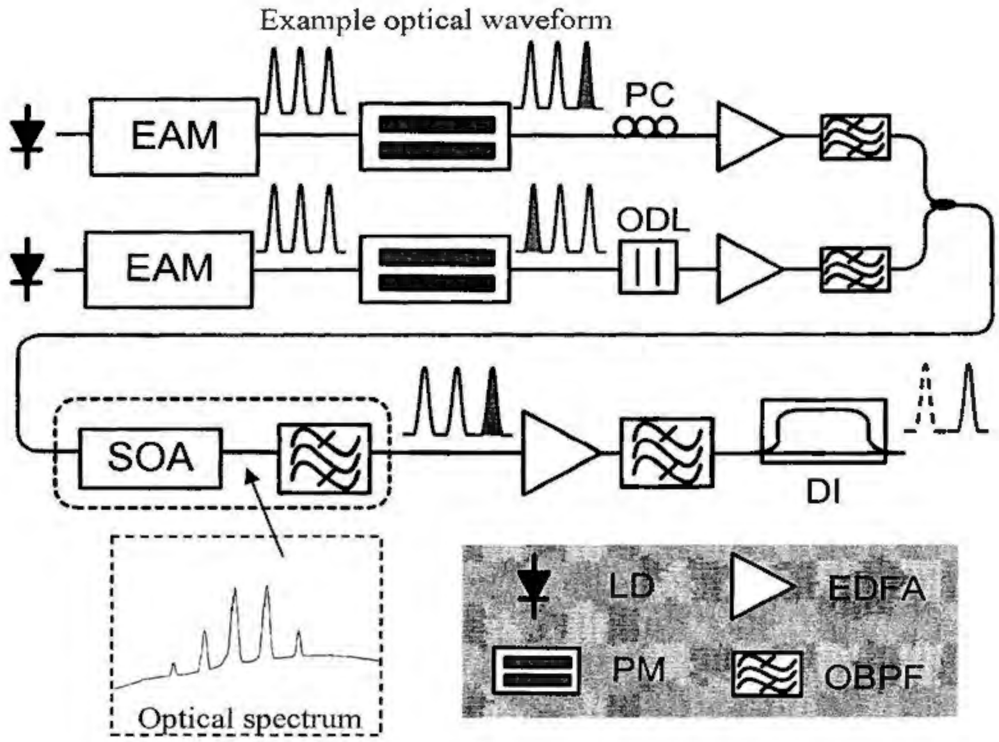

Fig. 4.6 Experiment setup of FWM-based all-optical XOR gate with two inputs. LD: laser diode; PM: phase modulator; EDFA: Erbium doped fiber amplifier; SOA: semiconductor optical amplifier; ODL: optical delay line; PC: polarization controller; OBPF: optical bandpass filter; DI: delayed interferometer. Inset shows the measured optical spectrum at the output of the SOA.

Fig. 4.6 shows the experimental setup. Using a pair of electroabsorption modulators (EAM), the RZ pulse streams were generated at 1547 nm and 1551 nm respectively. The optical pulses have a pulsewidth of about 15 ps and a repetition rate of 10.61 GHz. The pulse streams were then phase-encoded separately via optical phase modulators (PM) driven by 10.61-Gbit/s pseudo-random binary sequence (PRBS). The phase modulator has the same response at the two input wavelengths. As only two input signals were presented for FWM, the input field at a shorter wavelength (ω_1) was modulated with a depth of "π/2", instead of "π", according to equation (4). Another way to avoid using different modulation depths is to introduce a third CW wavelength to perform non-degenerate FWM. After having amplified by erbium-doped fiber amplifiers (EDFA), the DPSK coded pulse streams were then combined using a 3-dB fiber coupler. To ensure that the two input signals were copolarized and well aligned in time domain, a polarization controller (PC) and a tunable optical delay line (ODL) were inserted. The two combined DPSK signals were then fed into a commercial SOA with a small signal gain of 25 dB (polarization dependent gain ~0.6 dB, noise figure ~10 dB), biased at about 180 mA. The saturation output power of the SOA is 8.5 dBm; the gain peak is at 1538 nm with a 3-dB bandwidth of 42 nm. The average power launched into the SOA was about 6 dBm, with the two inputs at similar power level. From the output of the SOA, the FWM-generated signal at 1543 nm had an optical signal-to-noise-ratio (OSNR) of 20 dB and the FWM efficiency was about –20 dB, measured at a resolution bandwidth of 0.1 nm. It was then extracted by an optical bandpass filter with a 3-dB bandwidth of 0.1 nm before being DPSK-demodulated via a DI with a relative delay of 94.3 ps. The output waveforms were recorded using a 45-GHz p-i-n detector.

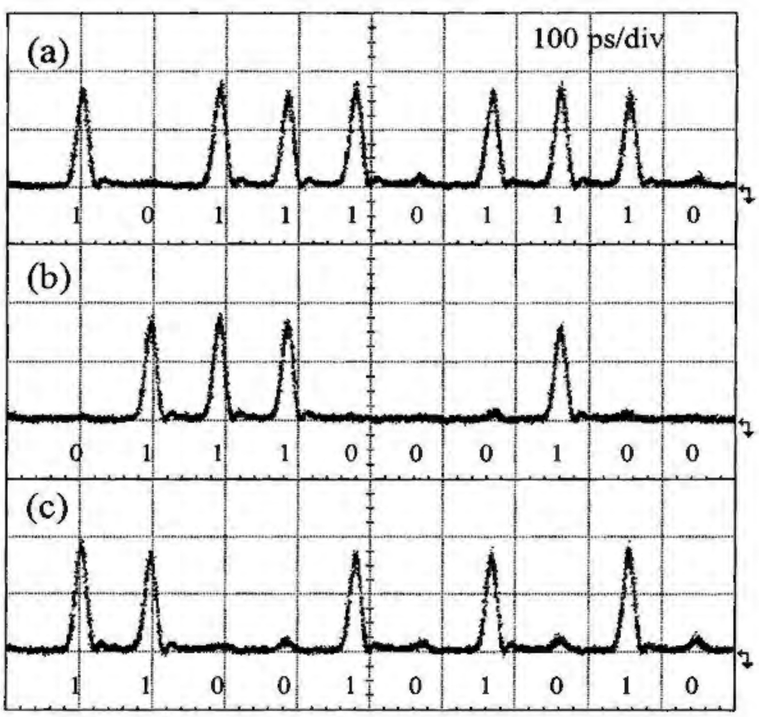

Fig. 4.7 10.61-Gb/s all-optical XOR gate demodulated input and output signals. (a): first input signal pattern "1011101110"; (b): second input signal pattern "0111000100"; (c): obtained XOR output at the FWM-generated wavelength, "1100101011". All waveforms are captured at the output of the DI.

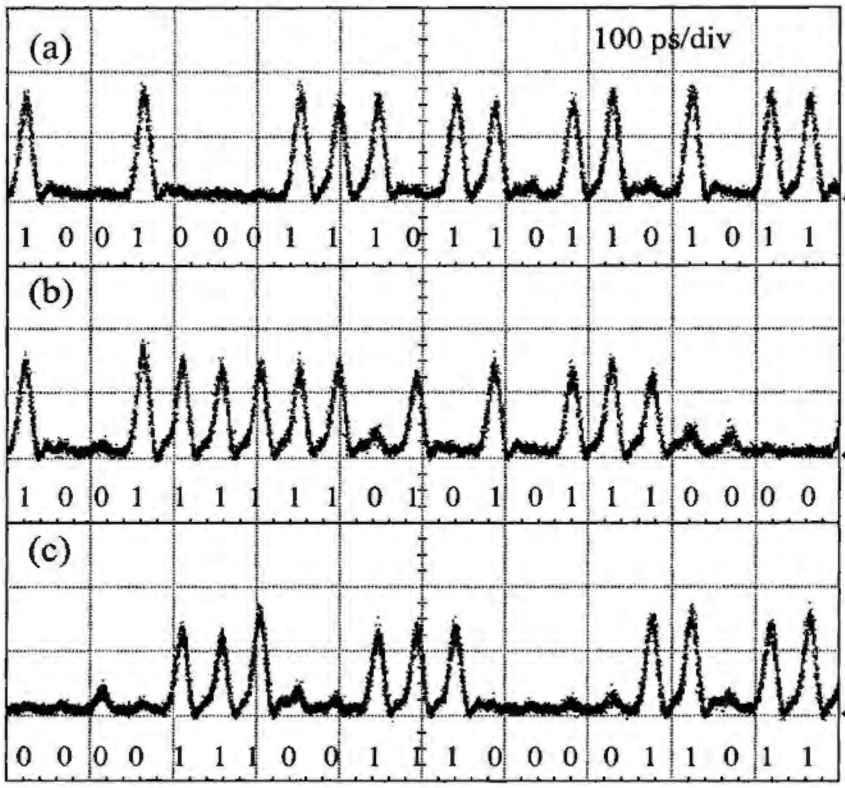

Fig. 4.8 21.22-Gb/s all-optical XOR gate demodulated input and output signals. (a): first input signal pattern "100100011101101101011"; (b): second input signal pattern "100111111010101110000"; (c): obtained XOR output at the FWM-generated wavelength, "000011100111000011011". All waveforms are captured at the output of the DI.

Fig. 4.7 (a) and (b) show the demodulated bit patterns for the first input signal ("1011101110") and the second input signal ("0111000100"). Fig. 4.7(c) shows the demodulated output from the FWM-based all-optical XOR gate ("1100101010"). The obtained results verified the effectiveness of the XOR operation by the proposed FWM method. The small amount of power appeared at "zero" bits could be mainly caused by the inaccurate phase modulation due to slight amplitude fluctuation in the modulator driving signal as well as the amplifier noises. To verify that the proposed all-optical XOR gate could be operated at high speed, the input signals were multiplexed to 21.22 Gbit/s, before being launched into the SOA. The corresponding obtained XOR output is shown in Fig. 4.8. Both the input and the output RZ-DPSK signals were demodulated by a DI with a relative delay of 47 ps. The degraded waveform could be explained by the inter-channel crosstalk during optical time division multiplexing as a result of insufficient pulse extinction ratio and relatively broad signal pulsewidth.

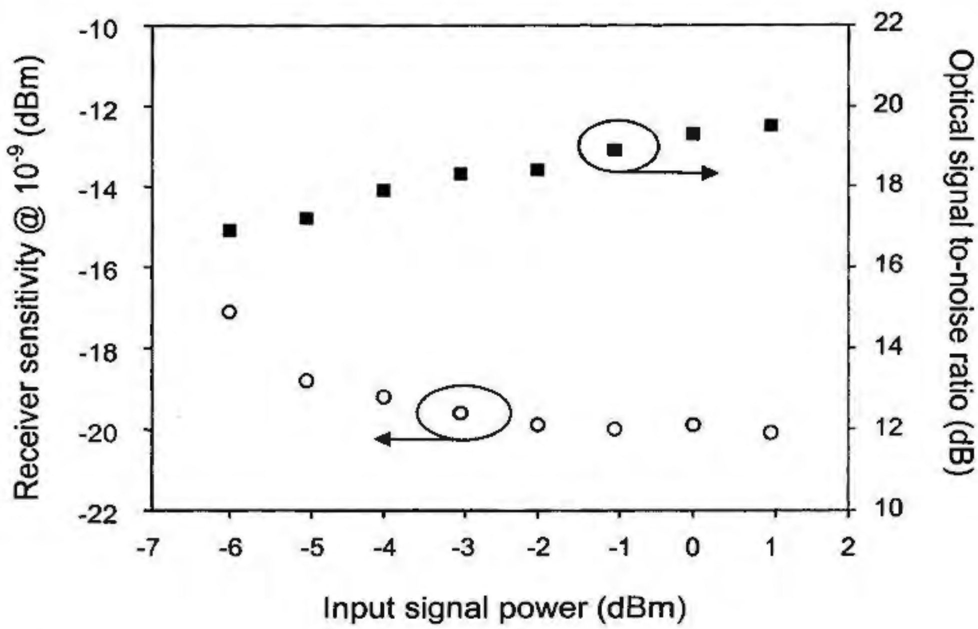

Fig. 4.9 The output signal receiver sensitivity and optical signal-to-noise ratio dependence on the input RZ-DPSK (10.61-Gb/s, 2^7-1 PRBS) signal power, in the two-input XOR gate functioning as a wavelength converter.

When one of the two inputs is a pulse stream without phase modulation, the XOR operation is a special case with one input all "0"s, which functions as a wavelength converter. By switching off the phase modulation on the input pulse stream at 1547 nm, the output at 1543 nm had the same data information with the input optical signal at 1551 nm. Using 2^7-1 PRBS, the bit error rates were measured and the converted signal at 1543 nm had less than 0.5-dB power penalty compared with the original input signal at 1551 nm. We have also studied the FWM-generated signal performance, when varying the input signal power. Previous works showed that with fixed CW pump power, there was an optimum input signal power (in OOK format) that led to optimal FWM-converted signal. Too small input signal power led to poor signal-to-noise ratio while too large input signal power induced inter-symbol interference (ISI) in the FWM-converted signal [15]. We fixed the pump power at 4 dBm and adjusted the input signal power within the safe power range for the SOA. If the receiver noise was dominated by spontaneous-signal beat noise, the OSNR could well reflect the converted signal performance. In Fig. 4.9, it is clearly shown that the OSNR (measured at 0.1-nm resolution bandwidth) of the converted output signal increased with the input signal power. The receiver sensitivity versus the input signal power is also presented in the same figure, showing that the improved OSNR has resulted in better receiver sensitivity. The results indicated that FWM based optical functions employing DPSK signals could achieve better performance at higher OSNR range, compared with OOK signals which were limited by ISI or patterning effect at high input signal power.

4.5 Demonstration of three-input XOR gate

To fully verify the logic integrity and the performance of our proposed FWM-based XOR gate, we have also experimentally investigated the three-input case. In addition, XOR gates with more than two data inputs are preferred in the applications such as data encoding, parity checking, and full adder, to avoid too many cascaded XOR gates. Fig. 4.10 shows the experimental setup. Three CW input light beams were firstly combined via fiber couplers, before passing through an EAM driven by a 10.61-GHz electrical clock for pulse carving. The generated 15-ps optical pulse trains were amplified, and were modulated by a 10.61-Gb/s 2^7-1 PRBS via an optical phase modulator (PM). The optical DPSK signals on the three wavelengths were then demultiplexed by an arrayed waveguide grating (AWG) and were decorrelated by two tunable ODL, as shown in Fig. 4.10. Due to the physical nature of polarization dependency of FWM, the three-input XOR gate is sensitive to the polarization states of the input signals. Thus two PCs were carefully adjusted so as to maximize the FWM efficiency of the generated ω_4 component ($\omega_4=\omega_1+\omega_2-\omega_3$). The three optical DPSK signals were then combined and fed into the SOA biased at 180 mA. The total average input power into the SOA was 4.5 dBm. A new light wave at ω_4 was generated, via FWM. This served as the XOR output signal, which was then extracted by a tunable OBPF with a 3-dB bandwidth of 1 nm and the output optical power was about -18 dBm. In the experiment, the DPSK signals were also demodulated by the fiber-based DI with a relative delay of 94.3 ps.

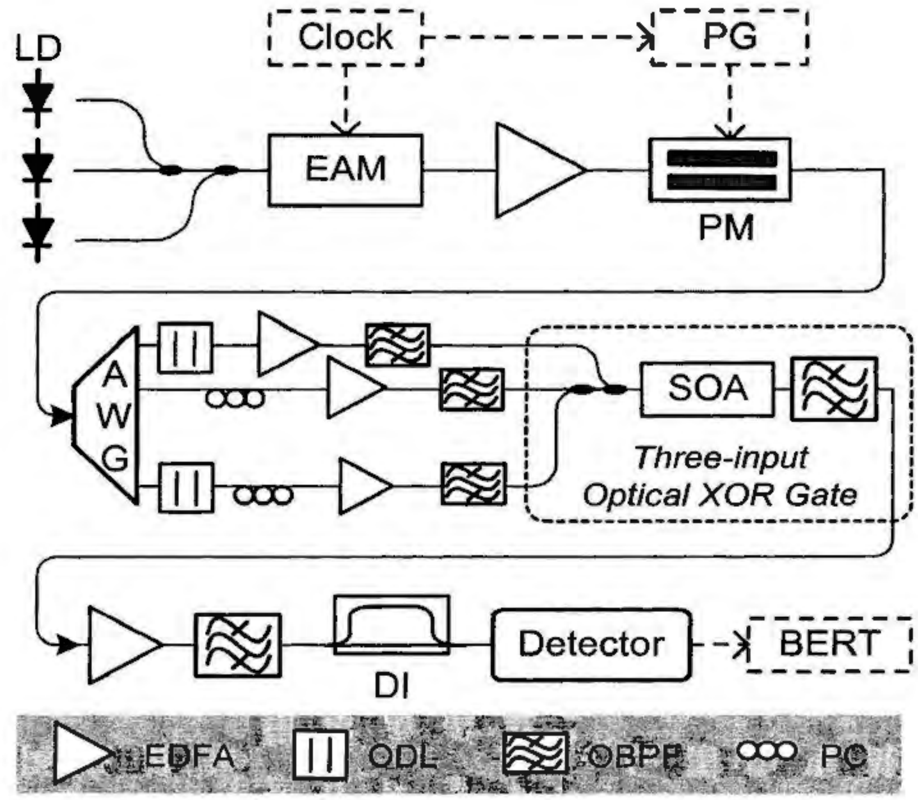

Fig. 4.10 Experimental setup of three-input XOR gate. LD: laser diode; EAM: electro-absorption modulator; PG: pattern generator; PM: phase modulator; AWG: array waveguide grating; SOA: semiconductor optical amplifier; DI: delayed interferometer; BERT: bit-error-rate tester; EDFA: erbium doped fiber amplifier; ODL: optical delay line; OBPF: optical bandpass filter; PC: polarization controller.

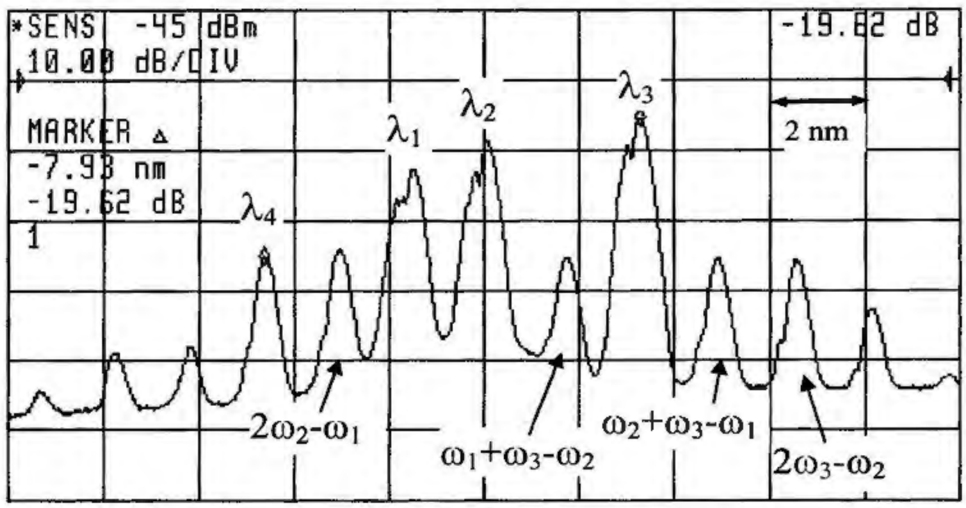

Fig. 4.11 The optical spectrum output from the SOA in the three-input XOR gate

Fig. 4.11 shows the output optical spectrum from the SOA generated by the FWM process. The three input wavelengths (λ_1= 1545.66 nm, λ_2 = 1547.23 nm, λ_3 = 1550.43 nm) were chosen near to the gain peak of the SOA, as well as in alignment with the AWG passbands. In addition to the generated wavelength λ_4 (corresponding to $\omega_4 = \omega_1+\omega_2-\omega_3$), the FWM process has also produced some other wavelength components (corresponding to $2\omega_2-\omega_1$, $2\omega_3-\omega_2$, $\omega_1+\omega_3-\omega_2$, $\omega_2+\omega_3-\omega_1$, $2\omega_3-\omega_2$, etc), as depicted in Fig. 4.11. The FWM efficiency, which is defined as the power ratio of the newly generated ω_4 component to the ω_3 component (with highest input power), was measured to be -19.6 dB. The OSNR of the ω_4 component was 21.3 dB, measured at 0.1-nm resolution bandwidth on the spectrum analyzer. The wavelengths of the three light beams (λ_1, λ_2, λ_3) were observed to be slightly red-shifted after the SOA, mainly due to their self- and cross-phase modulations [16].

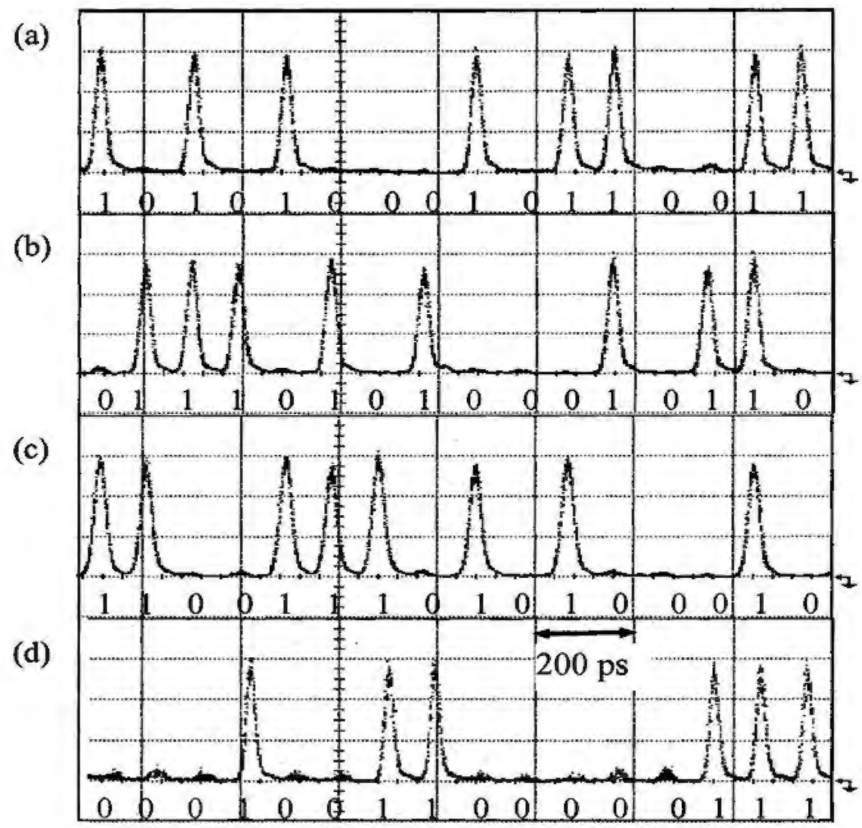

Fig. 4.12 16-bit demodulated DPSK waveforms of the three 10.61-Gbit/s input (a, b, c) and the XOR-output (d) signals. All waveforms are captured at the output of the DI.

The captured waveforms are shown in Fig. 4.12. A 16-bit sequence "1010100010110011" and its two delayed versions served as the three data inputs (Fig. 4.12 a, b, c). Fig. 4.12(d) shows the demodulated DPSK waveform output from our demonstrated optical XOR gate, with the correct XOR result "0001001100000111". The degraded extinction ratio of the XOR output signal might be attributed to the accumulated phase noises produced in the EDFAs and the SOA, in addition to the incomplete phase modulation of the input signals. We have also observed that the FWM components at ($\omega_1+\omega_3-\omega_2$) and ($\omega_2+\omega_3-\omega_1$) carried the same XOR result, but with worse signal quality due to more filtering leakage induced crosstalk from the neighboring strong optical frequencies.

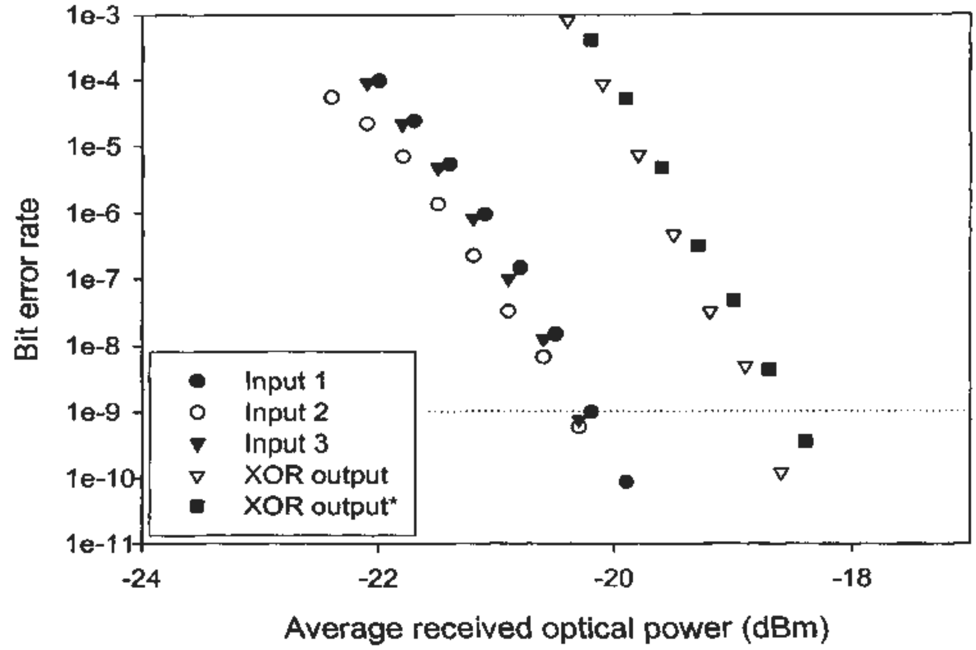

Fig. 4.13 BER measurements of the three DPSK input (●,○,▼ all 2^7-1 PRBS) and the XOR-output (▽ 2^7-1 PRBS, ■ 2^{10}-1 PRBS) signals.

We have performed bit-error-rate (BER) measurements to precisely investigate the logic integrity and the performance of the demonstrated FWM-based three-input optical XOR gate. A PRBS sequence with a word length of 2^7-1 and two of its delayed versions served as the three data inputs. We computed and edited the XOR result into the BER tester to evaluate the output XOR data. The measured BER for the three input and the output signals were plotted in Fig. 4.13. The three input signals had similar performance and the XOR output signal had less than 2-dB power penalty at BER=10^{-9} compared with the input signals. The power penalty might be attributed to the noises induced by the EDFAs and the SOA, and the slightly degraded extinction ratio, as discussed before. Note that the noise variance of the XOR output would be larger than that of each input, according to Eq.(3). The BER measurements using 2^{10}-1 PRBS as the input signal source showed similar data records, implying very small pattern dependence in the XOR performance. The data points for the 2^{10}-1 PRBS input signals were too close to those using 2^7-1 PRBS and thus were not drawn in the same figure. Although this demonstration was at 10.61 Gb/s, such FWM-based all-optical XOR gate was capable of processing optical signals at much higher bit rate, due to the ultrafast intraband processes of FWM in SOA.

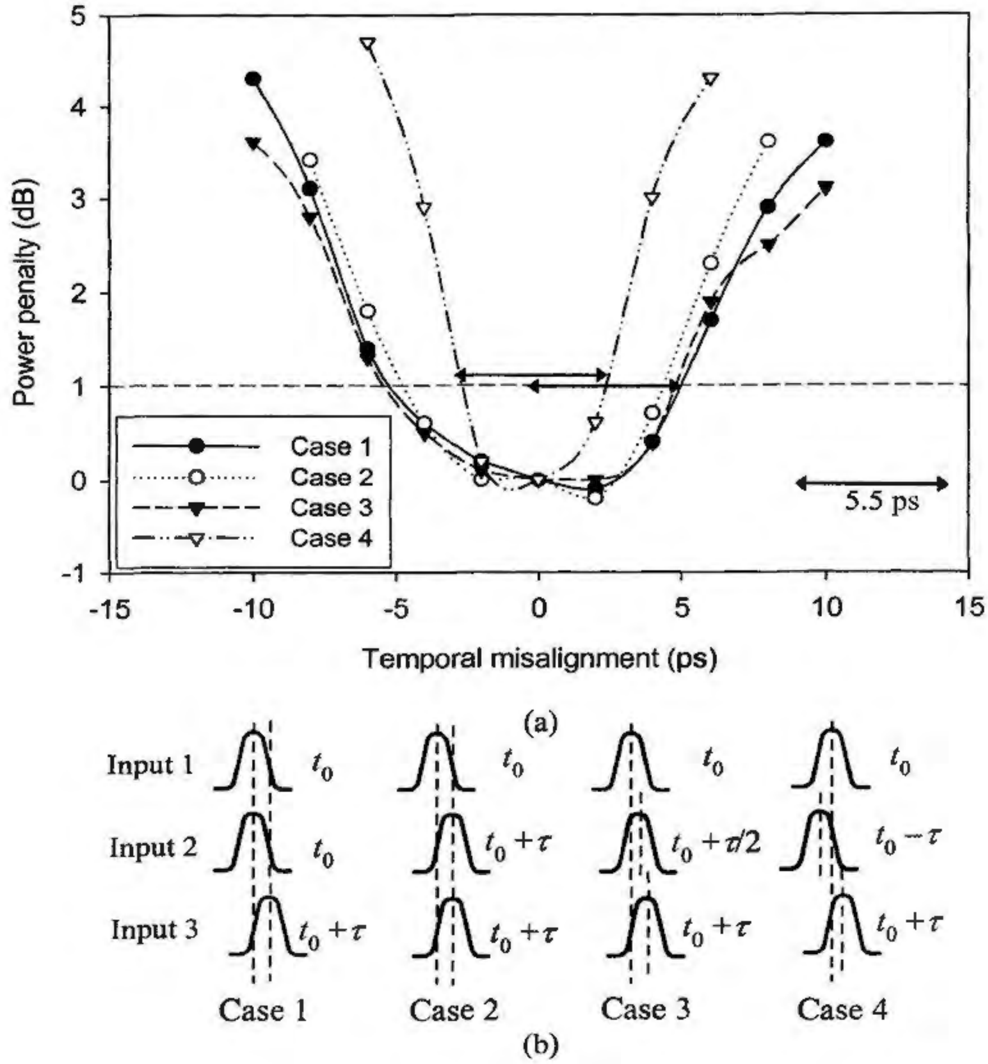

Fig. 4.14 The influence of temporal misalignment of the three input signals on the output XOR signal performance. (a) power penalty. (b) four cases of temporal misalignment.

The effective XOR operation requires good overlapping of optical fields among the input RZ-DPSK signal pulses. Any improper synchronization among the input signals would decrease the FWM efficiency as well as the output signal quality. We have experimentally measured the temporal switching window of the three-input XOR logic gate, to study the effect of temporal misalignment among the input signals. Fig. 4.14(a) shows the measured power penalties of the FWM-generated XOR signal with respect to four different cases of temporal misalignment among the input signals, as illustrated in Fig. 4.14(b). In Case 1, two inputs were well aligned and the third one was misaligned by a time period τ. In Case 2, one input had no temporal drift and two inputs had a temporal drift of τ. In Case 3, all three inputs were out of good synchronization where two of them had respective temporal drift of $\tau/2$ and τ relative to the third one. Experimental investigation obtained similar records of output power penalty for these three cases. The induced output penalties in Case 1 and Case 2 were slightly different due to the slight difference in input powers and SOA gain at different wavelengths, though they were intrinsically the same in terms of the mode of input asynchronous. In all of these three cases, one input had a misalignment of τ and another one was at different positions within the range of $[0, \tau]$, and their output performance were very similar to each other. Hence, this implied that the output performance would be determined by the maximum temporal misalignment τ among the input signals. The study in Case 4 further proved this statement, in which the second and the third inputs had a temporal drift of τ and $-\tau$, respectively, with respect the first input, as depicted in Fig. 10(b). In this case the maximum misalignment was 2τ. The misalignment tolerance, defined as the maximum temporal misalignment among the three inputs at 1-dB power penalty, was around 5.5 ps, which was about one-third of the input pulse width.

4.6 Summary

We have proposed a high-speed all-optical XOR logic gate based on FWM in SOA, which can intrinsically accommodate three-input XOR operation. We have successfully demonstrated the XOR gates in both two-input and three-input cases. The two-input XOR gate can also serve other all-optical processing functions such as wavelength conversion. The experiment of wavelength conversion for 10.61-Gb/s RZ-DPSK signals showed less than 0.5-dB power penalty. The best conversion performance occurred at the highest OSNR value within the safe input power range of the SOA. Moreover, three-input XOR gate is preferred in multiple-input applications, to reduce the number of XOR gates cascaded. Experiments showed less than 2-dB power penalty of the output XOR signal compared with the input signal receiver sensitivity. Besides, the maximum pulse misalignment among the three input RZ-

DPSK signals should be no greater than one-third of the input pulse width in order to avoid severe performance degradation.

References

[1] B.S. Robinson, S.A. Hamilton, S.J. Savage, E.P. Ippen, "40 Gbit/s all-optical XOR using a fiber-based folded ultrafast nonlinear interferometer," in *Optical Fiber Communications Conference (OFC)* 2002, paper ThY2, 2002.

[2] J. H. Kim, Y. M. Jhon, Y. T. Byun, S. Lee, D. H. Woo, and S. H. Kim, "All-optical XOR gate using semiconductor optical amplifiers without additional input beam," *Photonics Technology Letters*, vol. 14, pp. 1436–1438, Oct 2002.

[3] A.J. Poustie, K.J. Blow, A.E. Kelly, R.J. Manning, "All-optical full adder with bit-differential delay," *Optics Communications*, vol. 168, pp. 89-93, 1999.

[4] H. Soto, D. Erasme, and G. Guekos, "5-Gb/s XOR optical gate based on cross-polarization modulation in semiconductor optical amplifiers," *Photonics Technology Letters*, vol. 13, pp. 335–337, Apr. 2001.

[5] K. Zoiros, T. Houbavlis, "Ultrafast all-optical Boolean XOR logic using semiconductor optical amplifier-assisted Sagnac switch," *Conference on Quantum Electronics and Laser Science (QELS)* 2005, Vol. 2, pp. 960-962, 2005.

[6] C. Bintjas, M. Kalyvas, G. Theophilopoulos, T. Stathopoulos, H. Avramopoulos, L. Occhi, L. Schares, G. Guekos, S. Hansmann, and R. Dall'Ara, "20 Gb/s all-optical XOR with UNI gate," *Photonics Technology Letters*, vol. 12, pp. 834–836, 2000.

[7] R. P. Webb, R. J. Manning, G. D. Maxwell, and A. J. Poustie, "40 Gbit/s all-optical XOR gate based on hybrid-integrated Mach–Zehnder interferometer," *Electronics Letters*, vol. 39, pp. 79–80, 2003.

[8] Y.R. Shen, "Basic considerations of four-wave mixing and dynamic gratings," *Journal of Quantum Electronics*, vol. QE-22, pp.1196-1203, 1986.

[9] A. D'Ottavi, E. Iannone, A. Mecozzi, S. Scotti, P. Spano, J. Landreau, A. Ougazzaden, J. C. Bouley, "Investigation of carrier heating and spectral hole burning in semiconductor

amplifiers by highly nondegenerate four-wave mixing," *Applied Physics Letters*, vol. 64, pp.2492-2494, 1994.

[10] J.A Armstrong et al, "Interactions between light waves in a nonlinear dielectric," *Physics Review*, vol. 127, pp. 1918-1939, 1962.

[11] P.D Maker et al, "Study of optical effects due to an induced polarization third-order in the electric field strength," *Physics Review A*, vol. 137, pp. 801-818, 1965.

[12] G.P. Agrawal, "Population pulsations and nondegenerate four-wave mixing in semiconductor laser and amplifiers," *Journal of Optics Society of America B*, vol. , pp. 147-159, 1988.

[13] J. Zhou et al, "Efficiency of Broadband Four-Wave Mixing Wavelength Conversion Using Semiconductor Traveling-Wave Amplifiers," *Photonics Technology Letters*, Vol. 6, pp. 50-52, 1994.

[14] J. Zhou et al, "Four-Wave Mixing Wavelength Conversion Efficiency in Semiconductor Traveling-Wave Amplifiers Measured to 65 nm of Wavelength Shift," *Photonics Technology Letters*, Vol. 6, pp. 984-987, 1994.

[15] D.F. Geraghty, R.B Lee, M. Verdiell, M. Ziari, A. Mathur, K.J. Vahala, "Wavelength conversion for WDM communication systems using four-wave mixing in semiconductor optical amplifiers", *Journal of Selected Topics in Quantum Electronics*, Vol. 3, no. 5, pp. 1146-1155, 1997.

[16] G.P. Agrawal, N.A. Olsson, "Self-phase modulation and spectral broadening of optical pulses in semiconductor laser amplifiers," *Journal of. Quantum Electronics*, Vol. 25, no. 11, pp. 2297-2306, 1989.

5 A Simple Label Pattern Recognition Scheme for Phase-modulated Label Signals

5.1 Introduction to all-optical label recognition

As introduced in previous chapters, with the rapid growth of Internet traffic, optical label switching has been emerging as an attractive technology to maximize bandwidth utilization and minimize routing latency of future optical networks. Among various optical labeling schemes, bit-serial labeling can guarantee high signal performance of both the label and the payload [1-10]. Since the label is placed before the payload in time, it can be optically processed without influence or crosstalk onto the payload.

A few bit-serial label pattern recognition approaches based on optical signal processing have been reported [5-8]. One approach employed nonlinear optical processing (e.g. optical serial-to-parallel conversion) plus successive electrical post-processing [5-6]. A basic schematic is shown in Fig. 5.1. It could recognize different label patterns by programming the electronics but both its optical and electrical modules were quite complicated.

Another method utilized all-optical correlation based on nonlinear optical processing [7-8], which largely relaxed the requirement on electronics. For example, the optical label information was coded as the time gap between two specific pulses in the optical label signal in [7], and it was recognized using an all-optical signal processing circuit. The circuit contained the time gap information and utilized nonlinear effects in SOA. If the time gap information in the label matched with that in the circuit, the label was recognized. Therefore, there was no complicated electronic circuit required. However, each correlator could recognize only one label pattern and special label data format was required, which strongly limited the feasibility of this scheme.

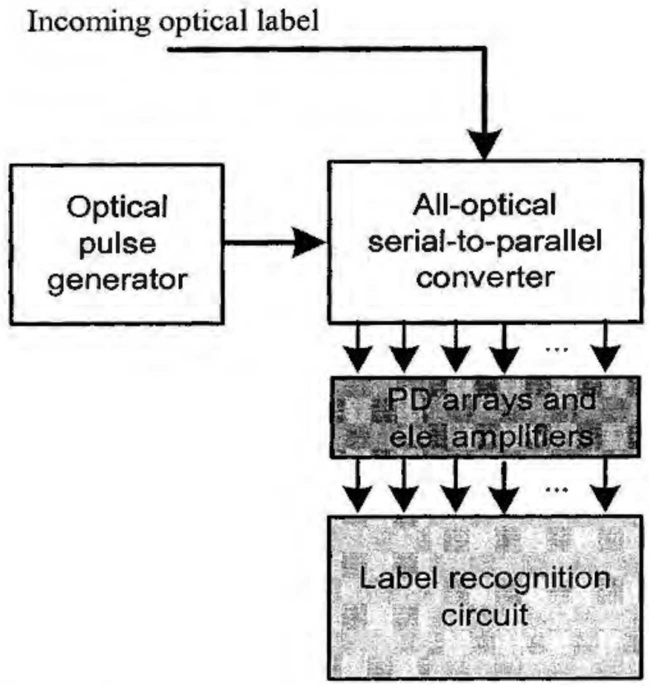

Fig. 5.1 The schematic diagram of the optical label recognition approach based on nonlinear processing (all-optical serial-to-parallel conversion) and electronic post processing [5].

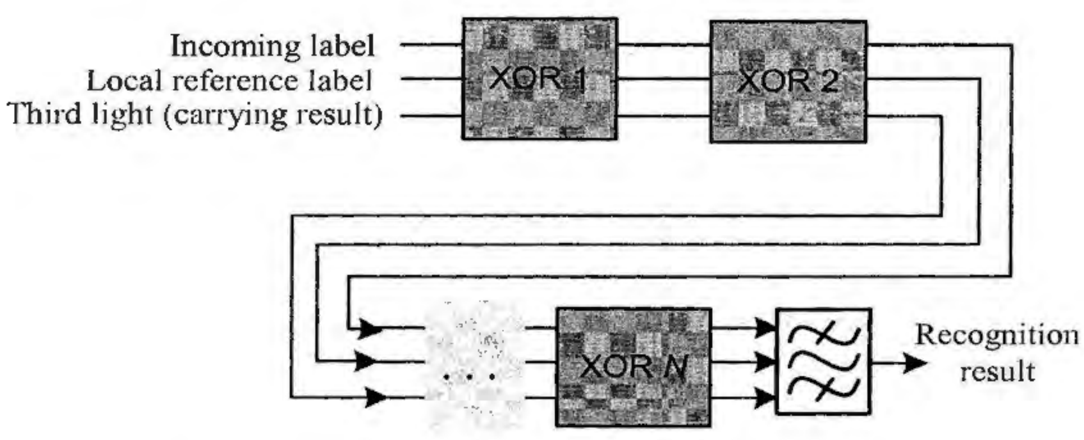

Fig. 5.2 Optical label recognition based on all-optical logic XOR gate [7].

Recently, optical label processing based on all-optical logic XOR gate has aroused much interest [9-10]. The optical correlator demonstrated in [9] compared the incoming label pattern with the local reference pattern bit by bit through XOR operation, and a third signal was used to carry and summarize the bitwise comparison results together. This scheme could recognize any label pattern because of the introduction of the local pattern. However, this scheme would involve N XOR gates for N-bit label, which was costly, complicated, and might have cascadability problem due to noise accumulation.

5.2 Proposed label recognition scheme

In this project, we propose a new optical correlator for phase modulated (PM) bit-serial label recognition. It can recognize any label pattern with the assist of a local reference pattern. Moreover, it handles label bit comparison in parallel, thus offering much more simple and robust operation. We employ a local optical pattern to interplay with the incoming label pattern via cross-phase modulation (XPM) in the dispersion-shifted fiber (DSF). After that the incoming label pattern is fed into a delayed interferometer (DI). The output will have no optical pulse or at least one optical pulse depending on whether the labels are matched or not. Therefore the decision of successful recognition can be simply achieved by measuring the output optical power. Moreover, it can recognize any incoming label pattern according to the local pattern, and can be reconfigured to accommodate variable-length label patterns.

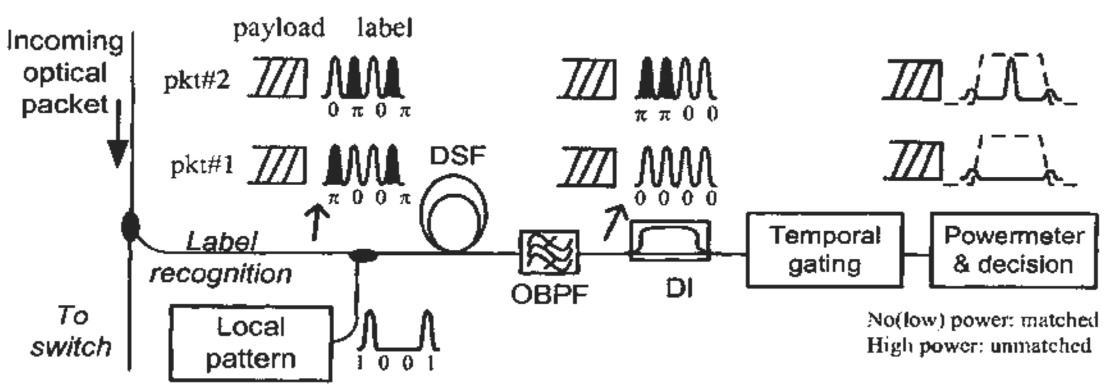

Fig. 5.3 Schematic of the proposed all-optical label recognition scheme. Two example packet label patterns and their corresponding output are shown.

Fig. 5.3 shows the principle of operation of our proposed all-optical PM label recognition scheme. In a network core router, part of the incoming packet power is tapped off for label recognition. The bit-serial PM label is aligned and combined with an optical pulse train, which is intensity modulated by a designated local label pattern. Then they are fed into a segment of DSF. Since the locally generated optical pattern is intensity modulated and has strong optical power, it can change the phase of the PM incoming label signal via XPM in the DSF. If the binary pattern encoded in the incoming PM label signal is the same with that in the local signal, the incoming label pattern signal would be changed to have equal phase in all of its pulses. By using an optical delay-line interferometer (DI), which has a relative delay between two arms equivalent to the label period, the destructive port of the DI would have no pulse output. On the contrary, if the incoming PM label pattern does not match the local optical pattern, there would be at least one pulse with its phase being different from others in the XPM-modified label signal after the DSF. As a result, there would be at least one optical pulse output from the DI's destructive port. For common bit-serial PM labeling, a PM label and its phase-complementary label are regarded to be the same (e.g. pattern "1010" can be encoded as either "$\pi 0 \pi 0$" or "$0 \pi 0 \pi$"), thus a label pattern is also judged to be matched with its complementary pattern in our scheme. According to the output power measurements, we can judge if the incoming label pattern matches with the local pattern. The optical pattern recognition module may vary its local pattern to re-check the incoming label pattern according to its requirement, controlled by the switch management unit. In this way the all-optical label pattern recognition is realized.

Fig. 5.3 also shows two examples of the label recognition procedure. The packet #1 (pkt#1) has a label of "$\pi 0 0 \pi$" (corresponding binary pattern "1001") while pkt#2 has a label of "$\pi 0 \pi 0$" (corresponding to "1010"). The local optical pattern is set to be "1001", matching with the label of pkt#1. After passing through the DSF, the local pattern "1001" changes the label signal "$\pi 0 0 \pi$" into "$(2\pi)(0)(0)(2\pi)$," which is equivalent to "0000" because of phase periodicity. In the DI output port, the four optical pulses destructively interfere with their one-bit delayed version and result in three central bit periods without power and two small side pulses. The generation of the two side pulses is because of the empty guardbands present before and after the label, and the power of each side pulse is 1/4 of that of every input full pulse. The three central bit periods can be temporally gated to remove the payload and the residual side pulses, and thus no power can be seen by the optical power meter. On the contrary, the label signal of pkt#2 "$\pi0\pi0$" is changed into "$00\pi\pi$" by the local pattern "1001," therefore after the DI the changed phase "$00\pi\pi$" has an output of a full pulse and two small side pulses. The power meter can detect the power of the full pulse after the time gating. In this way the two cases (pkt#1 is matched and pkt#2 is unmatched) can be simply differentiated by the power meter measurement, with a decision threshold between "nearly no power" and "with power". The temporal gating unit can be a fast electro-optical switch. Even if its switching time is not fast enough, there are only two side pulses to be included in the gating window due to the sufficiently long label guardbands. The two side pulses together have half of the power of a full optical pulse, which will narrow the decision threshold range but the recognition module can still work.

According to the principle of our proposed PM label recognition scheme, it is needed to modify the optical phase of the target label bits with a precise depth of π. This is different from most of other XPM based interferometric optical processing functions, in which good performance can be achieved as soon as a probe signal is modified by a certain value in phase (usually not necessarily π). In our case, on the contrary, the phase modification depth must be π as the incoming label signal has already been phase modulated. Otherwise, there will exist more than two phase levels and it may lead very poor performance or even recognition failure. Here we name the precise modification of π to the optical phase of selected bits as "all-optical phase recoding," as the target bit pattern is modified and recoded to be a new bit pattern. Although XPM in fiber has been thoroughly studied in terms of its induced transmission impairments, the XPM performance used to modify the phase value all optically has not been quantitively characterized before, to the best of our knowledge. Therefore, we firstly experimentally characterize the phase modification/recoding performance via XPM in next section.

5.3 Preliminary experimental study on phase recoding by XPM

In addition to our proposed label recognition scheme, all-optical phase recoding has a wide spectrum of applications in all-optical signal processing. We propose and study a simple all-optical approach to recode the phase information of an optical signal, by utilizing XPM in a piece of dispersion-shifted fiber (DSF). In addition to signal processing function as mentioned above, the all-optical phase modification approach can also conduct all-optical RZ to RZ-PSK and conventional RZ to CS-RZ format conversion. Compared with other phase recoding approaches, our proposed one is quite simple, and has no need to shift the wavelength of the data signal. Potentially, the operation based on XPM in fiber can support ultrahigh speed phase recoding. Next, we experimentally demonstrate the phase recoding in an optical RZ-DPSK signal. With delayed interferometric demodulation, the performance of the phase recoding can be easily investigated from the time-domain intensity. The obtained waveforms verified the effectiveness of our approach, and the BER measurements showed the recoded RZ-DPSK signal still exhibited good signal quality.

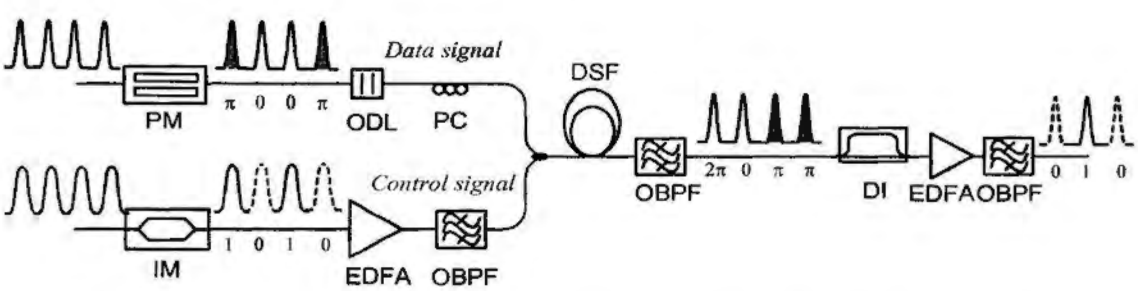

Fig. 5.4 Experimental setup. PM: phase modulator; IM: intensity modulator; ODL: optical delay line; EDFA: Erbium doped fiber amplifier; OBPF: optical bandpass filter; PC: polarization controller; DSF: dispersion-shifted fiber; DI: delay interferometer.

Fig. 5.4 shows the experimental setup. A semiconductor mode-locked laser diode (MLLD) generated an optical pulse sequence with ~1.5-ps pulsewidth at 1554.1 nm. A pattern generator operating at 10.61-Gb/s modulated the pulse sequence via an optical phase modulator. After passing through a tunable optical delay line (ODL) and a polarization controller (PC), the optical data signal was combined with a 10.61-Gb/s intensity-modulated control signal at 1545.3 nm. The pulsewidth of the control signal was around 20 ps, carved by an electro-absorption modulator (EAM). The DPSK data signal and the intensity-modulated control signal were coupled into a piece of 10-km dispersion-shifted fiber (DSF). Then an optical bandpass filter (OBPF) with a 2-nm bandwidth was used to extract the data signal. To observe and evaluate the phase modulation, a delay-line interferometer (DI) with a relative delay of 94.3 ps was used to demodulate the DPSK data signal.

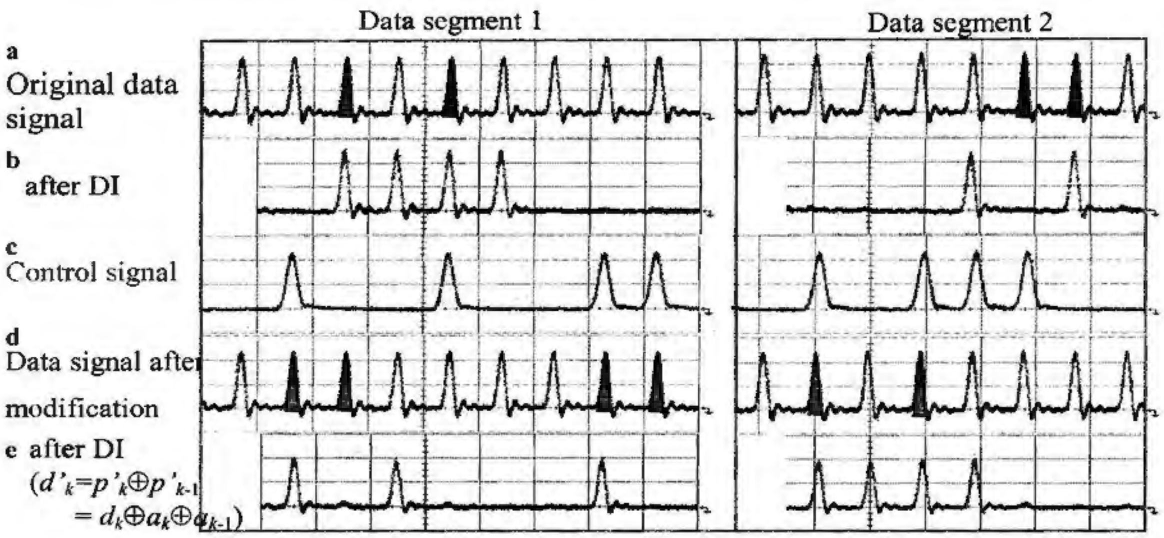

Fig. 5.5 Waveforms of the control signal (c) and the data signals: original data signal before (a) and after DI (b), recoded data signal before (d) and after DI (e). Time scale: 100 ps/div.

Due to optical Kerr effect in the DSF, the data signal experienced an additional phase shift due to self-phase modulation and XPM: $\Delta\phi = \gamma L_{eff}(P_{data} + 2P_{control})$, where γ is the nonlinear coefficient, L_{eff} is the effective fiber length, P_{data} is the data signal power and $P_{control}$ is the control signal power. In our scheme the data signal power is much less than the control signal power, therefore the phase shift caused by P_{data} is negligible and thus $\Delta\phi \cong 2\gamma L_{eff} P_{control}$. By properly adjusting the control signal power, $\Delta\phi$ can be tuned to approach π. When the control signal has a "0" level, there is no such additional phase shift applied onto the data signal and the phase information in the data signal is preserved, whereas the phase of data signal is added by π when the corresponding control signal bit is a "1". Due to phase periodicity, 2π is equivalent to a phase of 0. Therefore the phase information of the data signal can be properly changed according to the control signal. In our demonstration the data and the control signal average power input into the 10-km DSF were −15 dBm and 14 dBm respectively. In the DSF, although there was still some group velocity mismatch between the data and the control signals, their pulse overlapping could be guaranteed by the fact that the pulsewidth of the control signal was much larger than that of the data signal.

Fig. 5.5 shows the intensity waveforms of two segments of the data signal and the control signal. Fig. 5.5a shows the intensity waveform of the original DPSK data signal, which is an equal-level pulse train. The optical phase of the data signal was derived from the DI demodulated signal (Fig. 5.5b, 2e). We marked a shadow onto the pulse having a phase difference of π relative to the unmarked pulse. The control signal waveform is also shown in Fig. 5.5c. In general, the k^{th} original PSK bit p_k was recoded into $p'_k = p_k \oplus a_k$ by the control signal data p_k. On the other hand, if regarding the original data signal as a DPSK signal, its data $d_k = p_k \oplus p_{k-1}$ was changed into $d'_k = p'_k \oplus p'_{k-1} = p_k \oplus a_k \oplus p_{k-1} \oplus a_{k-1} = d_k \oplus a_k \oplus a_{k-1}$ by the control signal bits a_k and a_{k-1}. Taking the 1st data segment for example, the original phase-modulated data signal "00π0π0000" was changed into "0ππ0000ππ" by the intensity-modulated control signal "010010011." For the data segment 2, the original phase-modulated data signal "0000ππ00" was changed into "0π0π0000" by the intensity-modulated control signal "01011100."Because of DI demodulation, the first bit of the demodulated signal lost meaning and thus we did not show it here. After DI demodulation, the recoded data signal had good waveform and extinction ratio, indicating that the phase modification almost exactly equaled π.

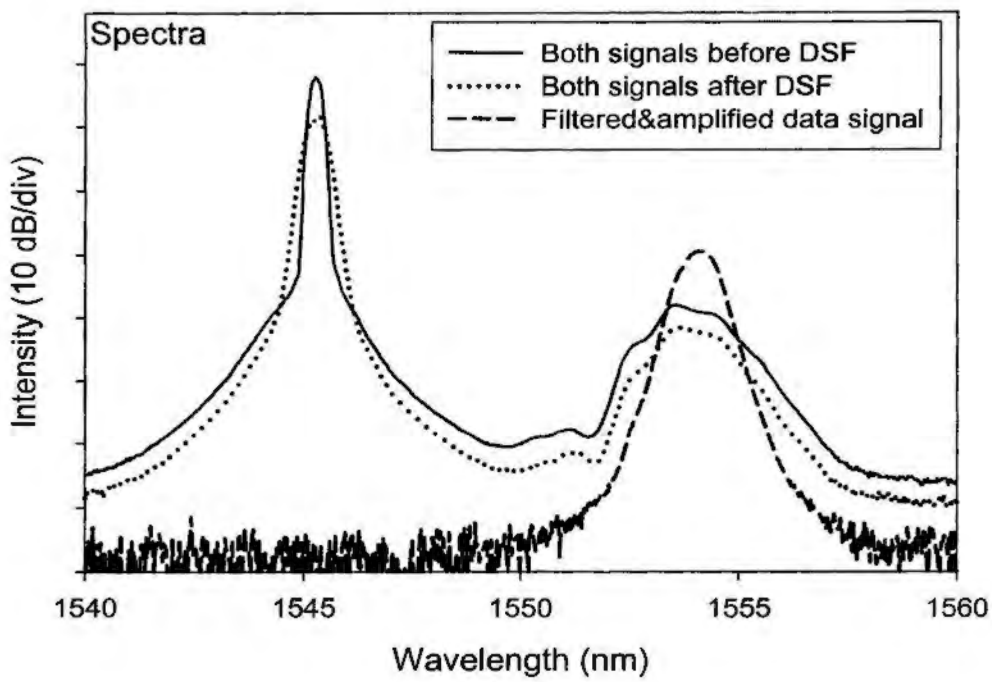

Fig. 5.6 The optical spectra of both the control and the data signals input before DSF (solid line), of both signals output after DSF (dotted line), of the filtered and amplified data signal (dashed line).

Fig. 5.6 shows the optical spectra of the control and data signals, measured with a resolution of 0.1 nm. The data signal spectrum centered at 1554.1 nm was obviously wider than the control signal, due to its much narrower time-domain pulsewidth. Self-phase modulation broadened the spectrum of the strong intensity-modulated control signal. However, because there was no soliton compression effect in the normal dispersion region, the spectrum broadening of the control signal was not severe and induced negligible crosstalk to the data signal. Moreover the control signal was easier to be kept in good quality in the normal dispersion region of the DSF than in the anomalous region [7]. We measured the bit error rates (BER) of the demodulated RZ-DPSK data signal, both before and after the phase recoding. The original DPSK data signal and the control signal were both from a 2^7-1 pseudo random binary sequence. Then we calculated the optical phase and the demodulation result of the data signal after phase recoding, according to the bit alignment relation of the data and control signals. We edited the resultant data values into the BER tester and found that the recoded optical data signal achieved error free with a receiver sensitivity of ~

−18.5dBm. This revealed the phase information was effectively and accurately recoded by the control signal.

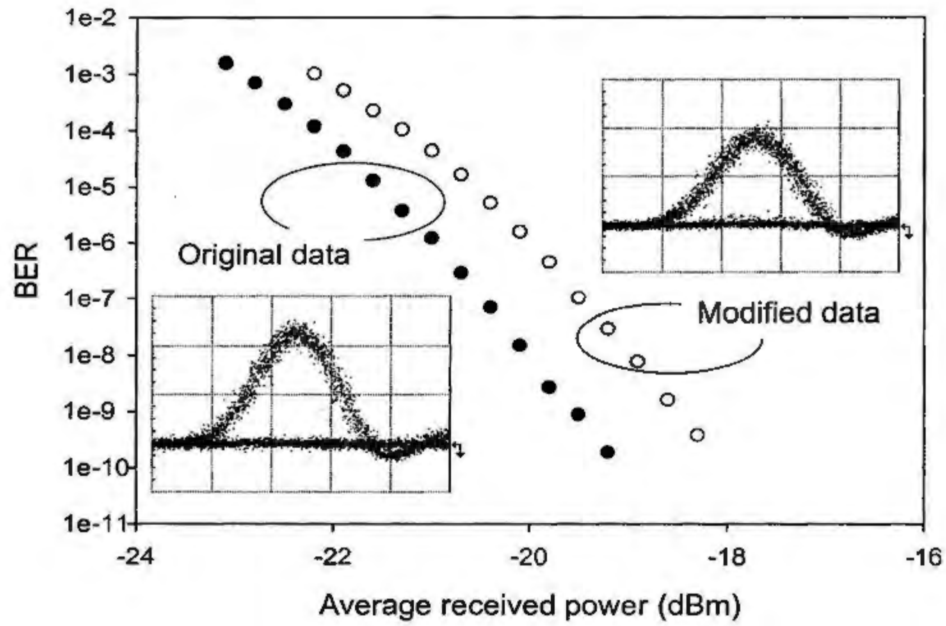

Fig. 5.7 BER measurements the original DPSK data signal (•) and the modified data signal (o) via XPM in DSF. Insets show the data signal eye diagrams of the two cases. Time base: 10 ps/div.

5.4 Experimental demonstration of all-optical label recognition

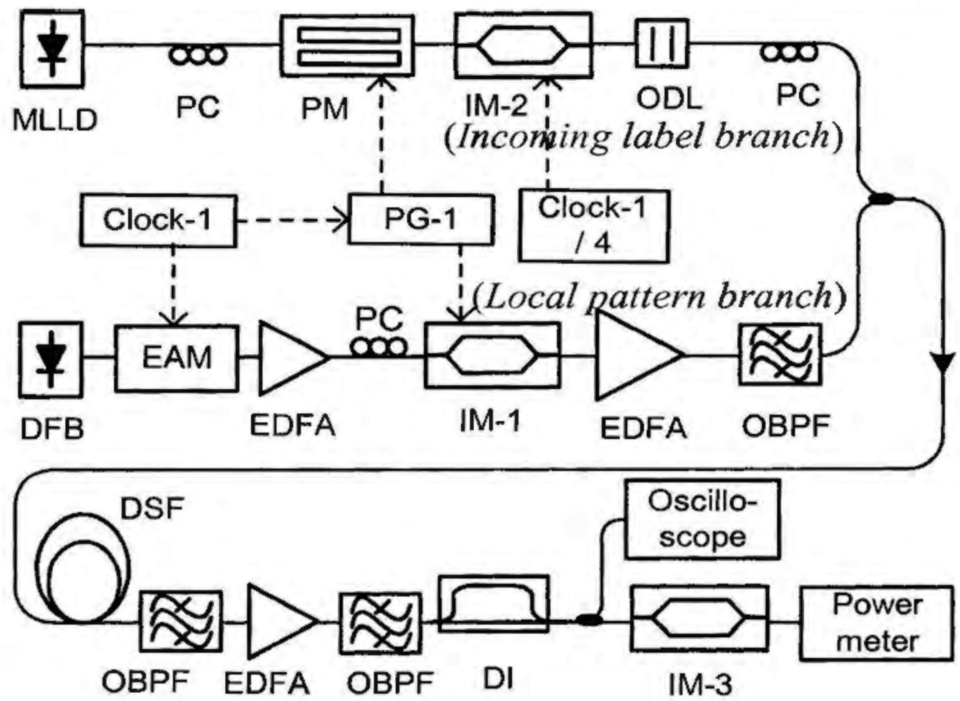

Fig. 5.8 Experimental setup. MLLD: mode-locked laser diode; PC: polarization controller; PM: phase modulator; IM: intensity modulator; ODL: optical delay line; EDFA: Erbium doped fiber amplifier; OBPF: optical bandpass filter; DFB: distributed feedback laser; EAM: electro-absorption modulator; DSF: dispersion-shifted fiber; DI: delay interferometer.

Fig. 5.8 shows the experimental setup. A semiconductor mode-locked laser diode (MLLD) generated an optical pulse sequence with ~1.5-ps pulsewidth at 1554.1 nm. A pattern generator (PG-1) operating at 10.61-Gb/s modulated the pulse sequence via an optical phase modulator. A 3-GHz intensity modulator (IM-2), driven by (10.61/4)-GHz square clock, was inserted to gate the continuous optical PM signal and produce 4-bit optical packet label. After passing through a tunable optical delay line (ODL) and a polarization controller (PC), the optical label signal was combined with a 10.61-Gb/s intensity-modulated control signal at 1545.3 nm. The pulse-width of the control signal was about 20 ps, being carved by an electro-absorption modulator (EAM). The incoming label signal and the intensity-modulated control signal were coupled into a piece of 4-km dispersion-shifted fiber (DSF). The power of the incoming label signal and the local control signal being input into the DSF were –17 dBm and +18 dBm respectively. Then an optical bandpass filter (OBPF) with a 2-nm bandwidth was used to extract the data signal. An optical delay interferometer (DI) with a relative delay of 94.3 ps was followed, and the output signal was separated and fed into a high-speed oscilloscope and another 3-GHz intensity modulator (IM-3, served as the optical temporal gating and driven by another PG) followed by an optical power meter.

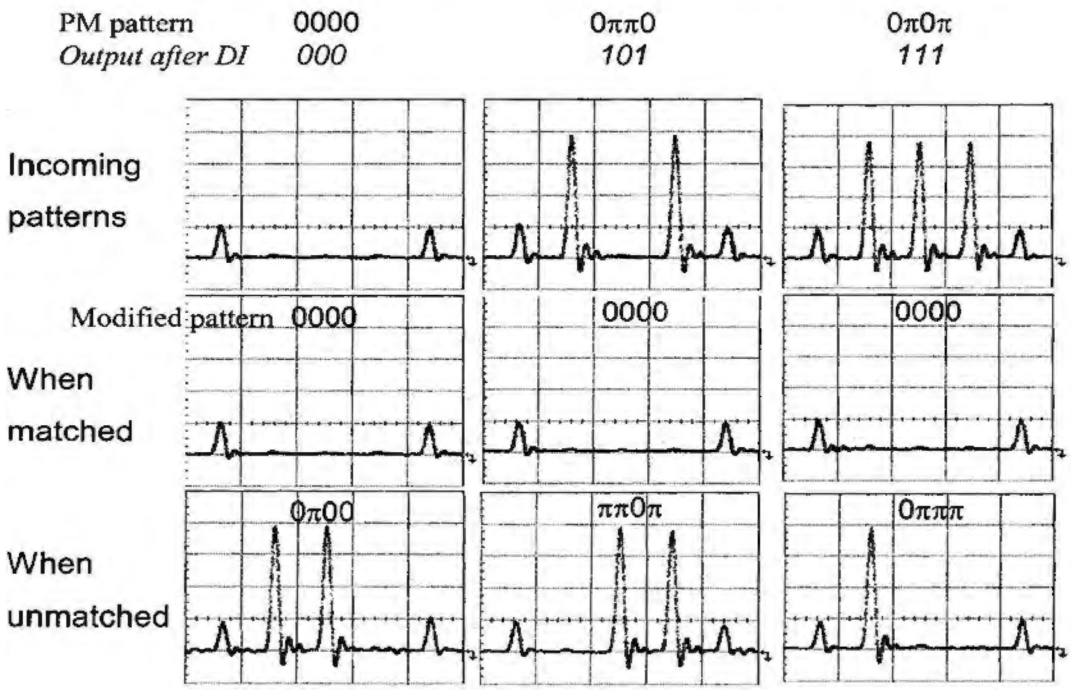

Fig. 5.9 Waveforms of the incoming label patterns before and after recognition. All waveforms were captured after the DI. Time base: 100 ps/div.

We first properly adjusted the ODL to align the incoming label with the same or different local pattern, as the matched or unmatched case, respectively. Fig. 5.9 shows the waveforms of three different 4-bit label patterns after the DI. The three incoming label patterns were "0000," "0ππ0" and "0π0π." The top row of Fig. 5.9 shows the intensity waveforms of the original three incoming label patterns at the output of the DI. The generation of the two small side pulses was due to the empty guard bands present before and after the label, and they could be removed after passing through the time gating device (IM-3). If the local patterns were matched patterns "0000," "0110" and "0101," then the three label patterns were all modified into the phase of "0000" and the DI outputted only two small side pulses (shown in the middle row of Fig. 3).

On the contrary, if the local patterns were unmatched ones, for example "0100," "1011" and "0010," the DI outputted at least one large pulse (shown in the bottom row of Fig. 5.9). The DI output in the pattern-unmatched cases certainly had much larger optical power than that in the matched cases, though there was very small amount of residual power in the matched case due to incomplete phase change and phase noises.

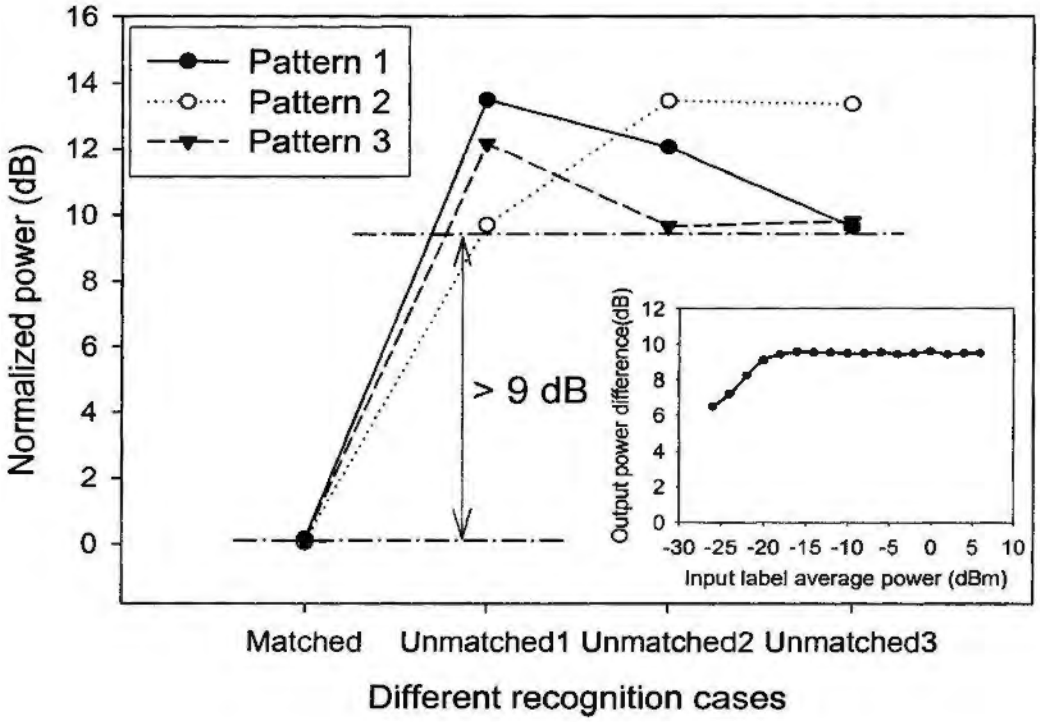

Fig. 5.10 Measured power in the pattern-recognized case and the pattern unmatched cases, for three incoming patterns "0000," "$0\pi\pi0$" and "$0\pi0\pi$."

Fig. 5.10 shows the measured optical power at the output of the recognition module with the three 4-bit label patterns. The matched case was observed when the incoming pattern and the identical local pattern were temporally pattern-aligned. On the other hand, they became unmatched when the incoming pattern and the local pattern were misaligned. We recorded and plotted the output power of recognition for the matched case and several unmatched cases. We found that the unmatched cases resulted in relatively large output power while the matched case gave very small power (normalized to 0 dB), as determined by the noise level and the power meter sensitivity. The worst case of differentiating the matched case and the unmatched cases had a substantial power difference (recognition contrast ratio) of greater than 9 dB, and thus could be easily processed by a simple electronic thresholding circuit.

At a label recognition module, the incoming optical packets may experience different optical paths and thus would have different signal qualities. Usually there should be a performance monitoring module at each core router to guarantee that the incoming packet quality is good enough for processing and forwarding. In our experiment we neglected such a module for simplicity, and assumed the packets fulfilled the performance requirement for the label recognition processing. Nevertheless, the incoming packet label power may be different from one another due to the optical path difference. We have measured the recognition dynamic range of the input PM label average power, as shown in Fig. 5.10 inset. For the input label power no less than –20 dBm, the power difference between the recognized case and unmatched cases (recognition contrast ratio) can reach 9 dB. When the input label power is too small, the optical signal-to-noise ratio was relatively poor after amplification, and thus the measured power at the output of recognition contained relatively more noise. Thus the input label average power is best to be no less than –20 dBm.

5.5 Summary

We have proposed a novel all-optical scheme for optical bit-serial PM label pattern recognition. The incoming PM label pattern is compared with an intensity-modulated local pattern in parallel via XPM. The comparison was realized via all-optical phase recoding of the incoming PM label by the local label pattern. If the incoming label and the local label had the same patterns, the recoded incoming label became to have the same phase in all of its pulses. This could be detected by measuring the optical power after feeding the recoded signal into a DI. The label recognition was thus realized in a simple way.

First, we experimentally investigated the proposed simple all-optical recoding approach. We modified the phase information of an optical data signal using another optical intensity-modulated signal, which is potentially an essential element for future all-optical signal processing modules. This technique is expected to be able to support ultrahigh speed operation because of ultrafast response of XPM in DSF. Furthermore, no wavelength conversion is needed in this method. Experimental demonstration showed 10.61-Gb/s RZ-DPSK signal was successfully recoded by a 10.61-Gb/s RZ-OOK signal. The data content of the recoded signal matched the calculated bit relations between the original data and the control signals. The BER measurement showed very small performance degradation of the data signal.

Then we demonstrated the reconfigurable all-optical label recognition scheme. The results showed that there was no optical pulse output when the incoming pattern was recognized. On the contrary, one or more optical pulses output indicated the incoming pattern did not match the local pattern. We could obtain the recognition result by simply measuring the DI output power. We tested three different 4-bit patterns and found the power difference between the matched case and the unmatched cases was at least 9 dB. This scheme can recognize any label patterns without additional complexity as compared with previous schemes, and can potentially support ultrafast label recognition at higher speed.

References

[1] D. J. Blumenthal, B. E. Olsson, G. Rossi, T. E. Dimmick, L. Rau, M. Masanovic, O. Lavrova, R. Doshi, O. Jerphagnon, J. E. Bowers, V. Kaman, L. A. Coldren and J. Barton, "All-optical label swapping networks and technologies," *Journal of Lightwave Technology*, vol. 18, no. 12, pp. 2058-2075, 2000.

[2] W. Hung, C.K. Chan, L.K. Chen, F. Tong, "A Bit-Serial Optical Packet Label Swapping Scheme using DPSK Encoded Labels," *Photonics Technology Letters*, vol. 15, no. 11, pp. 1630-1632, 2003.

[3] D. Klonidis, R. Nejabati, C. Politi, M. O'Mahony, "All-Optical Packet Switching of 40Gb/s Variable Length Packets Using Dual-Pump FWM Controlled by Fast Tunable Laser," in *European Conference on Optical Communication (ECOC)*, paper Th1.6.2, Stockholm, Sweden, 2004.

[4] J .J. V. Olmos, I. T. Monroy, J. P. Turkiewicz, Y. Liu and A. M. J. Koonen, "Self-controlled all-optical label and payload separator for variable length bursts in a time-serial IM/DPSK scheme," *Photonics Technology Letters*, 17, pp. 1692-1694, 2005.

[5] R. Takahashi, *et al*, "40-Gb/s label recognition and 1×4 self-routing using self-serial-to-parallel conversion," *Photonics Technology Letters*, Vol. **16**, no. 2, pp. 692-694, 2004.

[6] K. Chan, F. Tong, C.K. Chan, L.K. Chen, W. Hung, "An All-Optical Packet Header Recognition Scheme for Self-Routing Packet Networks", in *Optical Fiber Communication Conference (OFC)*, paper WO4, Anaheim, CA, USA, Mar 2002.

[7] N. Calabretta, G. Contestabile, E. Ciaramella, "All-optical label erasure/recognition of novel DPSK optical packets for optical packet switching," in *Optical Fiber Communication Conference (OFC)*, paper OtuC5, Anaheim, CA, USA, Mar 2005.

[8] M.T. Hill, A. Strivatsa, N. Calabretta, Y. Liu, H. d.Waardt, G.D. Khoe, H.J.S. Dorren, "1×2 optical packet switch using all-optical header processing", *Electronics Letters*, Vol. 37, no. 12, pp. 774-775, Jun 2001.

[9] J. M. Martinez, J. Herrera, F. Ramos, J. Marti, "All-optical address recognition scheme for label-swapping networks," *Photonics Technology Letters*, Vol. 18, no. 1, pp. 151-153, Jan 2006.

[10] A. J. Poustie, K. J. Blow, A. E. Kelly, and R. J. Manning, "All-optical parity checker with bit-differential delay," *Optics Communications*, vol. 159, pp. 208–214, 1999.

6 A WDM-PON with Centralized Light Sources and Multicast Overlay Using DPSK Signals

6.1 WDM-PON with centralized light sources

As introduced in Chapter 1, to facilitate the wavelength management and maintenance, the WDM-PON architecture with centralized light sources (CLS) at the optical line terminal (OLT) has emerged as an attractive solution [1-3]. With no wavelength-registered light source incorporated at the optical network unit (ONU), wavelength provisioning, monitoring and stabilization at every ONU are unnecessary and thus such wavelength independent (so-called "colorless") ONUs greatly eases the network maintenance and reconfiguration. In a realization of such a CLS PON, in additional to the downstream laser sources, extra laser diodes were installed at the OLT to provide light source for the upstream data which increased the system cost [2]. Some other demonstrations avoided this problem by directly re-use the downstream light as the upstream carrier at the ONU. In order to let the upstream signal be modulated onto the downstream light without interference, a portion of the temporal period of the downstream signal was left unmodulated and reserved for upstream data [1]. However, this reduced the downstream bandwidth and the upstream re-modulation had to synchronize with the unmodulated downstream time slots. Another approach of downstream light re-use at the ONU was to apply a semiconductor optical saturator/modulator [3] to erase the downstream data before the re-modulation. The use of such a proprietary component may be of high cost and be difficult to control. Moreover, the downstream signal should have a low extinction ratio so that data erasure could work, which sacrificed the downstream signal quality.

In the CLS PON demonstrations mentioned above, nonreturn-to-zero was employed as the line coding format. Recently, we have proposed to employ inverse-return-to-zero (IRZ) as the downstream signal format instead of nonreturn-to-zero to facilitate the upstream data re-modulation [4]. An optical IRZ signal carries power in both "one" and "zero" bits, which can provide the light source for the upstream signal in every time slot. The downstream light containing IRZ signals can be directly re-used at the ONU, without any data erasure procedure. On the other hand, employing IRZ only increases very small complexity compared with nonreturn-to-zero system.

An IRZ signal is formed by inverting the intensity level of a conventional return-to-zero signal, thus it carries a certain level of optical power in both "one" bits and "zero" bits. Therefore, the downstream optical power received at the ONU can be directly re-modulated by the upstream data. No downstream data erasure is needed and it can still maintain high extinction ratio of the downstream optical signal. Meanwhile, the downstream IRZ signal can be directly detected by a photodiode followed by an electrical inverting amplifier. This guarantees the complexity of the downstream receiver to be similar with a traditional receiver for nonreturn-to-zero signals.

Fig. 6.1 illustrates the WDM-PON architecture utilizing IRZ as the downstream signal format. Each transceiver at the OLT generates downstream IRZ signals and receives upstream re-modulated signals for the corresponding subscriber. The logic-AND operation between the downstream nonreturn-to-zero data and a clock signal can produce a return-to-zero shaped data signal. It is then used to drive a Mach-Zehnder intensity modulator (IM) biased at the quadrature point of the negative slope of the IM response curve, to generate the downstream IRZ signal. In this way, an electrical data bit "zero" modulates the CW light to possess optical power in its full bit period, while a return-to-zero electrical data bit "one" modulates the CW light as a dark pulse waveform. To increase the economical feasibility, an optical IRZ signal can also be generated by directly modulate a laser diode with the electrically inverted logic-AND result if the data rate is within the laser diode's modulation bandwidth. Hence, the generated IRZ signal carries finite optical power at both "one" levels and "zero" levels. On the other hand, it can be simply detected by a photodiode followed with an electrical inverting post-amplifier at the ONU.

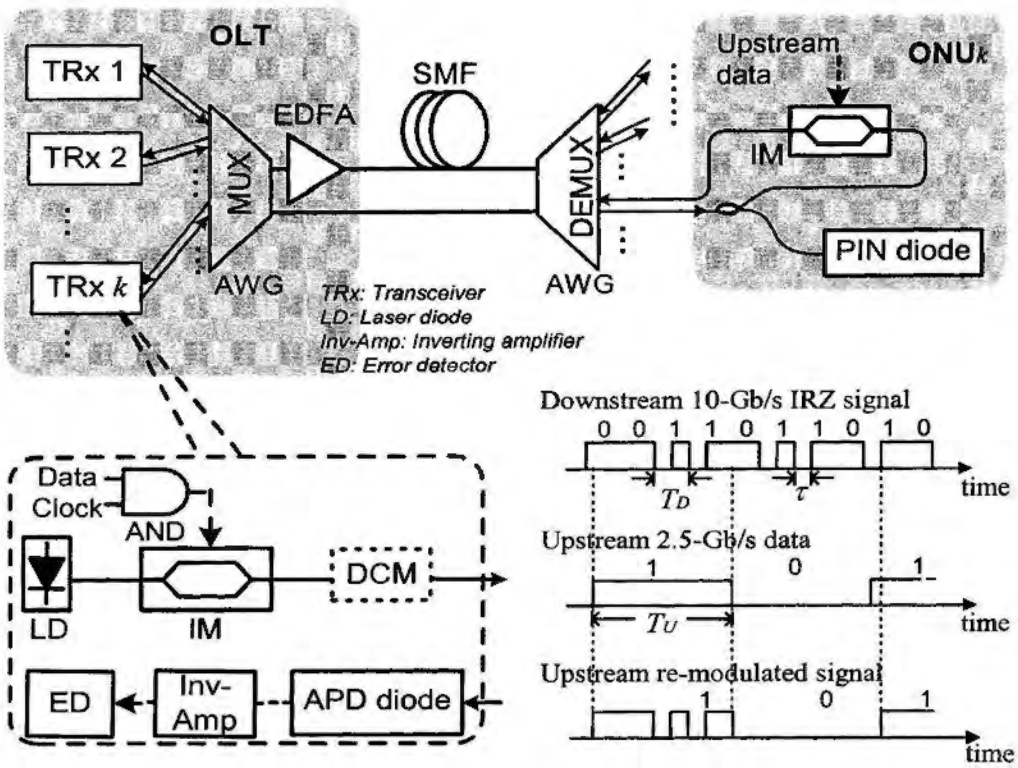

Fig. 6.1 The architecture schematic of the CLS WDM-PON employing downstream IRZ signals. The insets show the typical waveforms of the downstream optical IRZ signal, the upstream data signal, and the re-modulated upstream optical signal, respectively. AWG: arrayed waveguide grating; EDFA: Erbium doped fiber amplifier; SMF: single-mode fiber; IM: intensity modulator; DCM: dispersion compensating module; IM: intensity modulator.

The downstream IRZ signals from every transceiver in the OLT are WDM multiplexed, via an array waveguide grating (AWG), to the downstream fiber feeder. After transmission, the downstream traffic from the OLT is wavelength routed by another AWG at the remote node towards different ONUs. At an ONU, a portion of the received downstream signal power is tapped off for reception, while the remaining power is fed into an optical intensity modulator for upstream data re-modulation. The finite optical power in each bit of the downstream IRZ signal provides the light source for the upstream data in every bit slot. An example ideal IRZ waveform as well as the re-modulation process is described in Fig. 1 insets. The portion of downstream light carrying upstream nonreturn-to-zero data was then transmitted back to the OLT, through the remote node and the upstream fiber link. A pair of feeder fibers is used to avoid the possible Rayleigh backscattering induced performance degradation on both the downstream and the upstream signals.

3.2 WDM-PON with broadcast overlay

To realize more flexible network functions, some efforts have been paid to provide both point-to-point data service and broadcast video/data service in WDM-PONs [5-8]. As most of WDM-PONs were initially designed for point-to-point data transfer only, sometimes people also call the add-on broadcast video/data service is a broadcast overlay. These two service data could be transmitted via time division multiplexing, but complicated timing control is required and the downstream bandwidth needs to be shared.

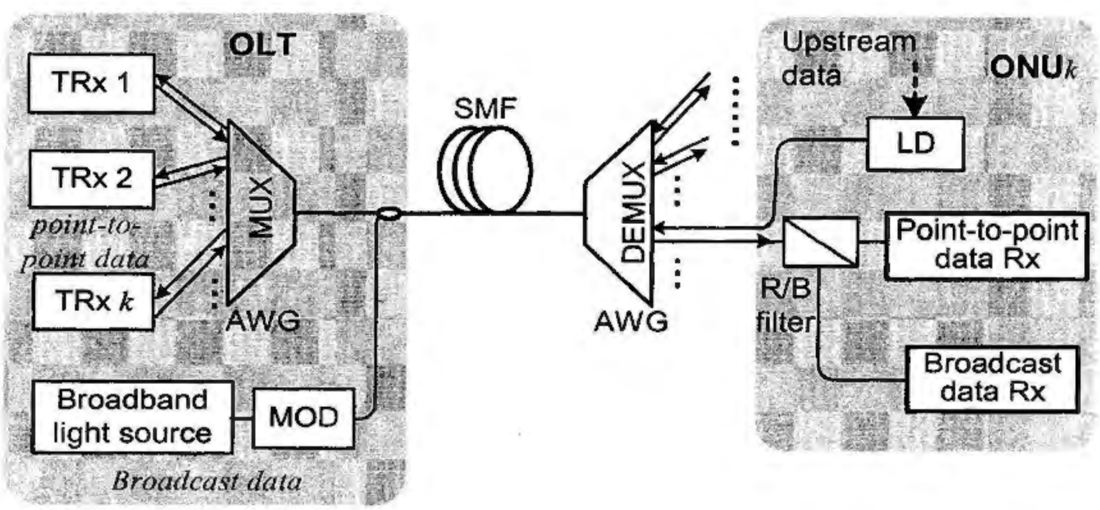

Fig. 6.2 A WDM-PON architecture with downstream broadcast overlay using broadband light source [5].

Another common approach was to use one or more additional light sources [5-6]. As shown in Fig. 6.2, a broadband light source, in a waveband different from the point-to-point light waves, is added at the OLT [5]. Then the downstream broadcast data is modulated onto the broadband light, and is combined with the downstream point-to-point data. Both of the two data sets are transmitted to the ONUs via the feeder fiber. At the remote node, every point-to-point wavelengths are routed to the corresponding ONU. Meanwhile, the broadcast data on the broadband light is routed to every ONU, benefited from the free spectral range (FSR) property of the AWG. Because of the added broadband light source, this scheme led to significant cost increase. Alternatively, a laser diode, instead of a costly broadband light source, can be used in the OLT to carry the broadcast data [6]. However, special routing design should be adopted at the AWG in the remote node, which led to additional complexity and insertion loss.

Some recent work proposed broadcast overlay on the same optical carrier with the downstream point-to-point data, based on subcarrier multiplexing (SCM) [7-8]. However, SCM technique requires high-frequency electronic components at both transmitter and receiver sides. In addition, the downstream capacity is limited due to the complexity in implementing high bit-rate baseband signal on a subcarrier.

In the above work, a light source is deployed in each ONU for each WDM upstream channel. However, as discussed in the previous section, employing centralized light sources at the OLT is an attractive approach for low-cost implementation. Since no wavelength registered light source is incorporated at the ONU, wavelength management at the ONU is unnecessary and thus greatly eases the network maintenance. At the ONU, the upstream data transmitter was realized by remodulating part of the received downstream signal power.

In this project, we propose a novel WDM-PON architecture to provide a downstream broadcast overlay on the conventional point-to-point data service. The proposed network offers both downstream services and upstream carrier provision with centralized light sources. In every wavelength channel, inverse-return-to-zero (IRZ) format is employed to carry the point-to-point data, while the differential-phase-shift keying (DPSK) broadcast/multicast data is superimposed onto it. With simple control in the transmitters at the OLT, the broadcast data can be selectively multicasted to specific subscribers. Moreover, using downstream IRZ signal format, the upstream data can be remodulated on the received downstream carrier, before being delivered back to the OLT.

3.3 Proposed WDM-PON architecture with centralized light sources and broadcast/multicast overlay

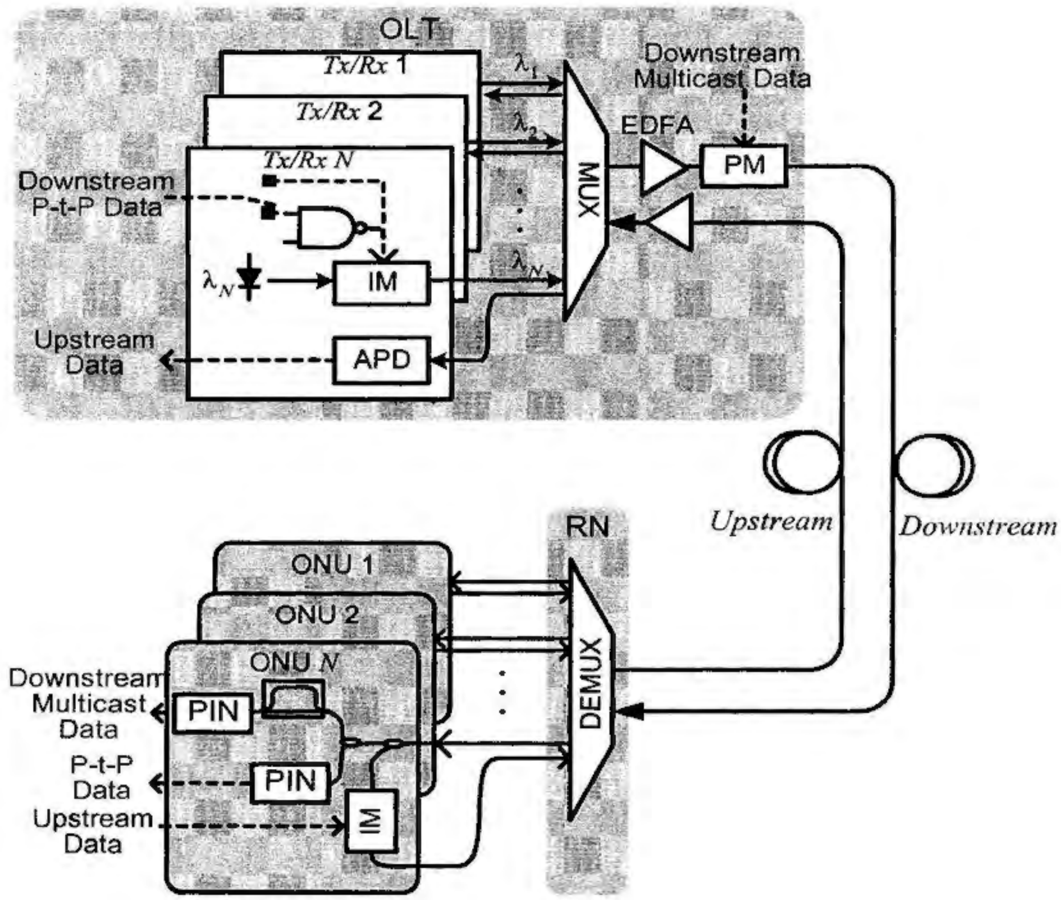

Fig. 6.3 Proposed WDM-PON architecture with centralized light sources and multicast overlay. IM: intensity modulator, PM: phase modulator; EDFA: Erbium doped fiber amplifier; OLT: optical line terminal; RN: remote node; ONU: optical network unit.

Fig. 6.3 depicts the proposed WDM-PON architecture with centralized light sources and multicast overlay. The downstream point-to-point data of every wavelength channel is generated from an IRZ transmitter. A logic NAND gate is used to produce an inversed return-to-zero shaped data signal, which is then used to drive an external modulator or a laser diode to generate an IRZ signal. The downstream IRZ signals from every transceiver in the OLT are WDM multiplexed, via an array waveguide grating (AWG) or equivalent. The multiplexed signals are then amplified and fed into an optical phase modulator (PM), driven by the pre-coded digital broadcast or multicast data. Since an IRZ signal consists of a period of high level at both "1" and "0" bits, the DPSK broadcast or multicast data can be successfully superimposed onto all the optical IRZ signals, without lost of bit information. In this way, every downstream wavelength carries both the IRZ point-to-point data and the DPSK multicast data.

When all the downstream point-to-point transmitters produce IRZ signals, the superimposed DPSK signal is broadcasted to all the ONUs. To realize multicast, a simple electronic control circuit can be added in each IRZ transmitter at the OLT. At normal operation, the transmitter generates an IRZ signal and the DPSK signal can be distributed to the corresponding ONU. To disable the DPSK data distribution, the control circuit triggers the point-to-point data signal to bypass the electronic NAND gate and directly drive the IM. Therefore, optical non-return-to-zero (NRZ) signal, instead of IRZ signal, is generated to carry the downstream point-to-point data. In this way, the DPSK broadcast data can be still modulated on the NRZ point-to-point signal, but it cannot be recovered at the ONU (unless theNRZ signal has an extinction ratio lower than 4.7 dB [9]). Therefore, downstream multicasting is realized. It is noteworthy that the multicast is centrally controlled in the OLT, and is transparent to every ONU receiver.

After downstream transmission, the downstream traffic from the OLT is wavelength routed by another AWG at the remote node (RN) towards different ONUs. At an ONU, a portion of the received downstream signal power is tapped off for reception. The IRZ or NRZ point-to-point data can be directly detected by a photodiode while the DPSK multicast data can be detected after demodulation. The remaining downstream power is fed into an optical intensity modulator for upstream data remodulation. As the downstream signal has a finite extinction ratio, the optical power in each bit can provide the light source for the upstream data in every bit slot. As the upstream bit rate (say 2.5 Gb/s) is usually lower than the downstream bit rate (say 10 Gb/s), no bit synchronization is required at the ONU.

3.4 Experimental demonstration

We have experimentally demonstrated downstream multicast and upstream remodulation of the proposed WDM-PON. Continuous-wave lights at 1546.9 nm and 1547.7 nm were IRZ (or NRZ) modulated by a 10-Gb/s 2^{31}-1 pseudo-random binary sequence (PRBS) and its complementary data, respectively, with an extinction ratio of around 8 dB. After wavelength multiplexing and power amplification, the WDM point-to-point signals were fed into a PM, driven by the decorrelated 10-Gb/s PRBS as the pre-coded broadcast data. In this experiment the point-to-point and the broadcast signals were bit synchronized, which could be simply realized by applying a common clock signal at the OLT. Then the composite signal was coupled into a 20-km dispersion-shifted fiber to emulate the downstream transmission link with proper dispersion compensation. At the ONU, a portion of the received downstream signal power was tapped off by a 3-dB optical power splitter, in which a half was fed into a photodiode for IRZ detection and the rest was demodulated by a delay interferometer (DI) for DPSK detection. The other portion of the received downstream signal was fed into an optical intensity modulator, driven by a 2.5-Gbit/s 2^{31}-1 PRBS as the upstream data, before being transmitted back to the OLT via another piece of 20-km dispersion-shifted fiber.

When the multicast was enabled, that is, when the downstream point-to-point signal was in IRZ format, the superimposed DPSK multicast data could be detected at the ONU. As every bit of an IRZ signal provided a period of high level as shown in Fig. 6.4(a), the demodulated DPSK signal showed a clear eye diagram as Fig. 6.4(b), though the horizontal width of the eye was narrowed. On the contrary, when the multicast was disabled, the demodulated DPSK signal on the point-to-point NRZ signal had a multiple-level eye as Fig. 6.4(c), agreeing with the theory [9]. Since the point-to-point signal had a relatively high extinction ratio of 8 dB, some "0" bits of the demodulated DPSK signal had a higher level than some "1" bits, causing significant detection errors. We have measured the bit error rate (BER) of the demodulated DPSK signal, as shown in Fig. 6.5. As the two WDM channels had very similar performance, only the BER for the 1546.9-nm channel was shown. The receiver sensitivity for the multicast data was less than −19 dBm (measured after DPSK demodulation) when multicast was triggered; while the BER could not be measured when multicast was disabled.

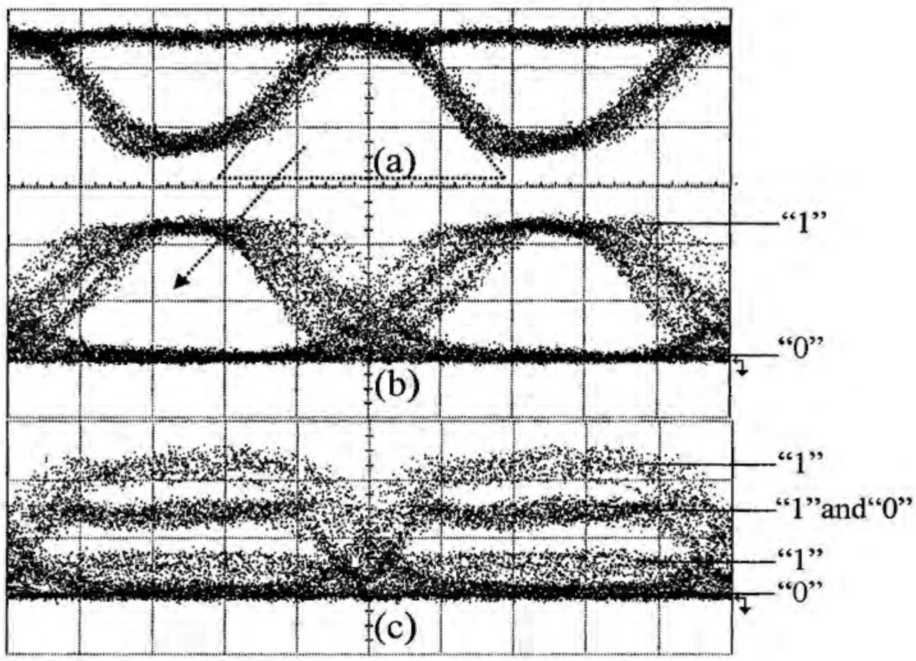

Fig. 6.4 Eye diagrams of (a) the 10-Gb/s downstream point-to-point data signal while in IRZ format (the high level of each bit in the trapezoid provided power for DPSK modulation), (b) the 10-Gb/s demodulated DPSK multicast signal when multicast was enabled, (c) the demodulated DPSK signal when multicast was disabled. Time scale: 20 ps/div.

Fig. 6.6 shows BER of the downstream point-to-point IRZ or NRZ signal. Negligible penalty was observed for both signals after transmission. For the upstream 2.5-Gb/s remodulated signal, an APD photodiode was employed at the OLT for detection, followed by an electrical low-pass filter with a 3-dB bandwidth of 1.87 GHz. It could effectively alleviate the degradation caused by the crosstalk from the downstream 10-Gb/s IRZ or NRZ signal. From the BER result in Fig. 6.7, the remodulated upstream signal had better performance when the downstream point-to-point signal was in IRZ format. This is attributed to the fact that the intensity variation of "0" and "1" bits of an IRZ signal is smaller than that of an NRZ signal. Such difference of the receiver sensitivities does not influence the normal operation of the system, as sufficient system margin has been designed for both cases.

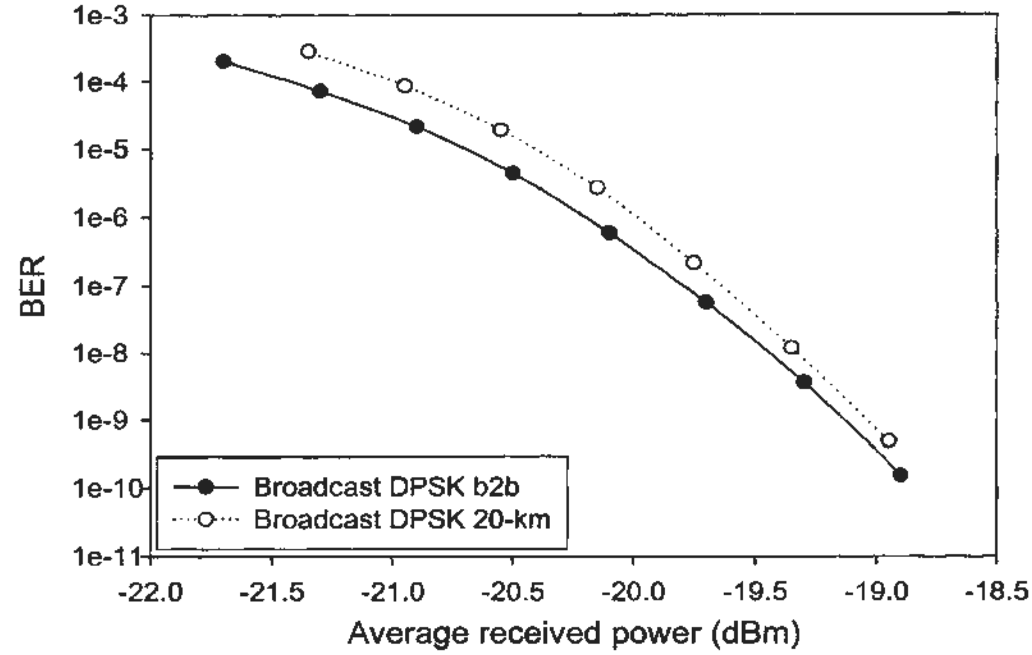

Fig. 6.5 BER of the downstream broadcast DPSK signal.

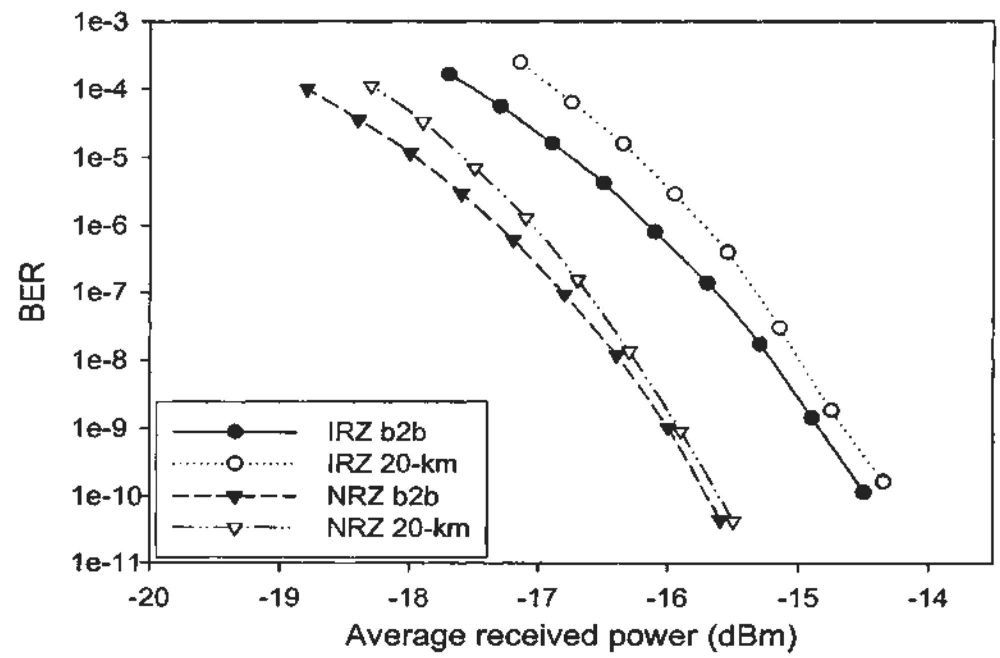

Fig. 6.6 BER of the downstream point-to-point signal.

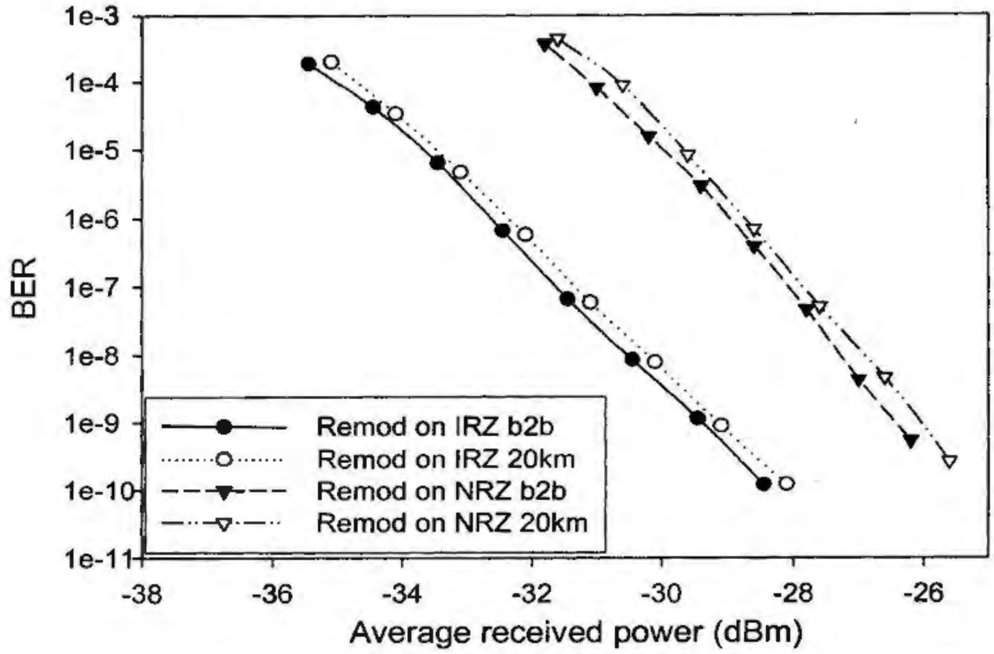

Fig. 6.7 BER of the upstream remodulated signal.

Table 6.1

	Modulation format	Received power	Receiver sensitivity	System margin
Downstream point-to-point	IRZ	−13 dBm	−15 dBm	2 dB
	NRZ	−13 dBm	−16 dBm	
Downstream multicast	DPSK	−16 dBm	−19 dBm	3 dB
Upstream Signal	Remodulated on IRZ	−20 dBm	−29 dBm	6 dB
	Remodulated on NRZ	−20 dBm	−26 dBm	

In the demonstration, the signal power of each channel fed into the downstream transmission link was around 3 dBm. The downstream loss caused by transmission and demultiplexing was 10 dB in total, thus the downstream power arrived at the ONU was –7 dBm. For 50/50 power splitting between downstream reception and upstream remodulation, the respective received power for DPSK demodulation and for IRZ or NRZ detection was –13 dBm, implying around 2-dB system margin for the downstream point-to-point signal and at least 3-dB system margin for the broadcast signal. Another portion of –10-dBm downstream light was remodulated by the upstream data, experiencing an excess loss of 7 dB. The optical power received at the receiver in the OLT for a channel would be around –32 dBm without amplification. However, by using a common amplifier before the AWG, at least 5-dB system margin could be provided for each upstream signal. The details of the system margin are summarized in Table 6.1.

For the downstream IRZ signal, its duty cycle determines the amount of optical power contained in the "one" bit, and thus would influence the performance of both the downstream signals and the re-modulated upstream signals. We define the duty cycle of the downstream IRZ signal as $\xi = \tau/T_D$, where T_D is the downstream signal period (T_D = 100 ps for 10-Gb/s signal), and τ is the width of the inversed pulse in the "one" level. The generated IRZ duty cycle in the experiments was estimated to be around 0.6. The ELPF at the receiver can be modeled as an integrator over a signal period [10]. Therefore for the downstream IRZ signal, the decision variables for the "one" and "zero" levels are $V_{D1} = \int_0^{T_D} R \cdot P_{D1}(t)\mathrm{d}t \big/ T_D = \xi PR$ and $V_{D0} = \int_0^{T_D} R \cdot P_{D0}(t)\mathrm{d}t \big/ T_D = 0$ respectively, where R is the photodiode's responsivity, $P_{D1}(t)$ and $P_{D0}(t)$ are the respective inversed temporal power profiles for the downstream "one" and "zero" levels. In access scenario without amplifier chains, it is reasonable to assume Gaussian noise statistics and the noise variances for "ones" and "zeros" are equal ($\sigma_1=\sigma_0=\sigma$); and the Q factor can be expressed as $(V_{D1}-V_{D0})/(2\sigma)$ and approximates 6 to achieve BER=10^{-9} [11]. That is, for the downstream $Q_D = (V_{D1}-V_{D0})/(2\sigma)=\xi PR/(2\sigma)=6$. Together with the expression of the average received downstream optical power $\overline{P}_D = (1/2)(1-\xi)P + (1/2)P = (1-\xi/2)P$, we have

$\overline{P}_D = (12\sigma)(1-\xi/2)/(R\xi)$ which is the receiver sensitivity of the IRZ signal. This can also be expressed with respect to the receiver sensitivity of a conventional nonreturn-to-zero signal (i.e. ξ=1) as $\overline{P}_{D,rec}[\text{dBm}] = \overline{P}_{D,rec,\xi=1}[\text{dBm}] + 10\log_{10} 2(1-\xi/2)/\xi$. Fig. 6.8 depicted the relation of $\overline{P}_{D,rec}$ (normalized with respect to $\overline{P}_{D,rec,\xi=1}$) against the value of ξ.

Similarly, the ELPF in the upstream receiver at the OLT also functions as an integrator over an upstream signal period T_U. The decision variable for bit "zero" is $V_{U0} = \int_0^{T_U} R\cdot P_{U0}(t)\mathrm{d}t \Big/ T_U = 0$ whereas for bit "1" $V_{U1} = \int_0^{T_U} R\cdot P_{U1}(t)\mathrm{d}t \Big/ T_U$ has many possible values, where $P_{U0}(t)$ and $P_{U1}(t)$ are the respective temporal power profiles for the upstream "zero" and "one" bits. The integration starting position can be at any timing point within a downstream bit and the integrating period may contain different downstream bit patterns. Here we consider a case where the starting position of an upstream bit is exactly the same as that of a downstream bit, in which an upstream re-modulated bit contains four full-period downstream bits. According to different bit pattern combinations of the four downstream bits, V_{U1} has five possible values (1-ξ)PR, (1-0.75ξ)PR, (1-0.5ξ)PR, (1-0.25ξ)PR, and PR, with their respective occurrence probabilities being 1/32, 1/8, 3/16, 1/8, and 1/32. Based on the above analysis, the error probability of the upstream signal can be derived by summing up the product of each error probability and its corresponding occurrence probability. We have numerically solved the error probability function and obtained the receiver sensitivity of the upstream re-modulated signal normalized with respect to the case using CW light as the upstream carrier (i.e., ξ=0), as depicted in Fig. 6.8. By respectively using the IRZ transmitter in our experiment and another method of IRZ generation based on dual-drive Mach-Zehnder IM [12], the downstream and upstream receiver sensitivities at ξ=0.6 and ξ=0.3 were also measured. It is shown that the calculations agree with the measured receiver sensitivities ("×" for the downstream IRZ signal and "O" for the upstream signal). These relations are useful to facilitate the system designs in terms of system margin, power budget, downstream/upstream power splitting ratio, etc.

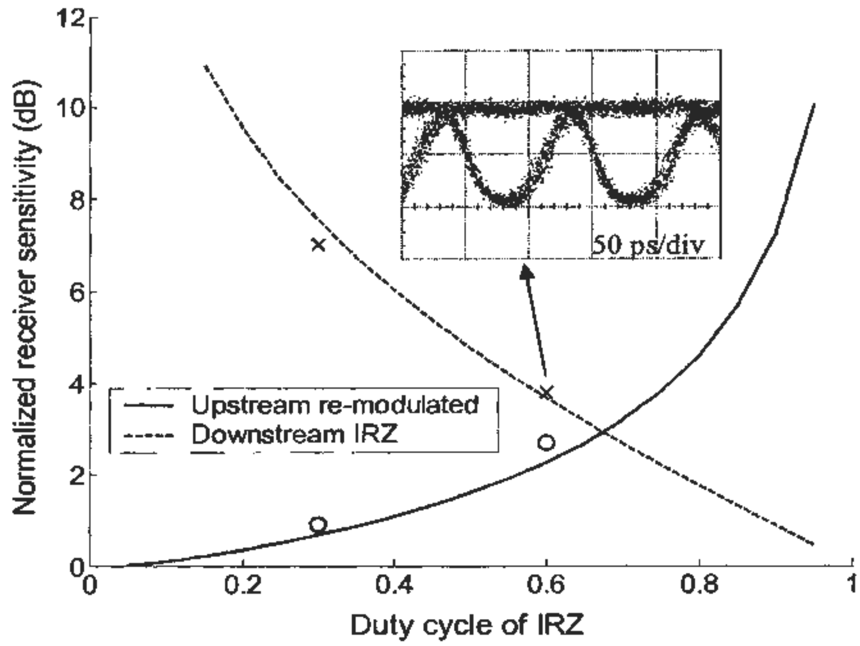

Fig. 6.8 The normalized back-to-back receiver sensitivities of the 10-Gb/s downstream IRZ and the 2.5-Gb/s upstream re-modulated signals versus the IRZ duty cycle. Symbols indicate the experimental measurements while lines indicate the theoretical performance. The inset shows the measured eye diagram of the downstream IRZ signal.

3.5 Summary

We have proposed and experimentally demonstrated a novel WDM-PON architecture to provide both downstream point-to-point data service and digital multicast service on the same light carrier. The multicast overlay adds only a little complexity to the existing WDM-PON structure, and offers better network flexibility by providing another downstream service of either broadcast or multicast. The multicast control is simple and centralized at the OLT. Experimental demonstration with 10-Gb/s downstream signals and 2.5-Gb/s upstream remodulated signals confirmed the feasibility of the proposed scheme.

References

[1] N.J. Frigo, P. P. Iannone, P.D. Magill, T.E. Darcie, M.M. downs, B.N. Sesai, U. Koren, T.L. Koch, C. Dragone, H.M. Presby, and G.E. Bodeep, "A wavelength-division multiplexed passive optical network with cost-shared components," *Photonics Technology Letters*, Vol. 6, no. 11, pp. 1365-1367, 1994.

[2] K.M. Choi, C.H. Lee, "Colorless operation of WDM-PON based on wavelength locked Fabry-Perot laser diode," in Proc. *31th European Conference on Optical Communication (ECOC)*, paper We3.3.4, Glasgow, UK, 2005.

[3] Y. Shibata, N. Yoshimoto, "2.5-Gbit/s wavelength channel data rewriter using semiconductor optical saturator/modulator for drop-and-rewrite WDM networks", in Proc. *29th European Conference on Optical Communication (ECOC)*, paper Th2.3.3, Rimini, Italy, 2003.

[4] N. Deng, C.K. Chan, L.K. Chen, "A centralized-light-source WDM access network utilizing inverse-RZ downstream signal with upstream data remodulation," *Optical Fiber Technology*, vol. 13, no. 1, pp.18-21, 2007.

[5] J. H. Moon, K.M Choi, C.H. Lee, "Overlay of Broadcasting Signal in a WDM-PON," in *Optical Fiber Communication Conference and Exposition and The National Fiber Optic Engineers Conference (OFC/NFOEC) 2006*, paper OTHK8.

[6] E.S. Son, K.H. Han, J.K. Kim, Y.C. Chung, "Bidirectional WDM passive optical network for simultaneous transmission of data and digital broadcast video service," *Journal of Lightwave Technology*, vol. 21, no. 8, pp. 1723- 1727, 2003.

[7] M. Khanal, C.J. Chae, R.S. Tucker, "Selective broadcasting of digital video signals over a WDM passive optical network," *Photonics Technology Letters*, vol. 17, no. 9, pp. 1992-1994, 2005.

[8] C.A. Chan, M. Attygalle, A. Nirmalathas, "Provision of independent services in WDM passive optical networks using closely separated dual baseband channels," in *Optical Fiber Communication Conference and Exposition and The National Fiber Optic Engineers Conference (OFC/NFOEC) 2007*, paper JWA48.

[9] M. Ohm, J. Speidel, "Quaternary optical ASK-DPSK and receivers with direct detection," *Photonics Technology Letters*, vol. 15, no. 1, 2003.

[10] G.J. Foschini, L.J Greenstein, G. Vannucci, "Noncoherent detection of coherent lightwave signals corrupted by phase noise," *Transaction on Communications*, vol. 36, no. 3, pp. 306-314, 1988.

[11] G.P. Agrawal, *Fiber-optic communication systems*, 3rd Ed., Wiley-Interscience, 2002.

[12] M. Ogusu, K. Ide, S. Ohshima, "0.8-b/s/Hz WDM of 40-Gb/s inverse-RZ signals without using polarization-division-multiplexing and pre-filtering techniques," in *9th Optoelectronics and Communications Conference (OECC)*, paper 13C2-2, Yokohama, Japan, 2004.

7 Conclusion

7.1 Summary of the thesis

In this thesis, we have investigated the signaling and related information processing technology of optical phase modulation, especially of the DPSK modulation format. The scope of the research is within the area of fiber-optic communication networks, ranging from the backbone transmission networks, then to the middle-level metro network, and at last to the last-mile optical access networks.

In details, we have proposed and experimentally demonstrated a novel OTDM scheme with hybrid modulation formats of ASK and DPSK, which can significantly enhance the demultiplexing performance. As the multiplexer of a conventional OTDM system is simple while the main difficulty lies in the demultiplexer, the significance of our proposed scheme is obvious: the simplification and improvement of the demultiplexer means the increased feasibility of OTDM systems. We have described the principle and experimental results in Chapter 3. First, a 42.44-Gb/s OTDM demultiplexing experiment showed that our proposed hybrid OTDM could enhance the tolerance to timing misalignment in demultiplexing by a factor of 2, compared with conventional OTDM with homogenous modulation formats. Second, we successfully demonstrated 84.88-Gb/s hybrid OTDM demultiplexing using a commercial EAM demultiplexer operated at normal condition. On the contrary, the attempt of demultiplexing a 84.88-Gb/s conventional OTDM signals failed, with the same operating condition. Again, this revealed that our proposed hybrid OTDM enhanced the tolerance to adjacent-channel crosstalk and thus improve the demultiplexing performance. Third, we demonstrated that a two-channel hybrid OTDM signal could be directly detected without demultiplexing, which was unimaginable using conventional OTDM.

For next-generation optical metro networks, high-speed optical packet switching is an attractive solution, among which all-optical processing is essential. Moreover, as discussed in Chapter 1, optical phase modulation is becoming the optimal choice of future systems due to its superior performance. Therefore, in Chapters 4 and 5, we have proposed a novel all-optical logic and an all-optical label recognition circuit, for optical phase modulated signals. Our proposed all-optical XOR gate for PSK or DPSK signals is based on FWM in SOA, which in nature can realize ultrahigh-speed operation with a compact configuration. We have demonstrated the world's first three-input XOR gate, which could effectively reduce the cascaded number of logic gates and improve the scalability in digital processing systems. In the experiment, we have measured the BER of the output signal of the all-optical XOR gate, which was often ignored by researchers in studying all-optical logic. BER measurements showed negligible power penalty for two-input XOR gate and less than 2-dB penalty for three-input XOR gate, respectively.

Followed in Chapter 5 we have proposed an all-optical label recognition scheme based on XPM in fiber. It can recognize any label pattern by reconfiguring the local pattern. The recognition result can be easily obtained by measuring the output optical power. We have demonstrated the recognition of three 4-bit label patterns, and studied the relation between the recognition sensitivity and the input label power.

In recent research of optical access technologies, CLS WDM-PON is a promising candidate. However, existing CLS WDM-PON architectures only support point-to-point data service. To implement stronger network functions and improve the downstream service, we have proposed a multicast overlay for CLS WDM-PON by utilizing DPSK modulation format. The downstream point-to-point signal is in IRZ format such that another set of DPSK multicast data can superimpose on it. At the ONU side, the composite IRZ-DPSK signal can be directly remodulated to carry the upstream data. That is, only one laser source is needed for each WDM channel, which nevertheless can carry both the two downstream services and the upstream service.

7.2 Suggestion on future work

Chapter 2 has proposed a hybrid OTDM scheme and investigated the two-channel OTDM system as a special case. For the two-channel hybrid OTDM system, either of the two channels can be directly detected without demultiplexing. This is a very simple method to double the capacity of a wavelength, without the need of upgrading any electronic or optical devices to higher speed.

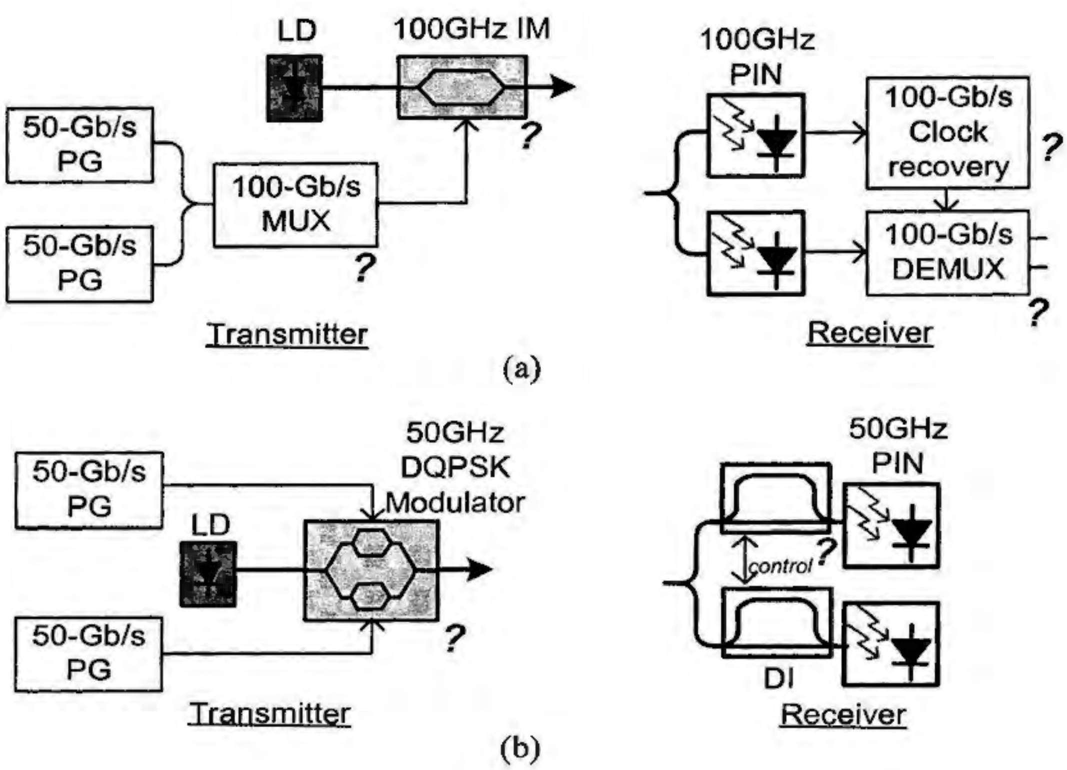

Fig. 7.1 100G Ethernet physical layer realized by 100-Gb/s ETDM (a) [1], and by 50-Gsymbol/s DQPSK (b) [2], respectively. The device accompanied with a question mark means the technical difficulty or non-practicability at present.

With the increase of local-area network traffic, gigabit Ethernet or 10-gigabit Ethernet is being widely deployed. The need of aggregating these 10-gigabit links is coming to the network providers of Internet infrastructure. Recently, the IEEE has formed a task force to study the next-generation 100-gigabit Ethernet (or simply, 100G Ethernet or 100GE) [1-3] and a completed standard may appear by 2010.

Currently, there have been several proposals to implement the physical layer of 100G Ethernet, as illustrated as follows.

In [2], the physical-layer 107-Gb/s signal was aggregated via electrical time division multiplexing (ETDM) before being modulated on optical carrier, as shown in Fig. 7.1(a). The 100-Gb/s (de)multiplexers are still in laboratory development status, and many 100-GHz essential electronic and optical components are not available. In [3], the immature 100-GHz components were avoided as 4-level format DQPSK was employed, which only needed to achieve 50 Gsymbol/s for 100 Gb/s. Therefore, commercially-available 50-Gb/s electronics would work well. However, DQPSK required relatively complex modulator and demodulator, and the performance was very sensitive to even a little phase noise.

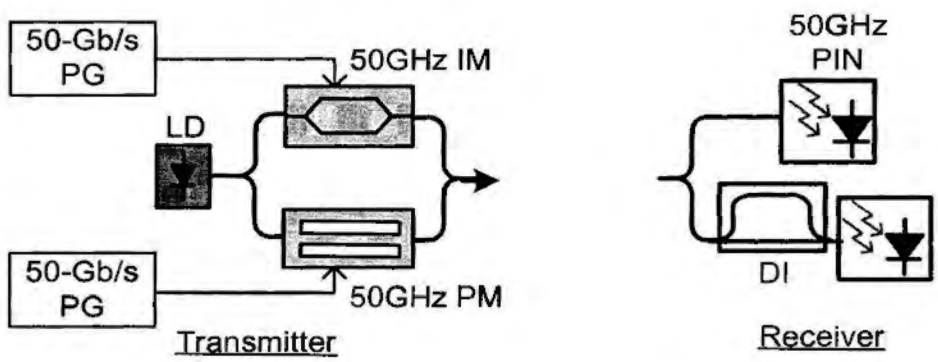

Fig. 7.2 100G Ethernet physical layer implemented by our proposed hybrid OTDM.

We consider it may be a better solution to employ our proposed hybrid OTDM to implement the 100G Ethernet physical layer. One 50-Gb/s ASK tributary can be combined with one 50-Gb/s DPSK tributary to form an aggregate 100-Gb/s OTDM signal, where only 50-GHz commercially available components are needed. More importantly, the two-channel hybrid OTDM signal does not need demultiplexing at the receiver side, which avoids the most cumbersome part of a conventional OTDM system. Fig. 7.2 shows our proposed transmitter and receiver for 100G Ethernet.

The next step of research is to investigate the signal performance at the receiver for the back to back case and after transmission, respectively. Under natural condition, the performance of the OOK tributary and the DPSK tributary data may not be the same. Therefore, to have an even performance for the two tributaries, some special design may need to be considered. The transmission link should also be well designed since the high-speed signal is very sensitive to fiber dispersion. Moreover, the compatibility with the higher network layers should also be considered, and the physical layer should be optimized for the functions and performance of the higher network layers.

The all-optical XOR logic gate proposed in Chapter 3 has the potential to support ultrafast operation due to the intraband process of FWM. After the successful demonstration and experimental investigation of the 10-Gb/s operation, the next step would be the demonstration of a 40-Gb/s three-input XOR gate for DPSK signals. The high-speed 40-Gb/s signal has higher requirement on the timing control of the three-input RZ-DPSK signals, which brings greater challenge in the implementation of the logic gate. Another merit of the proposed three-input logic gate is the reduced cascaded numbers of logic units in complicated logic operations. This issue is also expected to be quantitatively evaluated in the future work.

References

[1] 100G Ethernet Forum, http://www.100g-ethernet.com/ [online].

[2] K. Schuh, B. Junginger, E. Lach, G. Veith, "1 Tbit/s (10×107 Gbit/s ETDM) NRZ Transmission over 480km SSMF," in *Optical Fiber Communication Conference and Exposition and The National Fiber Optic Engineers Conference (OFC/NFOEC)* 2007, Anaheim, USA, paper PDP23.

[3] C. R. S. Fludger, T. Duthel, D. van den Borne, C. Schulien1, E-D. Schmidt, T. Wuth, E. de Man, G. D. Khoe, H. de Waardt, "10×111 Gbit/s, 50 GHz spaced, POLMUX-RZ-DQPSK transmission over 2375 km employing coherent equalisation," in *Optical Fiber Communication Conference and Exposition and The National Fiber Optic Engineers Conference (OFC/NFOEC)* 2007, Anaheim, USA, paper PDP22.

Bibliography

M.A. Wegleitner, "Maximizing the impact of optical technology," in *Optical Fiber Communication Conference and Exposition and The National Fiber Optic Engineers Conference (OFC/NFOEC)* 2007, Anaheim, USA, Plenary talk.

A.H. Gnauck, G. Charlet, P. Tran, P. Winzer, C. Doerr, J. Centanni1, E. Burrows, T. Kawanishi, T. Sakamoto, K. Higuma, "25.6-Tb/s C+L-Band transmission of polarization-multiplexed RZ-DQPSK signals," in *Optical Fiber Communication Conference and Exposition and The National Fiber Optic Engineers Conference (OFC/NFOEC)* 2007, Anaheim, USA, paper PDP19.

W. Hung, C.K. Chan, L.K. Chen, F. Tong, "An optical network unit for WDM access networks with downstream DPSK and upstream re-modulated OOK data using injection-locked FP laser," *Photonics Technology Letters*, vol. 15, no. 10, pp. 1476-1478, 2003.

E. Tangdiongga, Y. Liu, X. Shu, I. Bennion, H. De Waardt, G.D. Khoe, A.M.J. Koonen, H.J.S. Dorren, "640-to-40 Gb/s all-optical demultiplexing using a single SOA assisted by an optical filter," *IEEE Lasers and Electro-Optics Society Annual Meeting (LEOS)* 2006, Montreal, Canada, paper PD1.6.

C. Xu, X. Liu, and X. Wei, "Differential phase-shift keying for high spectral efficiency optical transmitters," *Journal of Selected Topics in Quantum Electronics*, vol. 10, no. 2, pp. 281-293, 2004.

P.A. Humblet and M. Azizoglu, "On the bit rate of lightwave systems with optical amplifiers," *Journal of Lightwave Technology*, vol. 9, pp. 1576-1582, 1991.

G.P. Agrawal, *Fiber-Optic Communication Systems*, 3rd Ed, Wiley-Interscience, New York, pp. 250-253, 2002.

L.G. Kazovsky, G. Kalogerakis and Wei-Tao Shaw, "Homodyne phase-shift-keying systems: past challenges and future opportunities," *Journal of Lightwave Technology*, vol. 24, no. 12, pp. 4876-4884, 2006.

A.H. Gnauck and P.J. Winzer, "Optical phase-shifted keying transmission," *Journal of Lightwave Technology*, vol. 23, no. 1, pp.115-130, 2005.

D.O. Caplan, M.L. Stevens and J.J. Carney, "High-sensitivity demodulation of multiple-data-rate WDM-DPSK signals using a single interferometer," in *Optical Fiber Communication Conference and Exposition and The National Fiber Optic Engineers Conference (OFC/NFOEC)* 2007, Anaheim, USA, paper OThD3.

A.H. Gnauck, X. Liu, S. Chandrasekhar, X. Wei, "Optical duobinary format from demodulation of DPSK using athermal delay interferometer," *Photonics Technology Letters*, vol. 18, no. 4, pp. 637-639, 2006.

I. Lyubomirsky, S. Shetty, J. Roman, and M. Y. Frankel, "Optimum 10-Gb/s NRZ receiver bandwidths for ultradense WDM transmission systems," *Photonics Technology Letters*, vol. 14, no. 6, pp. 870-872, 2002.

L. Christen, Y.K. Lize, S. Nuccio, J.Y. Yang, P. Saghari, A.E. Willner and L. Paraschis, "Fiber Bragg grating balanced DPSK demodulation," *IEEE Lasers and Electro-Optics Society Annual Meeting (LEOS)* 2006, Montreal, Canada, paper WP2.

H. Masuda1, A. Sano, T. Kobayashi, E. Yoshida1, Y. Miyamoto, Y. Hibino, K. Hagimoto, T. Yamada, T. Furuta, H. Fukuyama, "20.4-Tb/s (204×111 Gb/s) transmission over 240 km using bandwidth-maximized hybrid Raman/EDFAs," in *Optical Fiber Communication Conference and Exposition and The National Fiber Optic Engineers Conference (OFC/NFOEC)* 2007, Anaheim, USA, paper PDP20.

C. R. S. Fludger, T. Duthel, D. van den Borne, C. Schulien1, E-D. Schmidt, T. Wuth, E. de Man, G. D. Khoe, H. de Waardt, "10×111 Gbit/s, 50 GHz spaced, POLMUX-RZ-DQPSK transmission over 2375 km employing coherent equalisation," in *Optical Fiber Communication Conference and Exposition and The National Fiber Optic Engineers Conference (OFC/NFOEC)* 2007, Anaheim, USA, paper PDP22.

K. Schuh, B. Junginger, E. Lach, G. Veith, "1 Tbit/s (10×107 Gbit/s ETDM) NRZ Transmission over 480km SSMF," in *Optical Fiber Communication Conference and Exposition and The National Fiber Optic Engineers Conference (OFC/NFOEC)* 2007, Anaheim, USA, paper PDP23.

D. G. Foursa, A. Lucero, C.R. Davidson, J.-X. Cai, W. Anderson, Y. Cai, P.C. Corbett, W.W. Patterson, H. Li, M. Mazurczyk, M. Nissov, A. N. Pilipetskii, N. Bergano, " 2Tb/s (200x10Gb/s) data transmission over 7,300km using 150km spaced repeaters enabled by ROPA technology," in *Optical Fiber Communication Conference and Exposition and The National Fiber Optic Engineers Conference (OFC/NFOEC)* 2007, Anaheim, USA, paper PDP25.

H.G. Weber, R. Ludwig, S. Ferber, C. Schimidt-Langhorst, M. Kroh, V. Marembert, C. Boerner, and C. Schubert, "Ultrahigh-speed OTDM transmission technology," *Journal of Lightwave Technology*, vol. 24, no. 12, pp. 4616-4627, 2006.

J. P. Turkiewicz, E. Tangdiongga, G. Lehmann, H. Rohde, W. Schairer, Y.R. Zhou, E.S.R. Sikora, A. Lord, D.B. Payne, G.D. Khoe, H. de Waardt, "160 Gb/s OTDM networking using deployed fiber," *Journal of Lightwave Technology*, vol. 23, no. 1, pp. 225-235, 2005.

F. Futami, S. Ono, S. Watanabe, "160-Gb/s optical demultiplexing with enhanced timing tolerance by unequally aligning pulse position," in *European Conference on Optical Communication (ECOC)*, paper We2.2.6, Glasgow, UK, 2005.

E.S. Awad, P.S Cho, N. Moulton, J. Goldhar, "All-optical timing extraction with simultaneous optical demultiplexing from 40 Gb/s using a single electroabsorption modulator," *Photonics Technology Letters*, vol. 15, no. 1, pp. 126-128, 2003.

A.I. Siahlo, A.T. Clausen, L.K. Oxenlowe, J. Seoane, P. Jeppesen, "640 Gb/s OTDM transmission and demultiplexing using a NOLM with commercially available highly non-linear fiber," *Conference on Lasers and Electro-Optics (CLEO)* 2005, paper CTuO1, Baltimore, USA.

S.L. Jansen, M. Heid, S. Spalter, E. Meissner, C.-J. Weiske, A. Schopflin, D. Khoe, H. de Waardt, "Demultiplexing 160 Gbit/s OTDM signal to 40 Gbit/s by FWM in SOA," *Electronics Letters*, vol. 38, no. 17, pp. 978-980, 2002.

N. Yamada, S. Nogiwa, H. Ohta, "640-Gb/s OTDM signal measurement with high-resolution optical sampling system using wavelength-tunable soliton pulses," *Photonics Technology Letters*, vol. 16, no. 4, pp. 1125-1127, 2004.

A.I. Siahlo, J. Seoane, A.T Clausen, L.K. Oxenlowe, L.K.; P. Jeppesen, "320 Gb/s single-polarization OTDM transmission over 80 km standard transmission fiber," in *Optical Fiber Communication Conference and Exposition and The National Fiber Optic Engineers Conference (OFC/NFOEC)* 2005, Anaheim, USA, paper OFF3.

M. Nakazawa, T. Yamamoto, K.R. Tamura, "1.28 Tbit/s-70 km OTDM transmission using third- and fourth-order simultaneous dispersion compensation with a phase modulator," *Electronics Letters*, vol. 36, no. 24, pp. 2027-2029, 2000.

K. Chan, C.K. Chan, L.K. Chen, F. Tong, "Mitigation of pattern-induced degradation in SOA-based all-optical OTDM demultiplexers by using RZ-DPSK modulation format," *Photonics Technology Letters*, vol. 15, no. 9, pp. 1264-1266, 2003.

Y.C. Ku, K.Chan, C.K. Chan, L.K. Chen, "Patterning effect avoidance of SOA-based demultiplexer in 80-Gb/s OTDM system using RZ-DPSK modulation format," *Opto-Electronics and Communications Conference (OECC)* 2006, paper 7C1-4, Kaohsiung, Taiwan,

IETF work group, "draft-ietf-ccamp-gmpls-architecture-07.txt", work in progress, Internet draft in www.ietf.org, 2003.

D. J. Blumenthal, B. E. Olsson, G. Rossi, T. E. Dimmick, L. Rau, M. Masanovic, O. Lavrova, R. Doshi, O. Jerphagnon, J. E. Bowers, V. Kaman, L. A. Coldren and J. Barton, "All-optical label swapping networks and technologies," *Journal of Lightwave Technology*, vol. 18, no. 12, pp. 2058-2075, 2000.

W. Hung, C.K. Chan, L.K. Chen, F. Tong, "A bit-serial optical packet label swapping scheme using DPSK encoded labels," *Photonics Technology Letters*, vol. 15, no. 11, pp. 1630-1632, 2003.

N. Calabretta, G. Contestabile, A. D'Errico, E. Ciaramella, "All-optical label processor/erasure for label swapping of 12.5 Gbit/s spectrally separated bit-serial DPSK label and payload," *Electronics Letters*, vol. 41, no. 9, pp. 541-543, 2005.

X. Liu, Y. Su, X. Wei, J. Leuthold, and R. Giles, "Optical-label switching based on DPSK/ASK modulation format with balanced detection for DPSK payload," paper Tu4.4.3, in *European Conference on Optical Communication (ECOC)*, Rimini, 2003.

N. Deng, Y. Yang, C.K. Chan, W. Hung, and L.K. Chen, "Intensity-modulated labeling and all-optical label swapping on angle-modulated optical packets," *Photonics Technology Letters*, vol. 16, no. 4, pp. 1218-1220, 2004.

C. Lin, K.L. Deng, and C.K Chan, "Broadband optical access networks", in *Conference on Lasers and Electro-Optics in Pacific Rim (CLEO/PR)*, Vol. 2, pp. II-256, 2001.

M. S. Goodman, H. Kobrinski, M. P. Vecchi, R. M. Bulley, and J. L. Gimlett, "The LAMBDANET multiwavelength network: architecture, applications, and demonstrations," *Journal on Selected Areas in Communications*, vol. 8, no. 6, pp. 995-1004, 1990.

E. Hall, J. Kravitz, R. Ramaswami, M. Halvorson, S. Tenbrink, and R. Thomsen, "The Rainbow-II gigabit optical network," *Journal on Selected Areas in Communications*, vol. 14, no. 5, pp. 814-823, 1996.

M. Hickey and L. Kazovsky, "The STARNET coherent WDM computer communication network: experimental transceiver employing a novel modulation format," *Journal of Lightwave Technology*, vol. 12, no. 5, pp. 876-884, 1994.

N. J. Frigo, P.P. Iannone, P. D. Magill, T. E. Darcie, M. M. Downs, B. N. Desai, U. Koren, T. L. Koch, C. Dragone, H. M. Presby, and G. E. Bodeep, "A wavelength-division multiplexed passive optical network with cost-shared components," *Photonics Technology Letters*, vol. 6, no. 11, pp. 1365-1367, 1994.

N. Deng, C.K. Chan, L.K. Chen, "A centralized-light-source WDM access network utilizing inverse-RZ downstream signal with upstream data remodulation," *Optical Fiber Technology*, vol. 13, no. 1, pp.18-21, 2007.

I.T. Monroy, E. van Breusegem, T. Koonen, J.J.V. Olmos,; J. van Berkel, J. Jennen, C. Peucheret, E. Zouganeli, "Optical label switched networks: laboratory trial and network emulator in the IST-STOLAS project," *IEEE Communications Magazine*, vol. 44, no. 8, pp. 43-51, 2006.

H.G. Weber, R. Ludwig, S. Ferber, C. Schimidt-Langhorst, M. Kroh, V. Marembert, C. Boerner, and C. Schubert, "Ultrahigh-speed OTDM transmission technology," *Journal of Lightwave Technology*, vol. 24, no. 12, pp. 4616-4627, 2006.

J. P. Turkiewicz, E. Tangdiongga, G. Lehmann, H. Rohde, W. Schairer, Y.R. Zhou, E.S.R. Sikora, A. Lord, D.B. Payne, G.D. Khoe, H. de Waardt, "160 Gb/s OTDM networking using deployed fiber," *Journal of Lightwave Technology*, vol. 23, no. 1, pp. 225-235, 2005.

F. Futami, S. Ono, S. Watanabe, "160-Gb/s optical demultiplexing with enhanced timing tolerance by unequally aligning pulse position," in *European Conference on Optical Communication (ECOC)*, paper We2.2.6, Glasgow, UK, 2005.

E.S. Awad, P.S Cho, N. Moulton, J. Goldhar, "All-optical timing extraction with simultaneous optical demultiplexing from 40 Gb/s using a single electroabsorption modulator," *Photonics Technology Letters*, vol. 15, no. 1, pp. 126-128, 2003.

A.I. Siahlo, A.T. Clausen, L.K. Oxenlowe, J. Seoane, P. Jeppesen, "640 Gb/s OTDM transmission and demultiplexing using a NOLM with commercially available highly non-linear fiber," *Conference on Lasers and Electro-Optics (CLEO)* 2005, paper CTuO1, Baltimore, USA.

S.L. Jansen, M. Heid, S. Spalter, E. Meissner, C.-J. Weiske, A. Schopflin, D. Khoe, H. de Waardt, "Demultiplexing 160 Gbit/s OTDM signal to 40 Gbit/s by FWM in SOA," *Electronics Letters*, vol. 38, no. 17, pp. 978-980, 2002.

M. Nakazawa, T. Yamamoto, K.R. Tamura, "1.28 Tbit/s-70 km OTDM transmission using third- and fourth-order simultaneous dispersion compensation with a phase modulator," *Electronics Letters*, vol. 36, no. 24, pp. 2027-2029, 2000.

K. Chan, C.K. Chan, L.K. Chen, F. Tong, "Mitigation of pattern-induced degradation in SOA-based all-optical OTDM demultiplexers by using RZ-DPSK modulation format," *Photonics Technology Letters*, vol. 15, no. 9, pp. 1264-1266, 2003.

C. Schubert, J. Berger, S. Diez, H.J. Ehrke, R. Ludwig, U. Feiste, C. Schmidt, H.G. Weber, G. Toptchiyski, S. Randel, K. Petermann, "Compasison of interferometric all-optical switches for demultiplexing applications in high-speed OTDM systems," *Journal of Lightwave Technology*, vol. 20, no. 4, pp. 618-624, 2002.

S. Kieckbusch, S. Ferber, H. Rosenfeldt, R. Ludwig, C. Boerner, A. Ehrhardt, E. Brinkmeyer, H.-G. Weber, "Automatic PMD compensator in a 160-Gb/s OTDM transmission over deployed fiber using RZ-DPSK modulation format," *Journal of Lightwave Technology*, vol. 23, no. 1, pp. 165-171, 2005.

M.J. Guy, S.V. Chernikov, J.R. Taylor and D.G. Moodie, "Demonstration of the feasibility of dual frequency operation of an electroabsorption modulator for demultiplexing in a 16 channel 40Gbit/s OTDM system," *Electronics Letters*, vol. 32, no. 12, pp. 1138-1139, 1996.

D.G. Moodie, A.D. Ellis, and C.W. Ford, "Generation of 6.3 ps optical pulses at a 10GHz repetition rate using a packaged electroabsorption modulator and dispersion compensating fiber," *Electronics Letters*, vol. 30, no. 20, pp. 1700-1701, 1994.

T. Koonen, Sulur, I. T. Monroy, J. Jennen, H. Waardt, "Optical labelling of packets in IP-over-WDM networks," in *European Conference on Optical Communication (ECOC)*, Paper 5.5.2, 2002.

N. Chi, L. Xu, L. Chritiansen, K. Yvind, J. Zhang, P. Holm-Nielsen, C. Peucheret, C. Zhang, and P. Jeppesen, "Optical label swapping and packet transmission based on ASK/DPSK orthogonal modulation format in IP-over-WDM networks," in *Optical Fiber Communication Conference (OFC)*, Paper FS2, 2003.

D. Klonidis, R. Nejabati, C. Politi, M. O'Mahony, "All-Optical Packet Switching of 40Gb/s Variable Length Packets Using Dual-Pump FWM Controlled by Fast Tunable Laser," in *European Conference on Optical Communication (ECOC)*, paper Th1.6.2, Stockholm, Sweden, 2004.

J .J. V. Olmos, I. T. Monroy, J. P. Turkiewicz, Y. Liu and A. M. J. Koonen, "Self-controlled all-optical label and payload separator for variable length bursts in a time-serial IM/DPSK scheme," *Photonics Technology Letters*, 17, pp. 1692-1694, 2005.

B.S. Robinson, S.A. Hamilton, S.J. Savage, E.P. Ippen, "40 Gbit/s all-optical XOR using a fiber-based folded ultrafast nonlinear interferometer," in *Optical Fiber Communications Conference (OFC)* 2002, paper ThY2, 2002.

J. H. Kim, Y. M. Jhon, Y. T. Byun, S. Lee, D. H. Woo, and S. H. Kim, "All-optical XOR gate using semiconductor optical amplifiers without additional input beam," *Photonics Technology Letters*, vol. 14, pp. 1436–1438, Oct 2002.

A.J. Poustie, K.J. Blow, A.E. Kelly, R.J. Manning, "All-optical full adder with bit-differential delay," *Optics Communications*, vol. 168, pp. 89-93, 1999.

H. Soto, D. Erasme, and G. Guekos, "5-Gb/s XOR optical gate based on cross-polarization modulation in semiconductor optical amplifiers," *Photonics Technology Letters*, vol. 13, pp. 335–337, Apr. 2001.

K. Zoiros, T. Houbavlis, "Ultrafast all-optical Boolean XOR logic using semiconductor optical amplifier-assisted Sagnac switch," *Conference on Quantum Electronics and Laser Science (QELS)* 2005, Vol. 2, pp. 960-962, 2005.

C. Bintjas, M. Kalyvas, G. Theophilopoulos, T. Stathopoulos, H. Avramopoulos, L. Occhi, L. Schares, G. Guekos, S. Hansmann, and R. Dall'Ara, "20 Gb/s all-optical XOR with UNI gate," *Photonics Technology Letters*, vol. 12, pp. 834–836, 2000.

R. P. Webb, R. J. Manning, G. D. Maxwell, and A. J. Poustie, "40 Gbit/s all-optical XOR gate based on hybrid-integrated Mach–Zehnder interferometer," *Electronics Letters*, vol. 39, pp. 79–80, 2003.

Y.R. Shen, "Basic considerations of four-wave mixing and dynamic gratings," *Journal of Quantum Electronics*, vol. QE-22, pp.1196-1203, 1986.

A. D'Ottavi, E. Iannone, A. Mecozzi, S. Scotti, P. Spano, J. Landreau, A. Ougazzaden, J. C. Bouley, "Investigation of carrier heating and spectral hole burning in semiconductor amplifiers by highly nondegenerate four-wave mixing," *Applied Physics Letters*, vol. 64, pp.2492-2494, 1994.

J.A Armstrong et al, "Interactions between light waves in a nonlinear dielectric," *Physics Review*, vol. 127, pp. 1918-1939, 1962.

P.D Maker et al, "Study of optical effects due to an induced polarization third-order in the electric field strength," *Physics Review A*, vol. 137, pp. 801-818, 1965.

G.P. Agrawal, "Population pulsations and nondegenerate four-wave mixing in semiconductor laser and amplifiers," *Journal of Optics Society of America B*, vol. , pp. 147-159, 1988.

J. Zhou et al, "Efficiency of Broadband Four-Wave Mixing Wavelength Conversion Using Semiconductor Traveling-Wave Amplifiers," *Photonics Technology Letters*, Vol. 6, pp. 50-52, 1994.

J. Zhou et al, "Four-Wave Mixing Wavelength Conversion Efficiency in Semiconductor Traveling-Wave Amplifiers Measured to 65 nm of Wavelength Shift," *Photonics Technology Letters*, Vol. 6, pp. 984-987, 1994.

D.F. Geraghty, R.B Lee, M. Verdiell, M. Ziari, A. Mathur, K.J. Vahala, "Wavelength conversion for WDM communication systems using four-wave mixing in semiconductor optical amplifiers", *Journal of Selected Topics in Quantum Electronics*, Vol. 3, no. 5, pp. 1146-1155, 1997.

G.P. Agrawal, N.A. Olsson, "Self-phase modulation and spectral broadening of optical pulses in semiconductor laser amplifiers," *Journal of. Quantum Electronics*, Vol. 25, no. 11, pp. 2297-2306, 1989.

D. Klonidis, R. Nejabati, C. Politi, M. O'Mahony, "All-Optical Packet Switching of 40Gb/s Variable Length Packets Using Dual-Pump FWM Controlled by Fast Tunable Laser," in *European Conference on Optical Communication (ECOC)*, paper Th1.6.2, Stockholm, Sweden, 2004.

R. Takahashi, *et al*, "40-Gb/s label recognition and 1×4 self-routing using self-serial-to-parallel conversion," *Photonics Technology Letters*, Vol. **16**, no. 2, pp. 692-694, 2004.

K. Chan, F. Tong, C.K. Chan, L.K. Chen, W. Hung, "An All-Optical Packet Header Recognition Scheme for Self-Routing Packet Networks", in *Optical Fiber Communication Conference (OFC)*, paper WO4, Anaheim, CA, USA, Mar 2002.

N. Calabretta, G. Contestabile, E. Ciaramella, "All-optical label erasure/recognition of novel DPSK optical packets for optical packet switching," in *Optical Fiber Communication Conference (OFC)*, paper OtuC5, Anaheim, CA, USA, Mar 2005.

M.T. Hill, A. Strivatsa, N. Calabretta, Y. Liu, H. d.Waardt, G.D. Khoe, H.J.S. Dorren, "1×2 optical packet switch using all-optical header processing", *Electronics Letters*, Vol. 37, no. 12, pp. 774-775, Jun 2001.

J. M. Martinez, J. Herrera, F. Ramos, J. Marti, "All-optical address recognition scheme for label-swapping networks," *Photonics Technology Letters*, Vol. 18, no. 1, pp. 151-153, Jan 2006.

N.J. Frigo, P. P. Iannone, P.D. Magill, T.E. Darcie, M.M. downs, B.N. Sesai, U. Koren, T.L. Koch, C. Dragone, H.M. Presby, and G.E. Bodeep, "A wavelength-division multiplexed passive optical network with cost-shared components," *Photonics Technology Letters*, Vol. 6, no. 11, pp. 1365-1367, 1994.

K.M. Choi, C.H. Lee, "Colorless operation of WDM-PON based on wavelength locked Fabry-Perot laser diode," in Proc. *31th European Conference on Optical Communication (ECOC)*, paper We3.3.4, Glasgow, UK, 2005.

Y. Shibata, N. Yoshimoto, "2.5-Gbit/s wavelength channel data rewriter using semiconductor optical saturator/modulator for drop-and-rewrite WDM networks", in Proc. *29th European Conference on Optical Communication (ECOC)*, paper Th2.3.3, Rimini, Italy, 2003.

J. H. Moon, K.M Choi, C.H. Lee, "Overlay of Broadcasting Signal in a WDM-PON," in *Optical Fiber Communication Conference and Exposition and The National Fiber Optic Engineers Conference (OFC/NFOEC) 2006*, paper OTHK8.

E.S. Son, K.H. Han, J.K. Kim, Y.C. Chung, "Bidirectional WDM passive optical network for simultaneous transmission of data and digital broadcast video service," *Journal of Lightwave Technology*, vol. 21, no. 8, pp. 1723- 1727, 2003.

M. Khanal, C.J. Chae, R.S. Tucker, "Selective broadcasting of digital video signals over a WDM passive optical network," *Photonics Technology Letters*, vol. 17, no. 9, pp. 1992-1994, 2005.

C.A. Chan, M. Attygalle, A. Nirmalathas, "Provision of independent services in WDM passive optical networks using closely separated dual baseband channels," in *Optical Fiber Communication Conference and Exposition and The National Fiber Optic Engineers Conference (OFC/NFOEC) 2007*, paper JWA48.

M. Ohm, J. Speidel, "Quaternary optical ASK-DPSK and receivers with direct detection," *Photonics Technology Letters*, vol. 15, no. 1, 2003.

G.J. Foschini, L.J Greenstein, G. Vannucci, "Noncoherent detection of coherent lightwave signals corrupted by phase noise," *Transaction on Communications*, vol. 36, no. 3, pp. 306-314, 1988.

G.P. Agrawal, *Fiber-optic communication systems*, 3rd Ed., Wiley-Interscience, 2002.

M. Ogusu, K. Ide, S. Ohshima, "0.8-b/s/Hz WDM of 40-Gb/s inverse-RZ signals without using polarization-division-multiplexing and pre-filtering techniques," in *9th Optoelectronics and Communications Conference (OECC)*, paper 13C2-2, Yokohama, Japan, 2004.

100G Ethernet Forum, http://www.100g-ethernet.com/ [online].

Appendix

A.1 List of publications

JOURNALS:

N. Deng, C.K. Chan, L.K. Chen, "A Hybrid OTDM Scheme with Enhanced Demultiplexing Performance," to appear in *IEEE Photonics Technology Letters*, 2007.

N. Deng, C.K. Chan, L.K. Chen, "A Centralized-Light-Source WDM Access Network Utilizing Inverse-RZ Downstream Signal with Upstream Data Re-modulation," *Optical Fiber Technology*, vol. 13, no.1, 2007.

N. Deng, K. Chan, C.K. Chan, L.K. Chen, "An All-Optical XOR Logic Gate for High-Speed RZ-DPSK Signals by Four-Wave Mixing in Semiconductor Optical Amplifier," *IEEE Journal of Selected Topics in Quantum Electronics*, vol. 12, no. 4, pp. 702-707, 2006.

N. Deng, C.K. Chan, L.K. Chen, "Characterization of the Performance of Optical Amplitude-shift Keying–Differential Phase-shift Keying Orthogonally Modulated Signals," *OSA Optics Letters*, vol. 30, no. 8, pp. 818-820, 2005.

W. Hung, N. Deng, C.K. Chan, L.K. Chen, "A Novel Wavelength Shift Keying Transmitter Based on Optical Phase Modulation", *IEEE Photonics Technology Letters*, Vol. 16, no.7, pp. 1739-1741, 2004.

N. Deng, Y. Yang, C.K. Chan, W. Hung, L.K. Chen, "Intensity-modulated Labeling and All-optical Label Swapping on Angle-modulated Optical Packets," *IEEE Photonics Technology Letters*, Vol. 16, no. 4, 2004.

N. Deng, C.K. Chan, L.K. Chen, F. Tong, "Data Re-modulation on Downstream FSK Signal for Upstream Transmission in a WDM Passive Optical Network," *IEE Electronics Letters*, vol. 39, no. 24, 2003.

JOURNAL SUBMISSIONS:

N. Deng, C.K. Chan, L.K. Chen, C. Lin, "A WDM Passive Optical Network with Centralized Light Sources and Multicast Overlay," submitted to *IEEE Photonics Technology Letters*, 2007.

Z.X. Wang, N. Deng, C. Lin, C.K. Chan, "Polarization-Independent Operation in Four-Wave Mixing Using Dispersion-Flattened High-Nonlinearity Photonic Crystal Fiber with Small Birefringence," submitted to *IEEE/OSA Journal of Lightwave Technology*, 2007.

CONFERENCES:

N. Deng, C.K. Chan, L.K. Chen, C. Lin, "A WDM-PON Architecture with Selective-Broadcast Overlay," accepted by *European Conference on Optical Communication (ECOC) 2007.*

N. Deng, C.K. Chan, "Enhanced Tolerance to Demultiplexing Misalignment in an OTDM System with Hybrid RZ-ASK/DPSK Formats," in *Optical Fiber Communication Conference and Exposition and The National Fiber Optic Engineers Conference (OFC/NFOEC) 2007*, paper JWA51.

N. Deng, C.K. Chan, "A Novel OTDM Scheme with Hybrid RZ-ASK/DPSK Formats and Its Enhanced Tolerance to Demultiplexing Misalignment," in 7^{th} *IEEE Hong Kong Chapter LEOS Postgraduate Conference 2006*, paper C5.

N. Deng, C.K. Chan, L.K. Chen, "A Novel Phase-modulated Label Pattern Recognition Scheme Based on Parallel Bit Comparison Using Cross-phase

Modulation," in *European Conference on Optical Communication (ECOC) 2006*, paper We3.P.86.

N. Deng, C.K. Chan, "Optical Time Division Multiplexing of RZ-ASK and RZ-DPSK Signals and Their Detection without Optical Demultiplexing," in *European Conference on Optical Communication (ECOC) 2006*, paper Th3.5.6.

Z.X. Wang, N. Deng, C. Lin, C.K. Chan, "Polarization-insensitive widely tunable wavelength conversion based on four-wave mixing using dispersion-flattened high-nonlinearity photonic crystal fiber with residual birefringence," in *European Conference on Optical Communication (ECOC) 2006*, paper We3.P.18.

N. Deng, C.K. Chan, L.K. Chen, "Re-modulation of Upstream Data on Downstream Inverse-RZ Signals in Optical WDM Access Networks," *6th IEEE Hong Kong Chapter LEOS Postgraduate Conference 2005*, paper PSP9.

N. Deng, C.K. Chan, L.K. Chen, "Demonstration of an All-Optical Three-Input Exclusive-OR Logic Gate for High-Speed Optical DPSK Signals," in *European Conference on Optical Communication (ECOC) 2005*, paper Tu3.5.2.

G.W. Lu, N. Deng, C.K. Chan, L.K. Chen, "Use of Downstream Inverse-RZ Signal for Upstream Data Re-modulation in a WDM Passive Optical Network," in *Optical Fiber Communication Conference and Exposition and The National Fiber Optic Engineers Conference (OFC/NFOEC) 2005*, paper OFI8.

N. Deng, C.K. Chan, L.K. Chen, "Performance Characterization of Optical Orthogonal ASK/DPSK Signals," in *European Conference on Optical Communication (ECOC) 2004*, paper We4.P.138.

N. Deng, Y. Yang, C.K. Chan, L.K. Chen, W. Hung, "All-optical OOK Label Swapping on OFSK Payload in Optical Packet Networks," in *Proc. Optical Fiber Communications Conf. (OFC 2004)*, paper FO5.

N. Deng, W. Hung, C.K. Chan, L.K. Chen, F. Tong, "A Novel Wavelength Modulated Transmitter and Its Application in WDM Passive Optical Networks," in *Proc. OFC 2004*, paper MF79.

N. Deng, C.K. Chan, L.K. Chen, F. Tong, "Experimental Investigation of Re-modulating Upstream OOK Data on Downstream OFSK signal in a Two-way WDM Access Network," in *Conference of Lasers and Electro-Optics (CLEO/Pacific Rim) 2003*, paper W1J-(13)-4.

A.2 Participated research projects

"Next-Generation Broadband Optical Access for FTTH: WDM Access Network Architectures and Experimental Studies," Hong Kong Research Grant Council (HKRGC) #CUHK4142/06E.

"Broadband optical access networks-photonic technologies and architectural studies," CUHK Group Research Grant #4410010.

"Design of a novel high-speed optical frequency shift keying transmitter for optical transmission systems," Hong Kong Research Grant Council (HKRGC) #CUHK4106/05E.

"Study of photonic crystal fibers (PCF) for nonlinear optical frequency conversion and photonic sensor applications," Hong Kong Research Grant Council (HKRGC) #CUHK4144/05E.

"All-optical signal processing techniques for high-speed optical differential phase-shift-keying (DPSK) signals," Hong Kong Research Grant Council (HKRGC) #CUHK4240/04E.

"Optical networking techniques using high-speed constant intensity modulation," CUHK Direct Grant #2050296.

"Investigation of low-cost modulator for a proposed DWDM access network," Hong Kong Research Grant Council (HKRGC) #CUHK4191/01E.